PKA-MEDIATED REGULATION OF PROFILIN-1 – IMPLICATION IN SPROUTING ANGIOGENESIS

by

William Veon

B.S., University of South Florida, 2007

Submitted to the Graduate Faculty of

Swanson School of Engineering in partial fulfillment

of the requirements for the degree of

Doctor of Philosophy

University of Pittsburgh

2014

UNIVERSITY OF PITTSBURGH

SWANSON SCHOOL OF ENGINEERING

This dissertation was presented

by

William Veon

It was defended on

February 7, 2014

and approved by

Johnny Huard, Ph.D., Professor, Departments of Orthopaedic Surgery, Molecular Genetics, Biochemistry, Bioengineering, and Pathology

Donna Stolz, Ph.D., Professor, Department of Cell Biology and Physiology

Alan Wells, M.D., D.M.S., Professor, Departments of Pathology, Bioengineering, and Computational and Systems Biology

Dissertation Director: Partha Roy, Ph.D., Professor, Department of Bioengineering

Dissertation Co-Director: Sanjeev Shroff, Ph.D., Professor, Department of Bioengineering

PKA-MEDIATED REGULATION OF PROFILIN-1 – IMPLICATION IN SPROUTING ANGIOGENESIS

William Veon, Ph.D.

University of Pittsburgh, 2014

Angiogenesis is a process of vessel outgrowth from a pre-existing capillary that is implicated in many physiological and pathological conditions. Profilin-1 (Pfn1), a ubiquitously expressed actin-binding protein, has been previously shown to be up-regulated in vascular endothelial cells during capillary morphogenesis and required for endothelial cell migration, morphogenesis and invasion *in vitro*. In the first part of this study, we demonstrated that depletion of Pfn1 interferes with sprouting angiogenesis *in vitro* and *ex vivo*. In the second part, we further explored how Pfn1 might be biochemically regulated. Our studies suggested that a significant fraction of Pfn1 could exist in a number of phosphorylated states in cells. We showed that Pfn1 can be phosphorylated by Protein Kinase A (PKA) *in vitro* and in a PKA-dependent manner *in vivo*. By mass-spectrometry, we identified several potential PKA phosphorylation sites of Pfn1, one of which, T89, at least also appeared to be a bona fide modification site of Pfn1 *in vivo*. We performed biochemical and *in silico* analyses to determine the potential consequence of this phosphorylation on the properties of Pfn1. Finally, we showed that activating the PKA pathway affects ligand binding of Pfn1 in cells and negatively impacts both endothelial cell migration and sprouting angiogenesis. Collectively, these observations implicate a possible role for Pfn1 post-translational modification in the PKA-mediated regulation of sprouting angiogenesis.

TABLE OF CONTENTS

LIST OF TABLES

LIST OF FIGURES

ABBREVIATIONS AND ACRONYMS

2D	Two-Dimensional
3D	Three-Dimensional
A_C	Critical concentration of Globular-actin
A_{CB}	Critical concentration of the barbed end
A_{CP}	Critical concentration of the pointed end
ADF	Actin Depolymerizing Factor
ADP	Adenosine-5’-diphosphate
ADP-G-actin	Adenosine-5’-diphosphate-bound Globular-actin
ADP-Pi	Phosphate-bound Adenosine-5’-diphosphate
ADP-Pi-G-actin	Phosphate-bound Adenosine-5’-diphosphate-bound Globular-actin
AF6	ALL1-Fused Gene From Chromosome 6
ALS	Amyotrophic Lateral Sclerosis
Arp2/3	Actin-related protein 2/3 complex
ATP	Adenosine-5’-triphosphate
ATP-G-actin	Adenosine-5’-triphosphate-bound Globular-actin
C-terminal	Carboxy-terminal
CapZ	Capping Protein (Actin Filament) Muscle Z-Line
Cdc42	Cell division control 42

Cdh5	Cadherin 5
Cobl	Cordon bleu
ECM	Extracellular Matrix
Ena	Enabled
E#	Embryonic day #
EGF	Epidermal growth factor
ER	Estrogen Receptor
EVL	Ena/VASP-like
F-actin	Filamentous-Actin
FBS	Fetal Bovine Serum
FH1	Formin Homology Domain 1
FH2	Formin Homology Domain 2
FMNL1	Formin-Like 1
FRAP	Fluorescence Recovery After Photobleaching
FRET	Fluorescence Resonance Energy Transfer
G-actin	Globular-Actin
GFP	Green Fluorescent Protein
GST	Glutathione-S-Transferase
HEK-293	Human Embryonic Kidney 293
HMEC-1	Immortalized Human Microvascular Endothelial Cell line
HUVEC	Human Vein Umbilical Endothelial Cells
LIMK	LIM Domain Kinase
Lmod	Leiomodin

Lpd	Lamellipodin
MMP	Matrix Metalloproteinases
Mena	Mammalian Enabled
N-terminal	Amino-terminal
N-WASP	Neuronal-Wiskott-Aldrich Syndrome Protein
NMR	Nuclear Magnetic Resonance
NPF	Nucleation Promoting Factor
OHT	4-hydroxytamoxifen
P#	Postnatal day #
p42POP	Partner Of Profilin
Pfn	Profilin
Pfn1	Profilin-1
$PI(3,4)P_2$	phosphatidylinositol-3,4-bisphosphate
$PI(4,5)P_2$	phosphatidylinositol-4,5-bisphosphate
PIP_3	phosphatidylinositol-3,4,5-triphosphate
PKA	Protein Kinase A
PKCζ	Protein Kinase C-ζ
PLCγ1	phospholipase C-γ1
Polyproline	Poly-L-proline
Rac1	Ras-related C3 botulinum toxin substrate 1
Rho GTPAses	Rho family of small GTPases
RhoA	Ras homology family member A
RIAM	Rap1-GTP-Interacting Adaptor Molecule

ROCK1	Rho-associated coiled-Coil Kinase-1
ROCK2	Rho-associated coiled-Coil Kinase-2
siRNA	small interfering ribonucleic acid
SMN	Survival Motor Neuron Protein
SRF	Serum Response Factor
VASP	Vasodilator-stimulated phosphoprotein
VCP	Valosin Containing Protein
VEGF-A	Vascular Endothelial Growth Factor-A
VEGF-C	Vascular Endothelial Growth Factor-C
VEGFR2	Vascular Endothelial Growth Factor Receptor 2
WASP	Wiskott-Aldrich Syndrome Protein
WAVE	WASP family Verprolin-homologous protein
WH2	Wiskott-Aldrich Syndrome Protein-Homology 2
WIP	WASP Interacting Protein

PREFACE

I would first like to thank my mentors, Dr. Partha Roy and Dr. Sanjeev Shroff. I could not imagine reaching this plateau without their constant support, encouragement, and guidance. I am forever grateful for the patience they awarded me throughout the trials that came during this journey. I would also like to sincerely thank my thesis committee – Dr. Johnny Huard, Dr. Donna Stolz, and Dr. Alan Wells – for their support, advice, and critical evaluation of my work.

I also thank all of the members of Roy lab whom I have had the pleasure of working with, past and present: Dr. Li Zou, Dr. Tuhin Das, Dr. Zhijie Ding, Dr. Yongho Bae, Dr. Maria Jaramillo, Dave Gau, Chang Jiang, Marion Joy, and Dr. Sam Guo.

I would also like to thank Dr. Harvey Borovetz and Dr. Wendy Mars who always supported me when I was seeking financial support for the continuation of my studies.

Finally, I would like to express my sincerest thanks to my family. First, my wife, Yuri, for never letting me give up even when hope seemed unredeemable. Next, my parents for their constant support throughout my life. Last but not least, I would like to thank my daughter Chelsea. Our time together has given me newfound energy and drive. This is a shared achievement that I could not possibly have finished on my own.

1.0 INTRODUCTION

1.1 THE HUMAN PROFILINS

There are four known Profilin (Pfn) genes in the human genome – namely, PFN1, PFN2, PFN3, and PFN4 – that exhibit very distinct expression patterns [2-5]. In general, Pfns have been well-conserved through evolution and at least one Pfn gene has been found in nearly every eukaryotic cell type, from yeast and amoebae to plants and animals [6]. Pfn1, the only ubiquitously-expressed member and the focus of this study, is expressed throughout embryonic development and in every cell type except skeletal muscle upon adulthood [7, 8]. Pfn2a, the more common splice variant of Pfn2, is expressed most abundantly in the brain and certain phases of mouse embryogenesis although its mRNA is found in a variety of tissues. Expression of the Pfn2b variant is relatively limited [3, 9, 10]. Pfn3 and Pfn4 are exclusively expressed in the testes in spermatids and during spermatogenesis respectively [4, 5]. The sequence homologies of these Pfns and even comparable genes in other species are low, but *in vivo* function is relatively consistent. However, homozygous knockout of the PFN1 gene in mice resulted in embryonic lethality at the two-cell stage due to deficiencies in cytokinesis that could not be compensated by the more weakly expressed Pfn2a, highlighting its unique importance in cell survival and division [6, 7]. Because Pfn1 was originally isolated as a monomeric, globular (G)-actin sequestration factor, most studies, including the work presented hereafter, have focused on its

impact on the actin cytoskeleton [2, 11]. To put these studies in perspective, it is necessary to introduce them in the context of the understood mechanisms of actin polymerization and cell motility.

1.1.1 Proflin-1 Structure and Ligand Binding

Pfn1 has been found to complex with G-actin, poly-L-proline (polyproline) motif-bearing ligands, and membrane phosphoinositides. It is through these interactions that Pfn1 is thought to impact the actin cytoskeleton and cell migration [2, 12, 13]. The specific residues on Pfn1 involved in its interaction with these binding partners are well-established and have been confirmed through a series of mutagenesis studies [14-16]. At the same time, the three-dimensional (3D) structure of human Pfn1 has been solved through the use of both nuclear magnetic resonance (NMR) spectrometry and X-ray diffraction [1]. In general, Pfn1 folds into a single, compact globular domain that is bisected by an anti-parallel β-sheet (Figure 1) [17]. On one side both the amino (N)-terminal and carboxy (C)-terminal α-helices align roughly parallel to one another, while the other side is comprised of three smaller helices. A complex of Pfn1, G-actin, and polyproline peptide was also analyzed using X-ray diffraction by several groups [18, 19]. The polyproline peptide bound to Pfn1 between the N- and C-terminal helices and G-actin bound to Pfn1 on the opposite side showing specifically how Pfn1 could simultaneously interact with these two ligands. To date, no 3D structural analysis has been performed regarding the interaction of Pfn1 and phosphoinositides, but mutagenesis suggests the region of interaction overlaps both its G-actin and polyproline binding sites [15, 16].

Figure 1. *The Molecular Structure of Human Profilin-1*. The molecular structure of human Pfn1 as determined by multidimensional heteronuclear NMR spectroscopy [1]. The cartoon depicts both α-helices (red) and an anti-parallel β-sheet (yellow). The N-terminal and C-terminal α-helices are displayed at the top. The cartoon was generated using OpenAstex 3D Viewer.

1.2 PROFILIN-1-G-ACTIN INTERACTION: IMPACT ON THE DYNAMICS OF THE ACTIN CYTOSKELETON

Pfn1 was originally discovered in a complex with G-actin from echinoderm sperm that was termed profilactin (short for "profilamentous" or unpolymerized actin) [11]. As such, Pfn1 was unknowingly one of the first actin-binding proteins isolated [2]. Our understanding of the specific effect of Pfn1 on the actin cytoskeleton has evolved over time through numerous experiments and is still somewhat of a controversial subject. Though Pfn1 has several known

binding partners, the impact of its interaction with G-actin on the actin cytoskeleton has by far been the most thoroughly studied. To understand the context in which the role of the Pfn1-G-actin interaction, and Pfn1 in general, is currently defined, the model of actin polymerization must first be introduced.

1.2.1 Actin Polymerization

Purified G-actin that has been extracted from cells will spontaneously polymerize in solutions containing salt [20]. Under these conditions it was determined that, kinetically, the self-assembly can be segregated into three main phases: nucleation, elongation, and steady state.

Initially, unstable trimers of actin molecules will slowly form and act as nuclei from which filaments can grow [21-23]. Indeed, spiking a polymerization-competent solution with increasing concentrations of cross-linked actin nuclei significantly and proportionally reduced the time needed to reach steady state without affecting final filament length [24]. This implicates nucleation as the major rate-limiting step in spontaneous actin polymerization.

Filaments will then elongate bi-directionally [25]. There are two mechanisms by which we understand an actin filament can grow, though they are not mutually exclusive. The first mechanism is called exchange diffusion [26, 27]. In cells, G-actin is found almost exclusively bound to adenosine-5'-triphosphate (ATP) while filaments are largely composed of adenosine-5'-diphosphate (ADP)-bound actin monomers. As a result, it was originally thought that a hydrolysis reaction accompanied filament incorporation; however, further study revealed a lag between incorporation and conversion to ADP [26, 28, 29]. Radioactive labeling permitted the establishment of both ATP-bound and phosphate-bound ADP (ADP-Pi)-bound filament monomer intermediates upon ATP-G-actin incorporation into a growing filament [28]. Exchange

diffusion is a manner of growth where ATP-G-actin associates at either end of the filament and ATP-G-actin, ADP-Pi-bound G-actin (ADP-Pi-G-actin), and ADP-bound G-actin (ADP-G-actin) dissociate from the same end. Although ADP-Pi-G-actin and ADP-G-actin have begun to or have undergone nucleotide hydrolysis, once dissociated they are capable of nucleotide exchange [30]. This newly replenished ATP-G-actin, or previously established ATP-G-actin, can then be recycled back to the same end from which it dissociated.

Monomer incorporation would then be a function of the kinetic on- and off-rates for each nucleotide state. ATP-G-actin is generally readily incorporated where the conversion to an ADP-Pi-bound subunit is very fast. The completion of the hydrolysis reaction, resulting in an ADP-bound subunit, is relatively slow. ADP-bound filament monomers incorporated in this way are more stable than their ATP-bound counterparts and lack the capacity to regenerate ATP [30, 31]. In a condition in which both ends of the growing actin filament exhibited equal kinetic behavior, net polymerization or depolymerization in both directions would be equal; however, this is not the case. Hydrolysis of ATP-G-actin was observed to occur primarily on one end of the filament, called the barbed (or (+)) end [32]. Because hydrolysis of these subunits is both random and fast, exchange diffusion would suggest that a greater concentration of ATP-bound filament monomers are found at the barbed end. This phenomenon has been verified kinetically where the on-rate of ATP-G-actin at the barbed end was approximately 10-fold higher than that at the pointed (or (-)) end while off-rates were comparable [33, 34]. The critical concentrations of the filament ends – the concentrations of G-actin that are at equilibrium with either the barbed end (A_{CB}) or the pointed end (A_{CP}) respectively – are both functions of these kinetic values and are often used as characteristic quantities when defining actin filament growth. Due to the aforementioned differences in reaction kinetics, it is not surprising to find that A_{CB} and A_{CP} differ by 12-fold [35].

A concentration of G-actin above either A_{CB} or A_{CP} results in net association and growth at the respective end while lower G-actin concentrations result in net dissociation. Together, this means that if the concentration of available G-actin is maintained between A_{CB} and A_{CP}, polymerization will occur quickly at the barbed end while depolymerization will occur slowly at the pointed end.

These observations led to defining the other mechanism of filament growth, 'treadmilling' [26]. Though similar to exchange diffusion, in this case dissociated monomers are recycled exclusively from the pointed end to the barbed end rather than returning to the end from which they originally dissociated. Upon re-association at the barbed end, monomers move along the filament, undergoing ATP hydrolysis along the way. Confirmation of this in living cells came from Fluorescence Recovery After Photobleaching (FRAP) assays using fluorescent G-actin where recovery began at the membrane and progressed toward the cytoplasm [36]. Exchange diffusion and treadmilling are not mutually exclusive pathways and, in fact, both will occur simultaneously during filament elongation in cells.

Upon reaching steady state, when filament length no longer changes over time, the concentration of unpolymerized, unbound G-actin is typically referred to as the critical concentration (A_C). Based on biochemical analyses, the concentration of free, ATP-G-actin in cells is maintained at a value that kinetically yields no net growth or loss [37]. Additionally, polymerization as a function of only ATP-G-actin and filamentous (F)-actin results in treadmilling, or turnover, rates far slower than those observed *in vivo* [38]. Likewise, steady state is never reached *in vivo* as filament growth and destruction must be carefully and quickly regulated to promote actin-driven processes. As a result, the generation of actin filaments in cells likely involves co-factors and actin-binding proteins that alter critical concentration values. The rate of treadmilling is proportional to the difference between A_{CB} and A_{CP}, therefore any factor

that alters these values will impact filament turnover. Similarly, altering A_C could also play a role in filament turnover and length. Incidentally, critical concentration values can be influenced by several factors, most notably the association of G-actin with either ADP or ATP in its nucleotide binding site and the presence of certain actin-binding proteins.

1.2.2 Factors that Affect Critical Concentrations: Nucleotide Interaction

Although filament monomers are subjected to irreversible nucleotide hydrolysis, once dissociated they are capable of undergoing nucleotide exchange [30]. This cycle should provide the necessary supply of ATP-G-actin for re-incorporation at the barbed end, but it is theoretically possible to generate F-actin from pools of ADP-G-actin [33]. In this case, all three characteristic critical concentration values increased several-fold while the difference between A_{CB} and A_{CP} diminished meaning ADP-G-actin is less likely to be incorporated and treadmilling slows, but filaments are still present. It also suggests that nucleotide hydrolysis alone does not account for the marked difference in filament end kinetics and the innate structure of G-actin monomers can sufficiently yield polar filaments, though the difference is significantly less dramatic. Whether this is a physiologically relevant means of filament generation remains to be seen.

1.2.3 Factors that Affect Critical Concentrations: Profilin-1

Initial *in vitro* actin filament polymerization studies characterized Pfn1 as a G-actin-sequestration molecule that inhibited actin polymerization [39-41]. These conclusions were drawn from the fact that the presence of Pfn1 resulted in shorter filaments at steady state. Pure sequestration factors would reduce the pool of polymerization-competent G-actin while having

no impact on filament end dynamics, thus yielding shorter filaments. By the law of mass action, A_C would be independent of the presence of sequestration molecules; however, Pfn1 results in a well-documented reduction to A_C. Therefore, sequestration must be an incomplete explanation of Pfn1's impact of actin polymerization.

Pfn1 can also catalyze the nucleotide exchange of G-actin [42]. This would increase the ratio of ATP:ADP-G-actin and, because ATP-G-actin has a lower A_C than ADP-G-actin, the net result would be a pool of G-actin with an overall lower A_C. This catalytic capacity, however, does not likely contribute because nucleotide exchange is not rate-limiting in the absence of Pfn1 and plant Pfns that lack this capability reduce A_C as expected [43, 44].

Further analysis of Pfn1's role in actin polymerization revealed that the Pfn1-G-actin complex could interact with the barbed end and, following Pfn1 dissociation, the actin monomer incorporated into the filament [45-49]. This was proven to be the case for both ATP-G-actin and ADP-G-actin; however, Pfn1 fails to reduce A_C in pools of ADP-G-actin without the presence of ATP [50-52]. Therefore, the capacity of the Pfn1-G-actin complex to add to the barbed end alone does not sufficiently detail the reason for Pfn1's overall reduction of A_C, and the cause likely involves the hydrolysis of the G-actin-conjugated ATP.

In the presence of only ATP-G-actin, filaments grow mainly at the barbed end such that ATP-G-actin is incorporated and then converted to an ADP-bound monomer following a lag period. The presence of Pfn1 introduces a new population of ATP-G-actin that interacts with the barbed end with an association rate constant that is nearly indistinguishable from ATP-G-actin alone [47, 52]. The subsequent requirement of Pfn1 dissociation from its bound actin monomer to promote filament incorporation has been found to be mechanistically linked to ATP hydrolysis [48, 53]. Both ATP-G-actin and Pfn1-bound ATP-G-actin participate in filament growth in the

presence of Pfn1, but if the free energy change differed, one pathway would be favored. This energy imbalance is thought to be the cause of the observed reduction in A_C as Pfn1-mediated filament growth is slightly more energetically favorable. To this effect, two theories have been developed to explain the mechanistic link between ATP hydrolysis and Pfn1 dissociation.

The first and probably most widely-accepted theory involves the direct coupling of Pfn1-driven barbed end elongation to ATP hydrolysis [50]. This theory largely comes from the fact that Pfn1 displays a dramatically lower binding affinity for ADP-G-actin than ATP-G-actin [50, 54]. In this case, a Pfn1-ATP-G-actin complex will interact with the barbed end where it will remain until ATP hydrolysis results in Pfn1 release due to reduced affinity. This is supported by the fact that barbed end growth in the presence of high concentrations of Pfn1-ATP-G-actin was limited by the rate of ATP hydrolysis [51, 54].

The more recent theory involves an indirect coupling pathway [53]. In this case, the ATP hydrolysis of a specific monomer is not a requirement for Pfn1 dissociation. This theory relies on exchange diffusion as the mechanism of filament growth. In general, Pfn1 can increase the rate of exchange diffusion by acting as pump that concentrates ATP-G-actin at the barbed end. This arises from the fact that Pfn1-bound ATP-G-actin can only be incorporated at the barbed end as it can't interact with the pointed end [47]. Pfn1 adds monomer in the same fashion as before, but the increased ATP-G-actin presence, incorporation, and hydrolysis leads to higher energy filaments that can provide the energy for dissociation. This mechanism is therefore Pfn1-dependent, but does not require Pfn1 dissociation to be directly coupled to a specific hydrolysis event. Many aspects of this theory are still being developed as it is still in its infancy. It is important to note, though, that thermodynamic analyses supported the legitimacy of both models with regard to Pfn1-mediated reduction of A_C [44].

In addition, in agreement with the same thermodynamic study, Pfn1 is thought to decrease A_{CB} as a result of the slightly energetically favorable incorporation of Pfn1-bound ATP-G-actin compared to that of unbound ATP-G-actin. This would increase the difference between A_{CB} and A_{CP} leading to greater turnover. In fact, *in vitro* F-actin polymerization experiments have verified Pfn1, while causing filament length to be relatively shorter at steady state, does indeed increase the rate of turnover [43]. Both of these effects are in line with Pfn1 decreasing A_C and A_{CB}.

1.2.4 Profilin-1 Works in Tandem with Other Factors to Promote Elongation and Turnover

Besides Pfn1, a number of other factors can impact critical concentration values. These proteins have a synergistic effect when combined with Pfn1 in solution to either further enhance turnover or elongation. Though there are many actin-binding proteins, those that have been thoroughly studied in combination with Pfn1 include Actin Depolymerizing Factor (ADF)/cofilin-1, Thymosin-β4, and Capping Protein (Actin Filament) Muscle Z-Line (CapZ).

ADF/cofilin-1 (cofilin), as its name would suggest, induces the rapid depolymerization of F-actin *in vitro* [55]. Much like Pfn1, the exact activity of cofilin in actin polymerization is controversial with its role constantly evolving with new findings. Cofilin preferentially binds both ADP-G-actin and ADP-bound filament monomers compared to their ATP-bound counterparts [56]. This interaction allows it to play a role in the kinetics of filament growth in an end-specific manner, much like Pfn1. In general, it is thought cofilin interacts with ADP-bound filament monomers at the pointed end and induces their dissociation. This characteristic alone would dramatically increase A_{CP}, and although A_C is also increased, the difference between A_{CB}

and A_{CP} would be such that the rate of treadmilling would increase. Though cofilin has more recently been shown to participate in filament severing at low concentrations and filament stabilization at higher concentrations, filament disassembly is likely its primary role at physiological concentrations [57]. Cofilin, then, primarily acts to increase A_{CP} in cells. Though not necessarily always additive, when combined with the capacity for Pfn1 to reduce both A_C and A_{CB}, cofilin and Pfn1 work synergistically to increase filament turnover to rates that approach those observed in cells [58].

Actin sequestration molecules play an important role in the ability of cells to rapidly produce filaments. The concentration of G-actin in resting cells is between 600- and 1200-fold higher than A_C [59, 60]. A large portion of this, then, would need to be made polymerization-incompetent to prevent spontaneous filament assembly. While there are conditions under which Pfn1 might act as a sequestration factor, Pfn1-associated G-actin levels cannot account for the observed neo-F-actin content in stimulated cells [61-63]. Other G-actin-sequestering molecules, such as Thymosin-β4, contribute to a greater extent [42, 64]. Consequently, the total G-actin pool sequestered by Thymosin-β4 is enough to describe the increase in F-actin content in stimulated platelets [65]. Though intracellular concentrations of this protein widely vary depending on the cell type, it is generally found in much larger quantities than Pfn1 [66]. G-actin bound to Thymosin-β4 cannot participate in either nucleation or elongation. Though pure sequestration factors would have no effect on A_C, Thymosin-β4 lowers A_C in a concentration-dependent fashion [67]. This suggests behavior that affects the energetics of actin polymerization that has not been explored. Though not obvious from their individual effects on the characteristic critical concentration values, Thymosin-β4 and Pfn1 can work synergistically to increase turnover. Mechanistically, it is thought Thymosin-β4 further decreases A_C by creating a pool of G-actin

from which Pfn1, now at a higher concentration relative to polymerization-competent G-actin, can continuously draw [50]. Kinetically this is a far more complicated case that may or may not involve ternary complexes. In general, however, by combining Thymosin-β4 and Pfn1 polymerization rates of F-actin approached the membrane velocity of fish keratocytes [47, 50, 68].

CapZ is the most abundant barbed end capping protein in human cells [38]. Though there are pointed end capping proteins, such as tropomodulin, the specific relevance of pointed end polymerization is not known. Therefore the general term 'capping proteins' typically refers exclusively to barbed end capping proteins and shall so be here. In terms of actin polymerization, capping proteins have a number of functions, not the least of which is there propensity to associate with the barbed end, preventing elongation. They have also been shown to be involved in nucleation and regulating Z-disk content in muscle cells [69]. With regard to their capacity to regulate barbed end growth, the presence of capping proteins increases A_C in a concentration-dependent manner [70, 71]. While this should theoretically slow overall turnover and result in shorter filaments, the side effect would be a dramatic increase in the elongation rate of uncapped filaments. This phenomenon is enhanced by the presence of Pfn1 acting to lower A_C [72]. Here the synergism is limited to enhancing the turnover of select filaments; however, the polymerization rates of even those uncapped filaments do not compare to those found in cells [71]. This, however, becomes an interesting mechanism by which cells can regulate the growth of specific filaments.

Pfn1 is generally considered a promoter of actin polymerization, but the current understanding of its capacity in this role requires that it bind G-actin. As of yet, there is no model of a G-actin-independent means by which Pfn1 can promote actin polymerization. Given this,

however, less than 20% of triton-soluble Pfn1 was found in complex with G-actin among several tested mammalian cell lines [73]. Interestingly, microinjection of actin nuclei and G-actin into quiescent epithelial cells resulted in filaments composed exclusively of exogenous actin [74, 75]. This suggests cells do not maintain large quantities of polymerization-competent Pfn1-G-actin complex. There are likely further regulatory steps that have yet to be described behind which a pool of polymerization-incompetent G-actin is kept until properly released. In addition, this shows unregulated actin polymerization is probably not a realistic pathway by which filaments are generated *in vivo*. Therefore, nucleation and elongation are most likely a function of other actin-binding proteins that are subject to more stringent regulation. This does not, however, diminish the roles of the proteins above as their activities in manipulating critical concentration values is still the key force that drives filament production by these nucleation and elongation factors. Pfn1 actually cooperates with a number of these actin-binding proteins to enhance their activity by providing polymerization-competent G-actin in much the same way as it promotes barbed end elongation.

1.3 PROFILIN-1-POLYPROLINE INTERACTION: IMPACT ON THE ACTIN CYTOSKELETON

Both Pfn1 and Pfn1-G-actin complexes can be purified using polyproline affinity chromatography [12, 76]. This property was known for nearly a decade before Vasodilator-Stimulated Phosphoprotein (VASP) was identified to bind Pfn1 through a polyproline-mediated interaction [77]. Because of Pfn1's relevance with regard to the actin cytoskeleton, a number of other actin-binding proteins with polyproline stretches were investigated. Currently known

interacting partners include Neuronal-Wiskott-Aldrich Syndrome Protein (N-WASP), WASP family Verprolin-homologous protein (WAVE), WASP Interacting Protein (WIP), VASP, Mammalian Enabled (Mena), Enabled/VASP-Like (EVL), Diaphanous homologs, Formin-Like 1 (FMNL1), palladin, Rap1-GTP-Interacting Adaptor Molecule (RIAM), and ALL1-Fused Gene From Chromosome 6 (AF6) [78-84]. A number of these proteins directly enhance the polymerization of F-actin by nucleating new filaments or promoting barbed end elongation.

In addition to its more classical role with regard to the actin cytoskeleton, Pfn1 interacts with the polyproline regions of a number of other factors involved in a myriad of cellular processes. Pfn1 has been shown to interact with proteins involved in cell-trafficking – Valosin Containing Protein (VCP), Clathrin, Huntingtin, and Annexin 1 [8, 85, 86]. Synaptic scaffolding proteins have also been found to be ligands – Gephyrin, Drebrin, Aczonin, and Delphin [87-89]. Finally, Pfn1 interacts with several nuclear factors – Exportin 6, Survival Motor Neuron Protein (SMN), and Myb-Related Transcription Factor, Partner Of Profilin (p42POP) [90-92]. While the physiological relevance of many of these factors has not yet been investigated, it is clear that Pfn1-polyproline interaction may be imperative in a number of vital signaling cascades.

Peptide-based analyses suggest Pfn1 requires at least six consecutive proline residues, and more likely between eight and ten residues, for efficient binding; however, many of the known ligands lack a sequence with this number [93, 94]. Investigation of the polyproline stretches of the proteins with which Pfn1 is known to interact reveals five uninterrupted proline residues is typical, but there is no consensus and a variety of lengths are found [95]. Based on the sequence of its polyproline stretch, VASP could be eluted from Pfn1 by a peptide comprised of three repeats of glycine (G) followed by five prolines (P) – $(GP_5)_3$ – showing five prolines was sufficient, but affinity was low [77]. A different site on VASP contains a stretch of prolines

separated by an alanine (A) and a leucine (L) – (GPPPAPPLP) – for which Pfn1 has a far greater affinity [18]. Together, there does not appear to be a defined polyproline sequence that Pfn1 binds, but rather other proximal residues and 3D conformation are probably also determinants.

1.3.1 Actin Nucleation Factors

Nuclei composed of a trimer of G-actin are unstable and their spontaneous formation far too slow to allow a cell to readily adapt and respond to stimuli. To this effect, several factors have been discovered that greatly enhance the speed at which surfaces capable of supporting elongation are generated.

The Actin-related protein 2/3 (Arp2/3) complex was the first molecule identified that could initiate new filament polymerization. When combined with a Nucleation Promoting Factor (NPF) such as WASP or WAVE family proteins, the Arp2/3 complex is activated promoting the polymerization of a daughter filament oriented at a 70^{o} angle relative to the growth of the mother filament [96, 97]. It is thought that the Arp2/3-NPF complex presents Arp2 and Arp3 in a conformation that mimics an actin dimer and is able to recruit at least a single G-actin molecule [98]. Further, while Arp2/3 does not interact with Pfn1, activation is greatly enhanced through the recruitment of Pfn1-G-actin complexes by WASP and WAVE. Arp2/3-mediated nucleation and branching is often referred to as dendritic branching and is typically associated with lamellipodial protrusion. Filaments nucleated in this fashion can only grow at the barbed end because they remain capped at the pointed end by Arp2/3.

Formins are another class of nucleating factors. Unlike Arp2/3-mediated nucleation, there is no requirement of a pre-existing filament. The Formin Homology Domain 2 (FH2) domain found in formins is both required and sufficient to promote actin filament nucleation [99]. This

means that, while necessary for formin function in other aspects of cytoskeletal dynamics that will be discussed later, Pfn1 does not play a role in formin-mediated nucleation. Though not completely understood, the mechanism by which formins nucleate filaments is related to actin dimer stabilization [100]. While Arp2/3 acts as a pointed end capping protein, formins cap the barbed end and protect it from inhibitory capping proteins such as CapZ. However, unlike many other capping proteins, formins do not prevent barbed end elongation and instead appear to 'walk' along the growing filament as they actually promote the association of G-actin [101]. Though classically associated with the formation of stress fibers, formins are found abundantly at the leading edge of motile cells [102]. Diaphanous-related formins appear to be highly activated at the leading edge of membrane ruffles and protrusions suggesting this pathway of nucleation may be responsible for a number of the observed filaments in a protruding lamellipodium [103, 104]. In direct support of this, electron tomography revealed that the actin mesh commonly observed in the lamellipodial region is not necessarily comprised of a high population of branched actin filaments but rather is densely populated by unbranched filaments with a high degree of overlap [105]. Comparative studies attempting to discern the supposed mutually exclusive roles of formin- and Arp2/3-mediated nucleation, due to the differences in post-elongation filament structure, have revealed both pathways are vital to proper lamellipodial protrusion and filopodial initiation and growth [106, 107].

Spire is a more recently discovered actin nucleation factor. Spire contains four sequential WASP-Homology 2 (WH2) domains, a G-actin-binding domain also found in a number of other actin-binding proteins, separated by short linking sequences [108]. Analysis using electron microscopy revealed that G-actin associated with Spire aligns approximately linearly. *In vitro* analyses showed nucleation by this factor proceeded at a rate similar to formins but generally

slower than Arp2/3. Indeed, over-expression of Spire resulted in Arp2/3-independent actin filament formation in mammalian cells [109]. Like Arp2/3 and formins, Spire appears to remain associated with the end of the growing filament, but there is evidence of association with both the barbed and pointed ends [110]. The proteins Cordon bleu (Cobl) and Leiomodin (Lmod) seem to nucleate actin filaments in a similar fashion, though each has only three actin-binding domains [111, 112]. None of these factors are known to interact with Pfn1.

1.3.2 Actin Elongation Factors

An abundant presence of inhibitory capping proteins *in vivo* makes it unlikely that most filaments grow freely at their barbed ends unless those capping proteins have been somehow inactivated locally [113]. Therefore, factors that can both protect barbed ends from capping protein inhibition and promote polymerization are probably responsible for most positive intracellular filament growth. To date, both formins and the Enabled/VASP (Ena/VASP) family of proteins have been identified as such factors.

As previously described, formins not only have the capacity to nucleate filaments, but will remain associated and continue to promote barbed end growth. Adjacent to the FH2 domain required for nucleation, the Formin Homology Domain 1 (FH1) can interact with Pfn1-G-actin complexes creating a locally available pool of polymerization-competent G-actin, though the mechanism of addition remains elusive [114]. The presence of both the FH1 domain and Pfn1 are required of formin-mediated elongation. Formins have been shown to increase the rate of elongation by as much as 5-fold relative to the growth of a free barbed end, but there is a high degree of variability among the classified formins [115].

Like formins, the Ena/VASP family of proteins can remain associated with a growing barbed end and promote its elongation [116, 117]. These proteins can also interact with Pfn1-G-actin complexes to create a local pool of utilizable G-actin, but this is not a requirement as it is with formins [18, 118]. Investigation of its role in the protection of the growing barbed end suggested VASP must be tethered to a substrate and clustered to elicit its effect [119]. In this light, Ena/VASP proteins are known to be capable of forming tetramers and, at least for short periods of growth, these complexes can protect barbed ends from capping proteins [120]. Likewise, Ena/VASP proteins can be recruited to the membrane of the growing lamellipodial edge by Lamellipodin (Lpd) where they are thought to be most active [121]. Although more modest than some formins, human VASP was found to increase the rate of filament elongation by as much as 2-fold over that of free barbed ends [119].

1.3.3 Profilin-1 Enhances the Activity of Some Actin-Binding Proteins through Polyproline Interaction

Although a number of techniques that assess the rate of actin polymerization have been developed, the use of certain mobile bacteria, such as *listeria monocytogenes* (*listeria*) and *shigella*, or beads coated with a specific factor of study, all of which utilize the native or some designated set of cytoskeletal components, has been common practice. Though the physiological relevance of such systems is not clear, they provide a somewhat high-throughput means of delineating how sets of factors cooperate in promoting actin polymerization. Minimalistic *in vitro* studies utilizing these tools have shown only Pfn1, cofilin, capping proteins, and Arp2/3 are required to produce polymerization speeds comparable to observed cell speeds [122]. Further study into the mechanism by which such a pool of actin-binding proteins could effectively

polymerize F-actin determined that these bacteria were coated with the protein ActA, a noted NPF with structural similarity to WASP [123]. It is therefore not surprising that WASP-coated beads also produced similar results in the same solution [124]. This has also been extended to the use of formin-coated beads. In this case, minimalistic studies showed only Pfn1 and cofilin were required to induce speeds that were much quicker than those of Arp2/3-mediated WASP-coated beads [125]. Pfn1 therefore appears to be an essential cog in both of the canonical, seemingly mutually exclusive pathways through which F-actin structures are produced; however, these findings do not define the impact of the Pfn1-polyproline interaction as its G-actin binding capacity alone, when in the presence of cofilin, can result in greatly enhanced filament turnover, a far more important property in *listeria* propulsion than filament length [58]. Because Pfn1 can interact with G-actin and polyproline simultaneously, the specific relevance of Pfn1-polyproline interaction can be studied by mutagenesis [14].

Interestingly, both a lack of Pfn1 and the presence of a Pfn1 that lacks polyproline binding-capacity are detrimental to the propulsion of *listeria*, suggesting an important role for this interaction [126-128]. The mobility of WASP-coated beads is increased by the presence of Pfn1 and, following depletion, could not be rescued by a polyproline binding-deficient mutant of Pfn1 [129]. Similarly, Pfn1 that lacked the capacity to bind to the formins found in yeast, a system commonly used to study formins because of their essential role in cytokinesis, whether because of mutation or interspecies incompatibility, led to deficiencies in cytokinesis due to diminished actin polymerization [100, 130]. In addition to WASP and formins, Pfn1 also enhances the capabilities of the elongation factor VASP. While not required for basal movement, VASP presents asymmetric surface association and has been found to be necessary for efficient, directional *listeria* propulsion [131, 132]. Further analysis revealed VASP required Pfn1

interaction to promote enhanced *listeria* motility [133]. This can be partially explained by the fact that VASP maximally enhanced the rate of barbed end elongation in the presence of polyproline binding-competent Pfn1 [120]. In motile breast cancer cells, Fluorescence Resonance Energy Transfer (FRET) analysis showed that Pfn1-VASP interaction is most highly concentrated in the membrane ruffles at the leading edge [134]. These data suggest Pfn1 promotes the polymerization of actin in cells through its interaction with other actin-binding proteins.

1.4 PROFILIN-1-PHOSPHOINOSITIDE INTERACTION: IMPACT ON THE ACTIN CYTOSKELETON

Pfn1 was first shown to interact with phosphatidylinositol-4,5-bisphosphate ($PI(4,5)P_2$) using lipid micelles in solution [13]. The first evidence of phosphoinositide interaction *in vivo* came from the observation of a population of Pfn1 that was localized at the membrane in regions with no discernible actin structures, but whether this was a result of $PI(4,5)P_2$ interaction is not known [135]. Further examination revealed Pfn1 has a greater affinity *in vitro* for phosphoinositides with a phosphate at the D3 position of the inositol ring – phosphatidylinositol-3,4-bisphosphate ($PI(3,4)P_2$) and phosphatidylinositol-3,4,5-triphosphate (PIP_3); however, $PI(4,5)P_2$ is the most abundant phosphoinositide, so it is likely that Pfn1 binds to the cell membrane predominantly through interaction with $PI(4,5)P_2$ even if its affinity is lower [136, 137]. Additionally, whether these affinities are relevant to true interaction *in vivo* has not been determined.

Compared to both actin and polyproline interactions, far less is known about the physiological relevance of Pfn1's interaction with membrane phosphoinositides. One attempt at understanding its impact used high-resolution imaging to visualize Pfn1 on the surface of $PI(4,5)P_2$ micelles, where Pfn1 interaction resulted in $PI(4,5)P_2$ aggregation and overall membrane instability [138]. A more recent study determined Pfn1 could play a G-actin binding-independent role in cell motility through its phosphoinositide binding-capacity by inhibiting the production of $PI(3,4)P_2$. It was theorized this was a result of blocking $PI(4,5)P_2$ metabolism, but specific evidence of this sequestration phenomenon remains elusive [139, 140]. This, in turn, led to the down-regulation of VASP localization to the membrane causing a general inhibition of membrane protrusion and reduced cell migration [141]. A number of other actin-binding proteins interact with phosphoinositides including cofilin and WASP as well as the cytoskeletal regulatory proteins, the Rho family of small GTPases (Rho GTPases), and these interactions are imperative to their function [142, 143]. Likewise, differential levels of these lipids correlate with cell polarization as a consequence of directed actin polymerization [144]. Therefore, Pfn1-phosphoinositide interaction is not likely benign and requires further investigation.

1.5 CELL MIGRATION AND THE ACTIN CYTOSKELETON

Most of our understanding of cell migration comes from two-dimensional (2D) single-cell motility time-lapse imaging. The results of such assays have led to a well-characterized series of steps which have been found to be both highly reproducible and universal among a variety of cell types. While the cytoskeleton is commonly segregated into three components – actin microfilaments, intermediate filaments, and microtubules – actin microfilaments, or the actin

cytoskeleton, are the most dynamic element allowing the cell to readily adapt to both chemical and mechanical stimuli by contributing to cell morphology and permitting motor protein-independent locomotion [38]. Accordingly, cell movement correlates with marked change in the actin cytoskeleton, where a mobile cell has extremely rapid and directed polymerization and turnover [37]. The cell will first polarize, defined by a 'front' and 'rear' correlating with differential protein localization and expression. At the front, or leading edge, F-actin formation and polymerization in the lamellipodium pushes the membrane forward creating an underlying large, flat region called a lamella [145]. Additionally, filopodia are long, finger-like projections that often arise from a sub-population of the F-actin growth in lamellipodia and likely play a role in environmental exploration [146]. Adhesions form and mature on the new surface providing a strong anchor for the final step – rear retraction resulting from actomyosin contraction and weakened rear adhesion. The sum of these events provides a net displacement in the desired direction. Therefore, cell migration is very much a function of proper cytoskeletal organization as well as the capacity of the cell to regulate the polymerization and depolymerization of structures in a coordinated manner.

1.5.1 Molecular Regulation of the Actin Cytoskeleton and Cell Migration

While there are a myriad of factors known to participate in the regulation of the actin cytoskeleton, the most thoroughly characterized and seemingly universal moderators of actin cytoskeletal dynamics are the Rho GTPases, [147]. They are thought to mediate polarization, protrusion, and the formation of focal adhesions and stress fibers by activating a series of protein kinases as well as a variety of actin-binding proteins, including elongation and nucleating factors. This implicates them in nearly every aspect of cell movement. Rho GTPases themselves require

the presence of various phosphoinositides and therefore are spatially regulated by their metabolism, one mechanism linking extracellular signaling to site-specific actin polymerization [148, 149]. In agreement with this hypothesis, it was determined that differential phosphoinositide levels correlated with cell polarization and directed cell movement [144]. The three most studied Rho GTPases remain among those first discovered: Ras homology family member A (RhoA), Ras-related C3 botulinum toxin substrate 1 (Rac1), and cell division control 42 (cdc42).

RhoA is often associated with long, unbranched actin filaments [150]. In its most classically defined role, RhoA was found to be imperative in cell retraction during migration, presumably through stress fiber formation and regulation [151]. While not typically associated with lamellipodial growth, it has been suggested RhoA is not only active at the growing front but temporally supersedes the activity of both Rac1 and cdc42 [152]. Regardless of the location, RhoA mediates the activity of formins. Upon activation downstream RhoA, formins not only have the capacity to facilitate actin filament nucleation by stabilizing actin dimers but can also remain perpetually associated promoting filament elongation [100, 125, 153]. There is evidence that formins play a role in both lamellipodial protrusion and filopodial extension, but the isoforms thus far studied in this context can also be activated downstream both Rac1 and cdc42 [154]. In addition, RhoA activates Rho-associated coiled-Coil Kinase-1 (ROCK1) which can in turn activate LIM Domain Kinases (LIMKs), kinases that phosphorylate and deactivate cofilin [155]. Through this pathway, it has been theorized that RhoA acts to limit destructive protrusive activity and promote persistent movement [156]. Therefore, RhoA can both positively and negatively regulate lamellipodial development, likely as a function of other factors and time.

In neutrophils, a common cell type in migration studies PIP_3 accumulation on the plasma membrane corresponds with directed actin polymerization. This was found to occur because it led to the activation of Rac1, a Rho GTPase often associated with the formation of dense, highly-branched actin networks and lamellipodial protrusions [150, 157-159]. This type of actin structure is most commonly associated with the activation of N-WASP, a ubiquitous member of the WASP family of proteins that is activated downstream Rac1 [160]. In some cell types, N-WASP has been shown to be indispensable in cell migration [161]. This, in turn, provides a platform on which Arp2/3 can bind and be activated, nucleating a new actin filament [162]. According to the temporal relationship established in the only study to simultaneously investigate RhoA, Rac1, and cdc42, Rac1 acts to stabilize RhoA-mediated membrane protrusion [152]. In fact, Rac1 and RhoA exhibit mutual inhibition of one another [163, 164]. This antagonism parallels the different actin structures each factor promotes.

Constitutively active cdc42 induces the production of numerous filopodia [165]. Much like Rac1, cdc42 has been shown to induce the activity of WASP; however subsequent inhibition of the WASP family proteins did not prevent filopodial formation [166]. It was later determined that the formin Diaphanous-Related Formin 3 (mDia2) can also be activated by cdc42 and is imperative to cdc42-mediated filopodial extension [167]. In addition, cdc42 does indeed play a role in lamellipodial protrusion. In fact, cdc42 can itself activate Rac1, where cdc42-null cells often exhibit reduced Rac1 activity [168, 169]. In agreement with the fact that filopodia often play a sensory role, cdc42 has been found to be imperative in chemotaxis, or movement along a chemical gradient, and directed cell migration in several cell types [170].

1.5.2 Transcriptional Regulation of the Actin Cytoskeleton and Cell Migration

Serum response factor (SRF) is a transcription factor that acts downstream RhoA in a G-actin-dependent manner and has been shown to be important in the transcriptional regulation of a number of factors involved in the regulation of the actin cytoskeleton [171]. Some of the relevant target genes include actin, Arp3, Pfn1, Mena, ADF, cofilin, and gelsolin [172]. As expected, SRF knockout mouse models exhibited impaired embryogenesis at the gastrulation stage highlighted by a complete lack of a mesoderm, presumably from reduced cell migratory capacity [173]. Similarly, conditional SRF knockout in the mouse forebrain resulted in deficiencies in neuronal migration [174]. In both cases, a significant decrease in F-actin content was observed, illustrating the imperative role of the actin cytoskeleton and its regulation to understanding the process of cell migration.

1.5.3 Impact of Profilin-1 Expression on Cell Migration

Based on its relevance with regard to the actin cytoskeleton, it stands to reason that Pfn1 expression would have a significant impact on cell migration. Previous analysis of the impact of Pfn1 on actin polymerization both with and without the presence of other actin-binding proteins revealed Pfn1 increases the rate of F-actin elongation and turnover. To this end, a variety of depletion studies have implicated Pfn1 as a positive regulator of cell migration. Chronologically, the first study assessing its influence showed Pfn1 expression was required for proper F-actin formation in *Dictyostelium discoideum* (soil-living amoeba), impacting both cytokinesis and motility [175]. This significance was also observed in the migratory processes involved in the development of a variety of higher-order, multi-cellular organisms. Deletion of chickadee, a Pfn1

homolog, in *Drosophila melangaster* (fruit fly) resulted in a number of defects downstream malformation of the actin cytoskeleton and deficiencies in the migration of some cell types [176]. In *Strongylocentrotus purpuratus* (purple sea urchin), mesenchymal cells undergoing migration and morphological change during gastrulation exhibited dramatically increased Pfn1 expression [177]. By corollary, it was found that Pfn1 activity downstream Daam1, a formin homolog, in *Xenopus* (African clawed frogs) was required for blastopore closure [178]. Similarly, an antisense morpholino oligonucleotide for Pfn1 impaired cell movement during gastrulation in zebrafish [179]. As for mice, several studies have shown Pfn1 knockout models are not viable and typically arrest at the two-cell stage; however, conditional knockout in the brain permits sufficient development for study [7]. It was determined that radial migration of cerebellar granule neurons during brain development required the expression of Pfn1 and in general, mice with brain-specific knockout of Pfn1 exhibited defects typical of impaired neuronal migration [180].

Though the previous studies uniformly confirm Pfn1 as a positive regulator of cell migration, its role in human cells is not as clear. Expression is actually down-regulated in a number of invasive adenocarcinomas [181-184]. Further study using metastatic breast cancer cell lines revealed Pfn1 expression was inversely correlated with a number of actin cytoskeleton-mediated activities, including cell migration [185, 186]. Interestingly, this phenomenon was also observed with non-cancerous mammary epithelial cells. Conversely, knockdown of Pfn1 in endothelial cells reduced random motility in both 2D and 3D settings and was characterized as having reduced protrusion velocity [187, 188]. Taken together, Pfn1 plays a role in cell migration and is important for a variety of processes, but there is not likely a universal definition for the impact of Pfn1 on cell migration.

1.6 ANGIOGENESIS REQUIRES CELL MIGRATION

Angiogenesis describes the formation of new capillary vessels from outgrowths of the pre-existing vascular network. It has been shown to be important in many pathological and physiological events including wound-healing and tumor progression [189]. In contrast, vasculogenesis describes the *de novo* formation of the vasculature in developing animals; however, most late-development and postnatal vascular remodeling and repair proceeds through the angiogenesis cascade [190]. Endothelial cells are basally quiescent where homeostasis is maintained through low levels of autocrine Vascular Endothelial Growth Factor-A (VEGF-A) [191]. Sprouting angiogenesis is initiated by comparatively high levels of pro-angiogenic factors, including VEGF-A and VEGF-C, leading to the activation of certain endothelial cells, known as 'tip' cells. Delta-like-4-Notch1 signaling suppresses the propensity of the tip cell phenotype in adjacent endothelial cells, preventing mass activation and promoting a higher level of control of vessel sprouting [192, 193]. The insult to these cells promotes loss of cell-cell barrier function and activation of Matrix Metalloproteinases (MMPs) that degrade the basement membrane and extracellular matrix (ECM) permitting invasion along a cytokine gradient [194-196]. As the sprout progresses, underlying 'stalk' cells dynamically compete for the lead position resulting in a high degree of cellular rearrangement [197]. Tip cells are characterized by the presence of long, thin directional actin-mediated protrusions known as filopodia that permit the assessment of various attractive and repulsive cues and ultimately guide growth [198, 199]. Similar to the axonal growth cone during the development of the nervous system, filopodia also facilitate tip cell-tip cell contact, supporting their essential role in tip cell function [200]. Finally, upon inter-sprout contact, the tip cell phenotype is suppressed and pericytes are recruited, promoting anastamosis [194-196, 201, 202].

Many of the understood steps in sprouting angiogenesis require proper cell migration and morphogenesis. Pro-angiogenic factors, such as VEGF-A, are known to promote endothelial cell migration and invasion [203]. Conversely, many anti-angiogenic factors elicit their effect, at least partially, by inhibiting endothelial cell migration [204-206]. The relevant migratory mechanisms involved in angiogenesis involve a combination of chemotaxis, haptotaxis, and mechanotaxis [207, 208]. Chemotactic migration, or movement resulting from a chemical cue or gradient, in response to VEGF-A is linked to Rho GTPase activity downstream Vascular Endothelial Growth Factor Receptor 2 (VEGFR2). Several *in vitro* and *in vivo* studies have shown inhibition of Rho GTPases to be detrimental to angiogenesis [209-212]. Tip cell filopodia require cdc42 [199, 213]. Rac1 is implicated in endothelial cell lamellipodial development and is required for directed migration [214]. Finally, RhoA contributes to, among other things, the activation of PI3K in endothelial cells which mediates membrane-bound phosphoinositide content, key regulators of actin cytoskeletal dynamics and cellular polarization [215]. Accordingly, VEGF-A-mediated endothelial cell migration and morphogenesis requires SRF [216]. Endothelial cell-specific knockout of SRF was embryonic lethal at Embryonic day 14.5 (E14.5) due to severe subcutaneous hemorrhaging and decreased vascular density as a result of deficient cell migration; however, endothelial cell differentiation and early vascular morphogenesis were not affected, leading to the hypothesis that vasculogenesis may not be as harshly impacted [217]. Conditional knockout of SRF negatively impacted angiogenesis in both physiological and pathological contexts. Postnatal re-vascularization of the retina was significantly reduced while tumor-mediated angiogenesis was decreased leading to impaired tumor growth [218]. SRF is also paramount to tip cell filopodia formation, where deletion leads

to improper vessel connections, highlighting the importance of the regulation of the actin cytoskeleton throughout the cascade of events describing sprouting angiogenesis [217, 218].

Much less is known about the regulatory pathways involved in endothelial cell haptotactic migration, or movement along a gradient of ECM-conjugated chemoattractant or adhesion site concentration, and mechanotactic migration, or movement resulting from mechanical stimuli. Before an endothelial cell can invade, the underlying ECM must be degraded by MMPs. Depending on the material encountered, migration can be promoted independent of chemoattractants [219]. The physiological relevance of this, however, has yet to be elucidated. Mechanotaxis is presumably more important for larger vessels, but it has been shown even in the microcirculation, migratory endothelial cells orient their lamellipodia parallel to the direction of flow. Rho GTPases are also closely tied to mechanotransduction and their localization correlates with the forces experienced by the cell; however, they appear to have a greater impact on the microtubule network in this context [207].

1.6.1 Profilin-1 in Angiogenesis

Morphogenesis in the context of angiogenesis is taken to be the formation of tubes in both 2D and 3D environments. Because of the migratory aspects involved, it is not surprising that several actin regulatory proteins – gelsolin, VASP, and Pfn1 – are up-regulated during this process [220]. Further characterization revealed Pfn1 was required for proper cord- and tube-morphogenesis [187, 188]. On a single-cell basis, Pfn1 generally promotes the activity of the actin cytoskeleton in endothelial cells and is imperative for proper migration and proliferation. In order to promote such activity, it was determined Pfn1 must maintain both G-actin and polyproline binding capacity. Additionally, while the pathway is unclear, Pfn1 also reduced secretion of MMP2, a

type IV collagenase, ultimately negatively impacting ECM invasiveness [188]. ***These data would support Pfn1 as a positive regulator of angiogenesis, but the impact of Pfn1 on sprouting angiogenesis has not been addressed (Specific Aims 1 and 3).***

1.7 POST-TRANSLATIONAL MODIFICATION OF PROFILIN-1

Advances in post-translational modification detection and purification as well mass spectrometry have revealed Pfn1 is modified on a number of residues (See Table 1). These studies included a variety of cell lines and tissue samples to investigate the proteome downstream a diverse set of treatments and conditions. In nearly every case the proteome was purified by some means for the modification of interest. It is important to note that most of this data was collected within the last 5 years and the physiological relevance of a majority of these modifications has yet to be investigated.

Table 1. *Known Profilin-1 Post-Translational Modifications.* A list of established Pfn1 post-translational modifications with their sources. Modifications surrounded by parentheses represent post-translational modification found from *in vitro* sample or treatment. All other modifications represent post-translational modification established using mass spectrometry from tissue or cell sample. (* only found with *Mus musculus* Pfn1)

Residue	Modification	Function	Citation
Y6	Phosphorylation	Unknown	[221]
K37	Ubiquitination	Unknown	[222]
K53	Ubiquitination	Unknown	[222-228]
S56	Phosphorylation	Unknown	[229, 230]
S57	Phosphorylation	Unknown	[230]
Y59	Phosphorylation	Unknown	[231, 232]
K69	Ubiquitination	Unknown	[222, 225, 227, 228]
S84	Phosphorylation	Unknown	[233]
K90	Ubiquitination	Unknown	[222, 227]
S91	Phosphorylation	Unknown	[230, 232]
K104	Acetylation	Unknown	[234, 235]
K104	Ubiquitination	Unknown	[222, 225-227]
K107	Acetylation	Unknown	[235]
K107	Ubiquitination	Unknown	[222, 227]
T108	Phosphorylation	Unknown	[230]
K115*	Ubiquitination	Unknown	[228]
K125	Acetylation	Unknown	[235]
K125	Ubiquitination	Unknown	[222, 225, 227, 228]
K126*	Ubiquitination	Unknown	[228]
Y128	Phosphorylation	Increases Affinity for G-actin	[231, 232, 236-249]
S137	(Phosphorylation)	Affects ligand affinity	[250-252]
Y139	(Nitration)	Increases affinity for polyproline peptide and decreases affinity for G-actin	[253, 254]

1.7.1 Regulation of Profilin-1-Ligand Interaction

The first attempt to describe the regulation of Pfn1-ligand interaction came from the fact that the phosphoinositide binding region overlaps both its G-actin and polyproline binding sites. In this

light, Pfn1 was shown to block phospholipase C-γ1 (PLCγ1)-mediated hydrolysis of $PI(4,5)P_2$ *in vitro* unless PLCγ1 was modified with a tyrosine phosphorylation. This effect, in turn, was theorized to free Pfn1 to bind G-actin and polyproline and promote actin polymerization [12, 13, 255, 256]. $PI(4,5)P_2$ therefore acts to sequester Pfn1, effectively inhibiting its activity. This model has yet to be either confirmed or refuted, but further information regarding the regulation of Pfn1 has come from its propensity to be post-translationally modified. The first such evidence of this came from the *in vitro* phosphorylation of Pfn1 at Serine 137 (S137) by Protein Kinase C-ζ (PKCζ) in the presence of $PI(4,5)P_2$, and to a lesser extent with other D3 and D4 phosphoinositides [250-252]. Treatment with PKCζ resulted in increased Pfn1 association with G-actin and polyproline peptide *in vitro* while no effect was observed on Pfn1 association with $PI(4,5)P_2$ [257]. Similarly, Rho-associated coiled-Coil Kinase-1 (ROCK1) can also phosphorylate Pfn1on S137 *in vitro*; however, mutagenesis at S137 decreased Pfn1 association with polyproline [86]. While contradictory, it should be noted that neither mass spectrometry nor phospho-enrichment was performed during the discovery of S137 phosphorylation as they were unavailable at the time, so the presence of confounding post-translational modifications is possible. Since this initial finding, a number of post-translational modifications of Pfn1 have been detected using more advanced techniques (See Table 1). To date, only modification at Tyrosine 128 (Y128) has been investigated. With regard to Pfn1-ligand binding, phosphorylation at Y128 moderately increased G-actin binding without affecting polyproline interaction in endothelial cells [232]. Similarly, interaction with $PI(4,5)P_2$ micelles was also unchanged. ***No other effort has been made to clarify what regulatory pathways mediate these modifications or their downstream impact (Addressed in Specific Aims 2 and 3).***

1.8 HYPOTHESIS AND SPECIFIC AIMS

Through its interaction with G-actin and polyproline, Pfn1 promotes the polymerization of the actin cytoskeleton resulting in membrane protrusion and promoting cell motility [258]. These processes are integral in sprouting angiogenesis and so Pfn1 may be an important factor. In this regard, Pfn1 has been found to be up-regulated during tube morphogenesis and is required for endothelial cell migration and invasion [187, 188, 220]. Therefore, I hypothesized that *Pfn1 promotes sprouting angiogenesis*. In addition, Pfn1-ligand interaction has proven vital to its intracellular function in endothelial cells [188]. Along with the discovery of a number of post-translational modifications that have been implicated in regulating Pfn1-ligand binding-capacity, I hypothesized that *Pfn1's involvement in the regulation of the actin cytoskeleton is determined by its post-translational modification state*. Finally, because of the importance of the actin cytoskeleton in cell migration and angiogenesis, I postulated that ***Pfn1's regulation of the actin cytoskeletal dynamics of endothelial cells undergoing angiogenesis is governed by post-translational modification***. To test the overall hypothesis, I proposed the following aims:

Specific Aim 1: *To determine whether Pfn1 is required for sprouting angiogenesis*.

Specific Aim 2: *To determine whether Pfn1 is post-translationally modified in unstimulated cells and what regulatory pathways may be involved.*

Specific Aim 3: *To explore the impact of the determined regulatory pathway on Pfn1 and sprouting angiogenesis.*

The completion of these aims would advance our understanding of sprouting angiogenesis by not only confirming the previously implicated importance of Pfn1 but also

introducing a novel layer of regulation – via Pfn1 post-translational modification – that may act as a signaling link between various extracellular stimuli and actin cytoskeletal dynamics. Unregulated actin polymerization is not likely a realistic pathway by which filaments are generated *in vivo*. There are a series of regulatory steps, many of which probably have yet to be described, behind which a pool of polymerization-incompetent G-actin is kept until properly released. Significant effort has been put forth in defining how actin-binding proteins are regulated such that actin polymerization can occur in a predictable manner, but Pfn1 is often overlooked and simply thought to seamlessly facilitate the function of a variety of nucleation and elongation factors. This study will begin to elucidate the regulation of Pfn1 in the context of sprouting angiogenesis. Because of the direct impact Pfn1 has on the actin cytoskeleton, knowledge of how it can be controlled and manipulated might provide a means of globally inhibiting angiogenesis regardless of the stimulant. Many anti-angiogenic therapies fail because they only target a single or possibly several pro-angiogenic pathways. Pfn1 activity, however, may be a ubiquitous necessity in the capacity of these stimulants to promote angiogenesis and therefore becomes a target for general suppression.

2.0 MATERIALS AND METHODS

2.1 CELL CULTURE

An immortalized Human Microvascular Endothelial Cell line (HMEC-1) and Human Embryonic Kidney 293 (HEK-293) were used for all *in vitro* experiments. HMEC-1 were cultured in MCDB-131 (Life Technologies) growth medium [10% (v/v) FBS (Corning), 1 µg-mL^{-1} hydrocortisone (Sigma), 50 U-mL^{-1} Penicillin (Life Technologies), 50 µg-mL^{-1} Streptomycin (Life Technologies)] supplemented with 10 mM L-Glutamine (Life Technologies) and 1 ng-mL^{-1} EGF (Life Technologies). Cells were obtained at passage 18 and used between passages 20-30 for experimentation. HEK-293 were cultured in DMEM/F12 (1:1) (Life Technologies) growth medium [10% (v/v) FBS, 100 U-mL^{-1} Penicillin, 100 µg-mL^{-1} Streptomycin]. HEK-293 were maintained on culture dishes (Corning) coated with type I collagen (BD Biosciences) for all experiments.

2.2 ANTIBODIES AND REAGENTS

Antibodies used in this study included: Pfn1 polyclonal antibody (Abcam), α-Tubulin monoclonal antibody (Sigma), c-myc polyclonal antibody (Sigma), GFP monoclonal antibody (Clontech), GFP polyclonal antibody (Life Technologies), actin monoclonal antibody (BD

Biosciences), VASP monoclonal antibody (BD Biosciences), acetylated-lysine monoclonal antibody (Cell Signaling), pRRXS/T PKA Substrate monoclonal antibody (Cell Signaling), Anti-phosphotyrosine monoclonal antibody (BD Biosciences) HRP-conjugated goat anti-mouse Ig monoclonal antibody (BD Bioscience), Peroxidase-conjugated mouse anti-rabbit IgG monoclonal antibody (Jackson Immunoresearch). For immunoblotting, the following concentrations were used: Pfn1 (1:2500) and α-Tubulin (1:2000), c-myc (1:1000), GFP monoclonal (1:1000) actin (1:1000), VASP (1:1000), acetylated-lysine (1:500), pRRXS/T PKA Substrate (1:1000), Anti-phosphotyrosine (1:1000), HRP-conjugated goat anti-mouse Ig monoclonal antibody (1:1000), Peroxidase-conjugated mouse anti-rabbit IgG monoclonal antibody (1:1000). Forskolin (Sigma) and H89 (Sigma) were prepared according to manufacturer's instructions.

2.3 CONSTRUCTS

Mus musculus Pfn1 was cloned into pGEX-5X-1 (GE Healthcare) bacterial expression vector. Phospho-mimetic point mutations were made using the following primers: S57D (sense: 5'-GGCAAAGACCGGTCAGATTTTTTCGTC-3'), S89D (sense: 5'-GGATCTTCGTGACAAGAGCACCGG-3'), S91D (sense: 5'-CGTACCAAGGACACCGGAGGAG-3'), T92D (sense: 5'-CCAAGAGCGACGGAGGAGCC-3'). For expression in eukaryotic cells, myc-tagged *Mus musculus* Pfn1 was cloned into pIRES2-AcGFP1 (Clontech) bicistronic expression vector. Phospho-dead point mutations were made using the following primers: T89V (sense: 5'-GGATCTTCGTGTCAAGAGCACCGG-3'). For production of retrovirus, EGFP-tagged *Mus musculus* Pfn1 and Pfn1-H133S was cloned into

pQCXIP (Clontech) retroviral vector as previously described [188]. Phospho-dead and phospho-mimetic mutation was made using the following primers: S137A (sense: 5'-CTCACCTGCGGCGTGCCCAGTACTG-3'), S137E (sense: 5'-CTCACCTGCGGCGTGAACAGTACTG-3').

2.4 SIRNA TRANSFECTION

The single-target Pfn1 siRNA was previously described with sense strand 5'-AGAAGGUGUCCACGGUGGUUU-3' (Thermo Scientific) [187]. A smart pool of non-targeting control siRNA (Thermo Scientific) contains the following sense strands: 5'-GGCCAGAAAUGUUCGGUGAUU-3', 5'-GUGGUUUGAUCAACAAGAAUU-3', 5-CAAUGUCACUGUCACCAAGUU-3', and 5'-GGUGGAACGCCUACAUCGAUU-3'. Transfection was performed with DharmaFECT reagent 1 (Thermo Scientific) and appropriate buffer from the same source with 100 nM siRNA according to the manufacturer's instructions. Cells were incubated in siRNA-containing solution for 24 hours and washed several times where this time point is considered '24 hours after transfection'. Extent of knockdown was analyzed 72, 96, or 120 hours after transfection.

2.5 DNA TRANSFECTION

DNA transfection was performed using XtremeGENE HP transfection reagent (Roche) according to manufacturer's instructions. Cells were re-plated for experiment 24 hours after transfection. Proteins were assayed 48 hours after transfection.

2.6 PROTEIN EXTRACTION FOR WESTERN BLOT

Cells were washed twice with ice-cold DPBS (Lonza) and maintained on ice throughout the extraction process. Lysis Buffer [25 mM Tris (Fisher Scientific) pH 7.5, 150 mM NaCl (Fisher Scientific), 5% (v/v) Glyercol (Fisher Scientific), 1 mM EDTA (Fisher Scientific), 1% (v/v) NP-40 (Sigma)] was supplemented with 0.1% (w/v) SDS (Bio-Rad), 5 µg-mL^{-1} Leupeptin (Sigma), 10 µg-mL^{-1} Aprotinin (Sigma), 1 mM PMSF (Sigma), 5 µg-mL^{-1} Pepstatin (Sigma), 1 mM activated Sodium Vanadate (Sigma), and 50 mM Sodium Fluoride (Sigma). Cells were scraped in the presence of Lysis Buffer, collected into a microcentrifuge tube, and incubated on ice for 30 minutes. Lysates were spun at 13000 RPM for 30 minute at 4^{o}C. The protein concentration of the supernatant was measured using a coomassie-based protein assay kit (Bio-Rad) and aliquots stored at -80^{o}C for Western blot analysis.

2.7 WESTERN BLOT

Equal masses of protein were reduced by boiling for 5 minutes in the presence of 2-mercaptoethanol (Fisher Scientific). Proteins were loaded on 15% or 17% Tris-HCl polyacrylimide gels and SDS-PAGE carried out using the Mini-Protean Tetra Cell electrophoresis system (Bio-Rad) according to manufacturer's instructions. Gels were washed of SDS by equilibrating in Bjerrum and Schaefer-Nielsen Transfer Buffer [48 mM Tris pH 9.2, 39 mM Glycine (Bio-Rad), 20% (v/v) Methanol (Fisher Scientific)] for 15 minutes. Proteins were transferred onto Nitrocellulose paper (Bio-Rad) in the same Transfer Buffer using Bio-Rad's system. Membranes were washed in TBS [50 mM Tris pH 7.5, 150 mM NaCl] for 5 minutes and blocked with TBS containing 5% (w/v) non-fat dry milk (Carnation) for 1 hour at room temperature with mild agitation. Incubation with primary antibody was carried out overnight at 4^{o}C with mild agitation in TBST [50 mM Tris pH 7.5, 150 mM NaCl, 0.1% (v/v) Tween 20 (Bio-Rad)] containing 5% (w/v) non-fat dry milk. Membranes were washed extensively with TBST and incubated with appropriate HRP-conjugated secondary antibody in TBST containing 5% (w/v) non-fat dry milk. Another round of washing was performed before proteins were visualized with ECL Western Blotting Substrate (Thermo Scientific) using Kodak Imaging Device.

2.8 PROTEIN EXTRACTION FOR 2D ELECTROPHORESIS

Cells were washed twice with ice-cold DPBS followed by two washes with ice-cold Tris/Sucrose Buffer [10 mM Tris, 250 mM Sucrose (Invitrogen)] and maintained on ice throughout the

extraction process. Dishes were placed at oblique for 5 minutes to collect residual fluid. Cells were scraped in the presence of 2D Lysis Buffer [2 M Urea (Fisher Scientific), 7 M Thiourea (Invitrogen), 4% (w/v) CHAPS (Sigma), 50 mM DTT (Roche)] and collected into a Bead-beater tube (Biospec) containing 50 mg Glass Beads (Sigma). Lysates were pulsed 4 times for 20 seconds each in a Mini Beadbeater (Biospec) with 2 minutes on ice between pulses. 0.1 U Benzoase Nuclease (Sigma) and 2 mM $MgCl_2$ (Fisher Scientific) were then added and solution incubated on ice for 30 minutes. The lysates were collected into microcentrifuge tubes and subjected to 2 rounds of centrifugation. The first round was 3500 RPM for 5 minutes to separate glass beads, where the supernatant was then subjected to 13000 RPM for 20 minutes to remove debris. The protein concentration of the supernatant was measured using the RC DC Protein Assay Kit (Bio-Rad) and aliquots stored at -80^{o}C or immediately subjected to isoelectric focusing.

2.9 ISOELECTRIC FOCUSING AND EQUILIBRATION

Isoelectric focusing was performed using the Zoom IPGRunner System (Invitrogen) and carried out per manufacturer's instructions with modification. Equal masses of proteins were used to make Rehydration Buffer [final concentrations: 2 M Urea, 7 M Thiourea, 4% (w/v) CHAPS, 50 mM DTT, 0.5% (v/v) Carrier Ampholytes (Invitrogen), 0.005% (w/v) Bromophenol Blue (Fisher Scientific), 50-150 µg Proteins]. Rehydration buffer was loaded into a Zoom IPGRunner Cassette (Invitrogen) and incubated with ZOOM IPG Strips (Invitrogen) as recommended for 1 hour at room temperature. In all cases, the pH range of the Carrier Ampholytes and IPG Strip were identical. Greater than 95% of the rehydration buffer was taken up by the IPG strip. IPG

strips underwent isoelectric focusing using the following program: 175 V for 30 minutes; linear ramp 175-2000 V over 45 minutes; 2000 V for 45-105 minutes depending on pH range. IPG strips were then stored at -80^{o}C or immediately equilibrated. IPG strips were incubated with Equilibration Buffer [6 M Urea, 2% (w/v) SDS, 50 mM Tris pH 8.8, 20% (v/v) Glycerol, 2% (w/v) DTT] for 25 minutes at room temperature with gentle agitation. IPG strips were briefly washed with Running Buffer [25 mM Tris pH 8.3, 192 mM Glycine, 0.1% (w/v) SDS] and sealed on Tris-HCl polyacrylimide gels with Running Buffer containing 0.5% Agarose (Invitrogen) and 0.005% (w/v) Bromophenol Blue. These gels were subjected to Western blot as previously described.

2.10 TIME-LAPSE IMAGING

Cells were sparsely-plated (~150000) in a 6-well plate (Corning) either coated with type I collagen (Millipore) or untreated and incubated over night. Time-lapse imaging was carried out using an Olympus IX71 Inverted Microcope (Olympus) in a LiveCell Microscope Stage Incubator (Pathology Devices) to maintain temperature at 37^{o}C, CO_2 at 5%, and relative humidity at 80%. Images were collected for 120 minutes at a 1 minute time interval using MetaMorph (Universal Imaging). Cell location was assessed using the center-of-mass of the nucleus and tracked using ImageJ.

2.11 MOUSE AORTIC RING ANGIOGENESIS ASSAY

The aortic ring angiogenesis assay was performed according to the protocol described by Baker, et al. with modification [259]. Thoracic aortas of 9-11 week-old mice were isolated and cleaned of fatty tissue and branching vessels until a uniform white tube was observed. Following excision and throughout the cleaning process, aortas were maintained in ice-cold Opti-MEM (Life Technologies) and kept in this state for no more than 4 hours to maintain the health of the cells. Cold Opti-MEM was carefully injected into the lumen to flush out any residual blood. The cleaned aortas were cut evenly with a width of ~1 mm. If the aortic rings were to be subjected to siRNA treatment, the rings were collected and 15-20 rings placed into a single 24-well plate (Corning) well for each condition. Transfection was carried out as described with appropriate volumes for a 24-well plate well per the manufacturer's instructions and rings treated for 24 hours at 37^{o}C. Aortic rings that did not undergo siRNA treatment were immediately embedded. Aortic rings were embedded in either 1 mg-mL^{-1} type I collagen diluted in DMEM (Life Technologies) or Growth Factor-Reduced Matrigel (BD Biosciences) in a 96-well plate (Corning). Matrices were polymerized by incubating at 37^{o}C for 45 minutes. Each well was supplemented with 150-µL Opti-MEM containing 2.5% (v/v) FBS and 30 ng-mL^{-1} VEGF-A 165 (Cell Signaling) and incubated for up to 96 hours at 37^{o}C. Sprouts were imaged 48, 72, and 96 hours following embedding.

2.12 IMMUNOFLUORESCENCE OF AORTIC RINGS

Immunofluorescent labeling of aortic rings was performed according to the protocol described by Baker, et al. with modification [259]. Aortic rings were washed once with DPBS and fixed using DPBS containing 3% (v/v) Formalin (Fisher Scientific) for 30 minutes at room temperature. The rings were then permeabilized by two consecutive treatments of DPBS containing 0.25% (v/v) Triton-X-100 (Fisher Scientific) for 15 minutes each at room temperature. Blocking was performed using DPBS containing 10% (v/v) Goat Serum (Sigma) for 1 hour at room temperature. To visualize Pfn1, aortic rings were incubated with DPBS containing 10% (v/v) Goat Serum and Pfn1 polyclonal antibody (1:200) overnight at 4^{o}C with mild agitation. The rings were then extensively washed with DPBS containing 0.1% (v/v) Triton-X-100. To visualize endothelial cells, 0.05 mg-mL^{-1} Rhodamine-conjugated Lectin (Sigma) was added to DPBS containing 10% (v/v) goat serum and Fluorescein (FITC)-conjugated Goat Anti-Rabbit (1:100; Jackson Immunoresearch) and incubated with the aortic rings for 2 hours at room temperature with mild agitation. This was followed by further washing and rinsing once with MilliQ water (Millipore). Fluorescence was viewed on an Olympus IX71 inverted microscope at a 4x magnification and imaged using MetaMorph.

2.13 GENERATION OF PROFILIN-1 CONDITIONAL KNOCKOUT ANIMALS

C57BL/6 genetic background mice that express Cre recombinase under the transcriptional control of the endothelial-specific receptor tyrosine kinase Tie2 (Tie2-Cre$^{+/-}$) were purchased from The Jackson Laboratory. These mice were crossed with C57BL/6 genetic background mice

with two copies of Pfn1 with loxP sequences flanking exon 1 ($Pfn1^{fl/fl}$) to create mice with endothelial-cell specific knockout of a single allele of Pfn1 ($Pfn1^{EC,+/-}$). Offspring were backcrossed with $Pfn1^{fl/fl}$ mice to create endothelial cell-specific Pfn1 knockout mice ($Pfn1^{EC,-/-}$). All animal experiments were performed in compliance with an approved protocol by the Institutional Animal Care Committee of the University of Pittsburgh.

2.14 GENOTYPING OF PROFILIN-1 CONDITIONAL KNOCKOUT ANIMALS

The genomic DNA of both the tails of pups and segments of aorta following sacrifice was extracted using a commercial kit (Promega). The presence of the loxP sequence was assessed using the following primers: (Primer 1; forward) 5'-TGGAGCGGATCCAGCGAAGG-3' and (Primer 2; reverse) 5'-GTCCCCAGCAGTCGGGACG-3'. The presence of Tie2-Cre was determined according to The Jackson Laboratory using the following primers: (Tie2-Cre; forward) 5'-GCGGTCTGGCAGTAAAAACTATC-3', (Tie2-Cre; reverse) 5'-GTGAAACAGCATTGCTGTCACTT-3', (PCR positive control; forward) 5'-CTAGGCCACAGAATTGAAAGATCT-3', and (PCR positive control; reverse) 5'-GTAGGTGGAAATTCTAGCATCATCC-3'. The recombinase activity of Cre was assessed using Primer 1 above and the following primer: (Primer 3; reverse) 5'-GGACACCAACCTCAGCTGGC-3'. All primers were purchased from IDT. Thermocycling was carried out using the StepOnePlus PCR Machine (Applied Biosciences) and performed according to recommendations from animal sources.

2.15 GENERATING ENDOTHELIAL CELL SPHEROIDS

750 HMEC-1 were suspended in MCDB-131growth medium containing 0.25% (w/v) methylcellulose (Sigma) and seeded into non-adherent round-bottom 96-well plates (Corning). The cells were allowed to aggregate for 24 hours at 37^{o}C.

2.16 ENDOTHELIAL SPHEROID SPROUTING ANGIOGENESIS ASSAY

In vitro sprouting angiogenesis of endothelial spheroids was assessed using a protocol described by Korff, T., et al. with modification [260, 261]. Collagen solution [1 mg-mL^{-1} type I collagen, 0.25% (w/v) methylcellulose] was made diluted in MCDB-131] and pH-adjusted using 5 N NaOH (approximately 1-µL-mL^{-1} solution). Spheroids were collected and mixed with the chilled collagen solution and 600-µL (typically containing 15-20 spheroids) was seeded into a pre-warmed 24-well plate (Corning). To permit complete polymerization, the gels were incubated at 37^{o}C for 1 hour. After polymerization, 500-µL of MCDB-131 growth medium was added to each well and incubated at 37^{o}C for 24 hours before analysis.

2.17 MASS SPECTROMETRY

Samples for mass spectrometric analysis were subjected to SDS-PAGE. The gels were washed 2 times with MilliQ water for 5 minutes each to remove SDS then stained with Coomassie Stain [0.1% (w/v) R250 (Fisher Scientific), 40% (v/v) Ethanol (Decon), 10% (v/v) Acetic Acid (Fisher

Scientific)]. Gels were destained using Destaining Solution [10% (v/v) Ethanol, 7.5% (v/v) Acetic Acid] until bands could be clearly discerned from background. The bands were excised with a sterile razor blade and placed in a microcentrifuge tube containing MilliQ water. These samples were delivered to the University of Pittsburgh Proteomics Facility for processing and analyzation. Gel bands were digested with trypsin and peptides were analyzed by nano reverse phase HPLC interfaced with an LTQ linear ion trap mass spectrometer. The tandem mass spectra (MS/MS) were analyzed by the SEQUEST search engine and identified peptides and proteins were further statistically validated with the Scaffold software. This project used the UPCI Cancer Biomarkers Facility that is supported in part by award P30CA047904.

2.18 IMMUNOPRECIPITATION

Cells were extracted and lysates prepared as described under the section Protein Extraction for Western Blot without SDS. Equal amount of protein were pre-cleared by constant mixing with 15-µL Protein G Plus/Protein A-conjugated Agarose Beads (Calbiochem) at 4^{o}C for 1 hour. Brief centrifugation was used to separate bead fraction and supernatant collected into pre-chill microcentrifuge tube. Lysates were incubated with 5 µg of appropriate antibody overnight at 4^{o}C with constant rotation. This was mixed with 50-µL Protein G Plus/Protein A-conjugated Agarose Beads and rotated at 4^{o}C for 2 hours. The beads were washed 3 times with Lysis Buffer and proteins eluted by boiling for 5 minutes in the presence of 2-mercaptoethanol. The eluate was directly loaded for SDS-PAGE and Western blot or stored at -80^{o}C.

2.19 GENERATION OF RETROVIRUS

Appropriate pQCXIP constructs and pVSVG (Clontech) were co-transfected into the packaging cell line GP2-293 (Clontech) as described. Cells were washed twice after 24 hours transfection and virus allowed to collect for following 48 hours. The conditioned media was collected and filtered through 0.45 µm Cellulose Acetate Filter (VWR) and used immediately for infection.

2.20 RETROVIRAL INFECTION AND CELL SELECTION

HMEC-1 were plated sub-confluently and treated with 4-mL retrovirus-containing conditioned medium in the presence of 2.5 µg-mL^{-1} Polybrene (Sigma) for 3 hours at 37^{o}C. MCDB-131 growth medium was then added to 10-mL and cell incubated 24 hours at 37^{o}C. This process was repeated once. Cells were washed several times with DPBS and allowed to recover in MCDB-131 growth medium for 24 hours. Cell selection was achieved using MCDB-131 growth medium containing 1 µg-mL^{-1} Puromycin (Sigma). Cells were selected until cell death subsided and maintained in MCDB-131 growth medium containing 0.25 µg-mL^{-1} Puromycin.

2.21 PHOSPHATASE TREATMENT

Cells were extracted and lysates prepared as described under the section Protein Extraction for Western Blot without SDS. Equal amounts of protein was aliquoted for each condition and supplemented with appropriate 10x buffer and 10x $MnCl_2$ and either MilliQ water or 1 U-ug^{-1} λ-

Protein Phosphatase (NEB). Samples were incubated at 30°C for 30 minutes. These samples were used to make Rehydration Buffer for 2D electrophoresis and subjected to isoelectric focusing. The presence of higher salt concentrations did not significantly affect focusing resolution.

2.22 PROTEIN EXPRESSION AND AFFINITY PURIFICATION

pGEX contructs were transformed into DH5α (Life Technologies) competent cells. Cells were grown at 37°C under constant agitation in the presence of antibiotics until the optical density at 600 nm was between 0.6 and 0.9. Cells were induced with 0.1 mM isopropyl-β-D-thiogalactopyranoside (IPTG) (Sigma) for 3 hours. Cells were lysed by sonication in the presence of Lysis Buffer containing bacterial protease inhibitors (Sigma). The lysates were allowed to incubate on ice for 30 minutes then centrifuged at 13000 RPM for 30 minutes. Supernatants were mixed with reconstituted Glutathione-Agarose Beads (Sigma) for 2 hours at 4°C with constant rotation. Beads were washed 5 times with Lysis Buffer and either underwent *in vitro* kinase treatment (See *In vitro* Kinase Assay section for further details) or incubated with lysates generated from HEK-293 as previously described overnight at 4°C with constant mixing. The beads were then washed 5 times with Lysis Buffer and proteins eluted by boiling for 5 minutes in the presence of 2-mercaptoethanol. The eluate was directly loaded for SDS-PAGE and Western blot or coomassie stain as previously described.

2.23 IN VITRO KINASE ASSAY

For GST-Pfn1, following washes with Lysis Buffer, beads were washed an additional 2 times with Kinase Buffer [20 mM BES (Sigma) pH 7, 20 mM EGTA (Fisher Scientific), 6 mM $MgCl_2$ (Fisher Scientific), 5 mM ATP (Sigma), 10 mM Phosphocreatine (Sigma), 1 mM DTT]. For His-Pfn1 (Cytoskeleton), 1.5 µg was added to Kinase Buffer for each treatment condition: with or without 0.5 U μL^{-1} Protein Kinase A (PKA) from bovine heart (Sigma). GST-Pfn1 beads were separated into three treatment groups: No treatment (maintained on ice) and with or without 0.5 U-μL^{-1} PKA. For the latter two groups, the GST-Pfn1 beads or His-Pfn1 was incubated at 30^{o}C for 1 hour with gentle mixing every 15 minutes. The reaction was stopped and proteins eluted by boiling for 5 minutes in the presence of 2-mercaptoethanol. Eluate was directly loaded for SDS-PAGE and Western blot of coomassie stain as previously described.

2.24 MULTIPLE SEQUENCE ALIGNMENT

Multiple sequence alignment was done using Clustal Omega (EMBL-EBI).

2.25 HOMOLOGY MODELING

A homology model of *Mus musculus* Pfn1 was created from a crystal structure of bovine Pfn1 bound to actin (PDB 2BTF). The model was created by manually performing the following mutations using Pymol: N9S, N41S, I49V, I100V, and M122L. All mutations could be

performed without introducing significant steric clashes. Additional Pfn1 models were created by mutating T89 to either valine or aspartic acid to mimic a phospho-dead and phosphorylated state. All simulations were performed with Amber version 12.3. The homology modules were solvated to form an octahedral water box that extends 12 Å beyond the protein. The system was neutralized with Na+ or Cl- ions. The system then underwent two rounds of minimization. A 100 ps equilibration run was performed with weak positional restraints on the protein during which the temperature was warmed from 0 K to 300 K. Simulations were performed using the particle mesh Ewald (PME) method with a nonbonded cutoff of 10 Å. Constant pressure periodic boundaries and isotropic position scaling were used to maintain a pressure of 1 atm. Langevin dynamics were used for temperature control. Simulations were performed at the Center for Simulation and Modeling using equipment funded through NSF Grant 12-29064. Three simulations of each model were run and every simulation was run for 144 hours, resulting in approximately 360ns of simulation per a run (an I/O error terminated the T89V simulation early) [Reproduced with the permission of Dr. David Koes, University of Pittsburgh (Collaborator)].

3.0 PROFILIN-1 IS REQUIRED FOR SPROUTING ANGIOGENESIS

3.1 INTRODUCTION

Cell migration requires the coordinated regulation of the actin cytoskeleton to produce membrane protrusion and rear retraction [38]. Pfn1, a G-actin-binding protein, participates in barbed end elongation and enhances the activity of other actin-binding proteins to promote actin polymerization [258]. Accordingly, a number of studies have implicated Pfn1 as being vital to cell migration in a variety of contexts [175-180]. Angiogenesis is the outgrowth of new vessels emerging from the existing vasculature and is critically dependent on endothelial cell invasion and migration [189]. It is therefore not surprising that Pfn1 has proven imperative to endothelial cell motility and morphology *in vitro* [187, 220]. Angiogenesis, however, is a more complex process that requires the coordinated actions of multiple cells that are dynamically regulated to invade and differentiate ultimately giving rise to a functional vessel. In this regard, Pfn1 has not been investigated in the context of endothelial cell undergoing sprouting angiogenesis.

3.2 RESULTS

3.2.1 Knockdown of Profilin-1 Reduces Endothelial Cell Motility on Multiple Substrates

The substrate on which or along which cells move plays a vital role in their behavior. Therefore assessing movement on relevant substrates will be necessary to begin to study the importance of Pfn1 in endothelial cells undergoing angiogenesis. Previous studies on the role of Pfn1 in general endothelial cell movement assessed single-cell random motility on plastic with no ECM component [187]. We first wanted to verify that the observed phenotype was not a function of the substrate on which the motility was assessed. Suppression of Pfn1 in HMEC-1, an immortalized microvascular endothelial cell line, was achieved by transiently transfecting a previously characterized single-target Pfn1 siRNA (Pfn1 siRNA) for the time indicated [187]. With this, greater than 95% knockdown of Pfn1 was achieved (Figure 2A). We seeded these cells on either plastic (untreated culture dishes) or collagen-coated dishes and assessed the average single-cell random 2D speed using nuclear tracking (Figure 2B). Pfn1 knockdown resulted in a 37% decrease in average cell speed on plastic, comparable to the previous report. Similarly, a 36% decrease in cell speed was observed on collagen substrate. Although there was a trend of lower overall speed for cells seeded on collagen, the decrease was not significant. These conditions, while limited to 2D analysis, indicate Pfn1 may play a general, yet vital, role in endothelial cell motility and therefore becomes an interesting potential target for regulating angiogenesis.

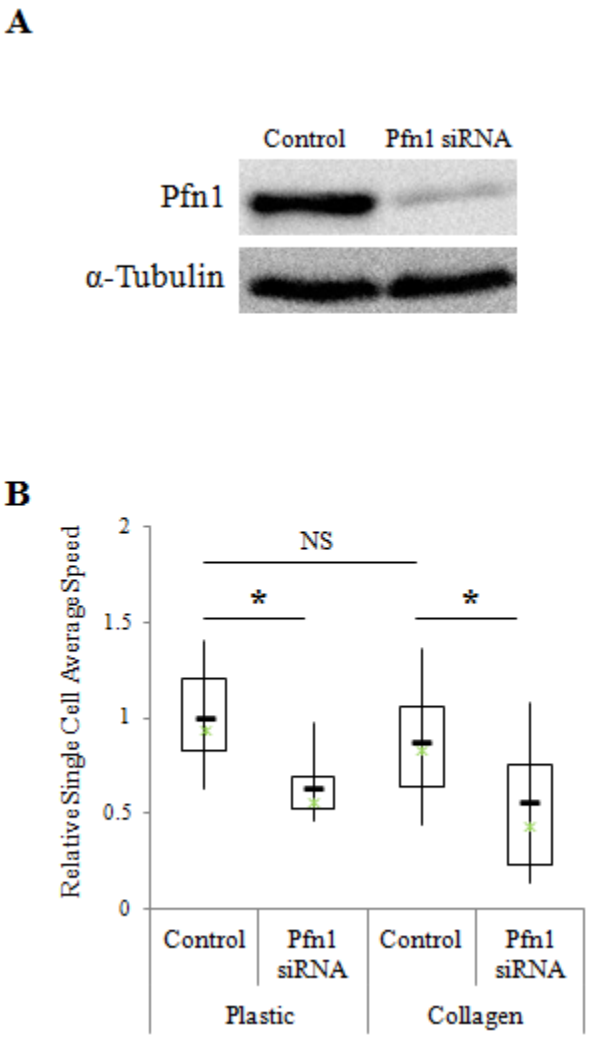

Figure 2. *Dependence of Profilin-1 siRNA-Mediated Reduction in HMEC-1 Motility on Substrate.*(A) Western blot showing suppression of Pfn1 expression in HMEC-1 treated with either smart pool non-target (Control) or single-target Pfn1 siRNA (Pfn1 siRNA) after 96 hours. (B) Box-and-whisker plots of the average cell speed of either Control or Pfn1 siRNA-treated HMEC-1 seeded on either an untreated cell culture dish (Plastic) or a collagen-coated dish (Collagen) normalized to the Control cells seeded on Plastic. The average speed of the Control cells on Plastic was 0.76 μm-min^{-1}. Time-lapse imaging was carried out 96 hours post-transfection after cells were incubated 24 hours on appropriate substrate. (* $p<0.001$; NS Not Significant)

3.2.2 Treatment with Profilin-1 siRNA Decreases Sprouting of Explanted Aortic Rings

Pfn1 has been implicated in some aspects of angiogenesis, but no study has directly explored its importance in neo-vessel sprouting [187, 188]. In this regard, we adopted the *ex vivo* mouse aortic ring assay to assess the overall impact of Pfn1 on sprouting angiogenesis [259, 262]. Aortic rings derived from three female FVB background mice were first treated with either Control or Pfn1 siRNA. These rings were subsequently embedded in collagen containing no serum and incubated with medium containing 2.5% FBS and 30 ng-mL^{-1} VEGF-A for 96 hours. Representative images for both Control and Pfn1 siRNA-treated rings following the 120 hour protocol are shown in Figure 3A. For Pfn1 siRNA-treated rings, the number of sprouts counted using phase contrast microscopy was significantly reduced at all time points (Figure 3B). The counts for the numbers of sprouts at the final time point were verified using an endothelial cell-specific lectin stain (Figure 3C-D). The decrease in the number of sprouts for Pfn1 siRNA-treated rings was found to be equally significant, where the counts using phase contrast microscopy were slightly conservative for both groups.

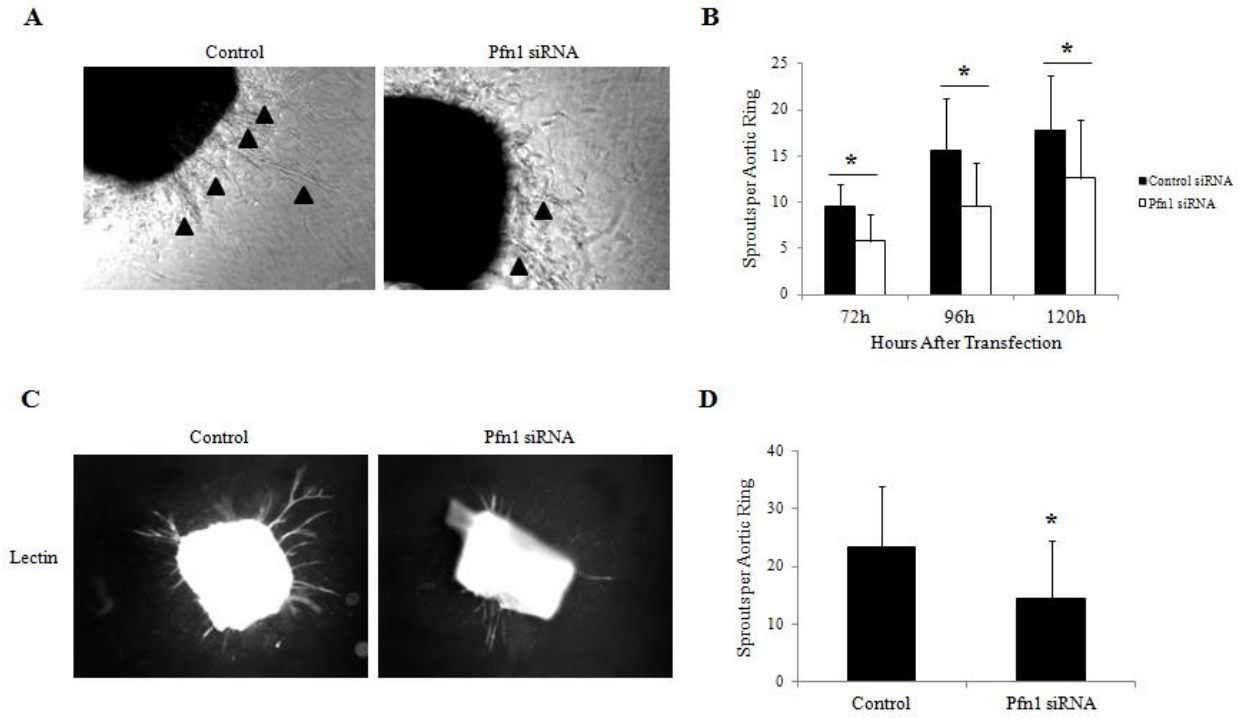

Figure 3. *Effect of Profilin-1 siRNA Treatment on Aortic Ring Sprouting Angiogenesis.* (A) Representative images of Control or Pfn1 siRNA-treated aortic rings cultured for 96 hours following 24 hours transfection. Arrows indicate sprouts that were counted in respective images (B) The number of sprouts was quantified using phase contrast microscopy 72, 96, and 120 hours after beginning transfection. (C) Representative images of Control or Pfn1 siRNA-treated aortic rings at the final time point stained with fluorescent-tagged lectin. (D) The number of sprouts was quantified, verifying the accuracy of the previous counts. (* $p<0.05$)

3.2.3 Sprouts Exhibiting Attenuated Profilin-1 Expression Appear Normal

Interestingly, there were a number of sprouts originating from aortic rings treated with Pfn1 siRNA that displayed global suppression of Pfn1 expression. That is, while individual sprouts likely contain multiple cells, the expression of Pfn1 was either comparable to the sprouts from the control-treated aortic rings or relatively low throughout the entire sprout. The Pfn1

expression of individual sprouts was determined using immunofluorescence (Figure 4A). Sprouts from aortic rings treated with Pfn1 siRNA were segregated as either having nearly unobservable levels of Pfn1 (Low Pfn1) or not (Avg Pfn1) and representative images of sprouts from each group are shown in Figure 4B. The ratio of sprouts designated as Low Pfn1 or Avg Pfn1 for both Control and Pfn1 siRNA-treated aortic rings is shown in Figure 4C. Treatment with control siRNA did not yield any sprouts that could be defined as having Low Pfn1. Of the sprouts that grew from Pfn1 siRNA-treated aortic rings, approximately 35% exhibited almost complete loss of Pfn1. This ratio can also be used as a crude measure of the efficacy of the siRNA treatment in attenuating Pfn1 expression in the *ex-vivo* system. Analysis of the properties of the individual sprouts between the segregated groups indicated that neither the length, as measured from the edge of the aortic ring to the end of the sprout, nor the frequency of bifurcation, as bifurcations per sprout, were not statistically different (Figure 4D-E).

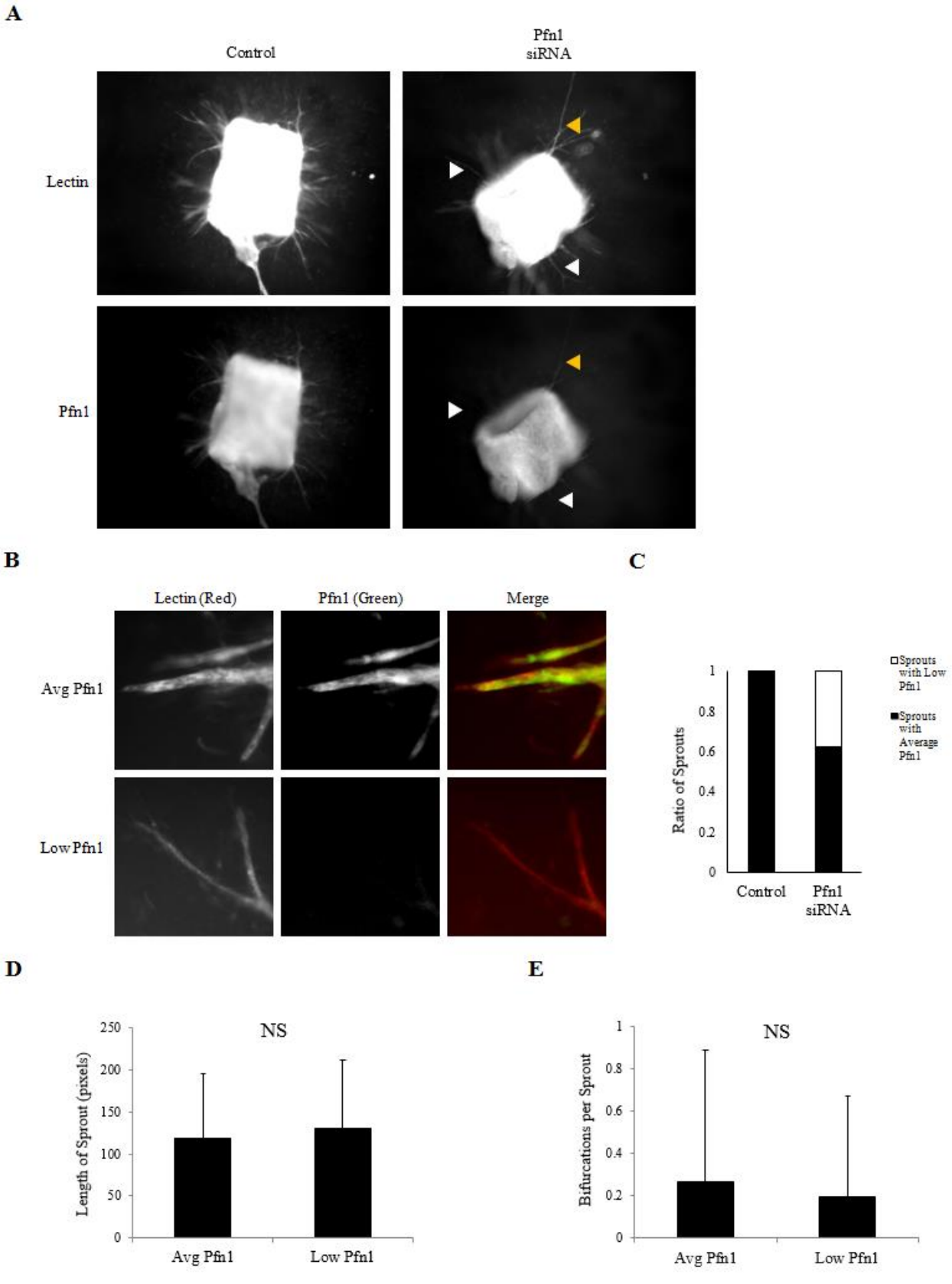
A
Control
Pfn1 siRNA
Lectin
Pfn1
B
Lectin (Red)
Pfn1 (Green)
Merge
Avg Pfn1
Low Pfn1
C
Ratio of Sprouts
1
0.8
0.6
0.4
0.2
0
Control
Pfn1 siRNA
Sprouts with Low Pfn1
Sprouts with Average Pfn1
D
NS
Length of Sprout (pixels)
250
200
150
100
50
0
Avg Pfn1
Low Pfn1
E
NS
Bifurcations per Sprout
1
0.8
0.6
0.4
0.2
0
Avg Pfn1
Low Pfn1

Figure 4. *End-point Analysis of Sprouts with Contrasting Profilin-1 Expression Levels.* (A) Representative images of Control or Pfn1 siRNA-treated aortic rings at the final time point stained for lectin and Pfn1. The yellow arrow indicates a sprout defined as having visible levels of Pfn1 (Avg Pfn1) while white arrows indicate sprouts designated as having low levels of Pfn1 (Low Pfn1). (B) Representative images of sprouts defined as having either Low Pfn1 or not Avg Pfn1. Aortic rings were stained with fluorescent-tagged lectin (red) and Pfn1 (green) and co-localization observed (Merge). (C) The number of sprouts in each of the Avg Pfn1 and Low Pfn1 groups were counted and displayed as a portion of 100% as a measure of the extent of knockdown. (D) The lengths of the sprouts between the two groups were compared. (E) The number of bifurcations per sprout was compared between groups. (NS Not Significant)

3.2.4 Endothelial Cell-Specific Profilin-1 Knockout Mice are Not Viable

While the prior experiments indicate Pfn1 is a factor that is generally important in angiogenic sprouting, the specific impact of Pfn1 on endothelial cells was not addressed due to the presence of a number of other cell types that were subjected to the same siRNA treatments. To look more specifically at the importance of Pfn1 in endothelial cells during sprouting angiogenesis, we attempted to create an endothelial cell-specific knockout mouse model. Using a Cre-loxP system for conditional knockout of specific genes, we mated $Pfn1^{fl/fl}$ mice (See Figure 5A) with Tie2-$Cre^{+/-}$ mice. Cre successfully removed the first exon creating $Pfn1^{EC,+/-}$ mice (See Figure 5B for typical genotying results). $Pfn1^{EC,+/-}$ mice were born at the expected frequency (See Table 2) and did not exhibit any obvious deficiencies compared to their $Pfn1^{EC,+/+}$ littermates.

To generate $Pfn1^{EC,-/-}$ mice, $Pfn1^{EC,+/-}$ mice were backcrossed with $Pfn1^{fl/fl}$ mice and the resulting genotype frequencies illustrated in Table 3. No $Pfn1^{EC,-/-}$ mice were born and using a binomial distribution, we found that the frequency is highly significant meaning this is not likely

a random occurance. Therefore, endothelial cell-specific knockout of Pfn1 is a lethal genotype, further implicating its importance in endothelial cell function.

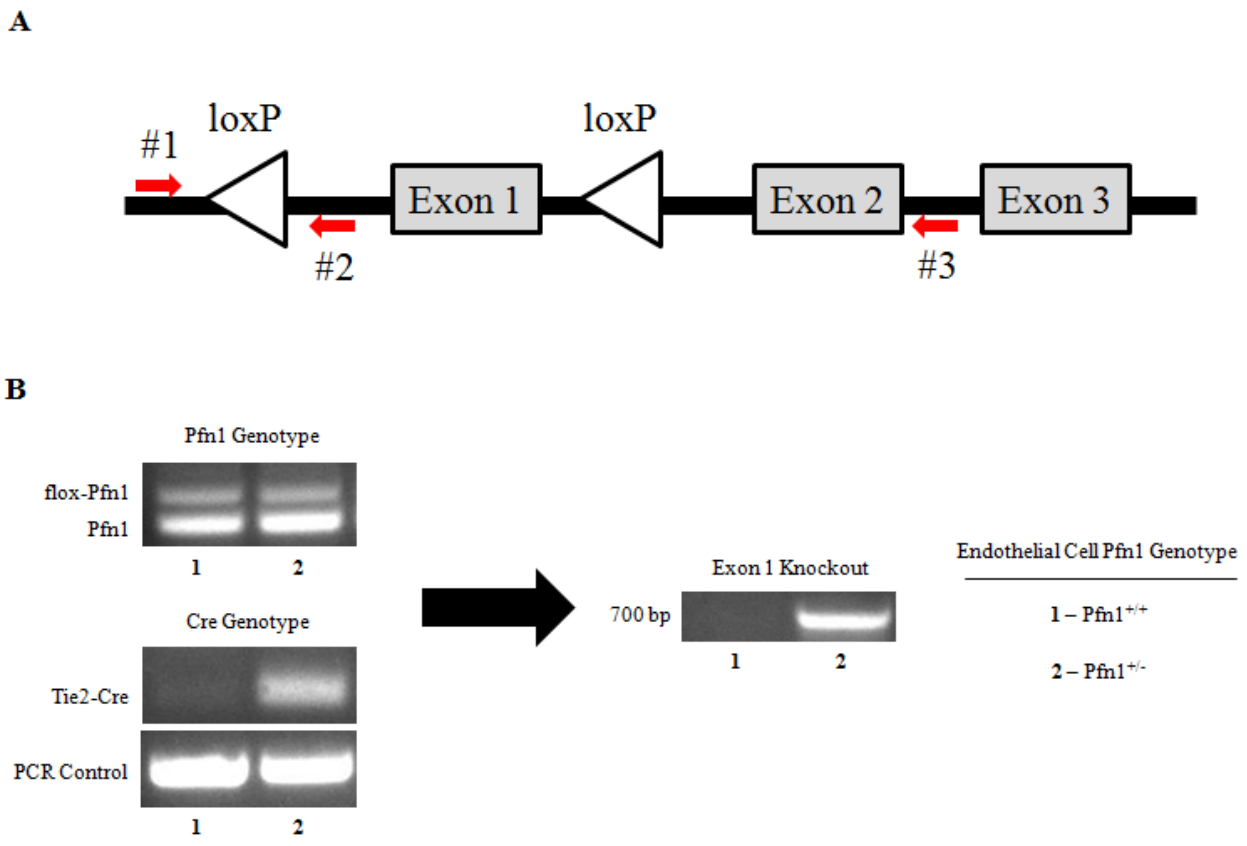

Figure 5. *Creation of an Endothelial-Specific Heterozygous Profilin-1 Mouse Model.* (A) A representation of the Pfn1 gene with loxP sequences and the locations of the primers used for genotyping. (B) Representative genotyping results. PCR conducted with Primer 1 and Primer 2 reveals the Pfn1 genotype. The lower molecular weight band (240 bp) is the wild-type allele while the higher molecular weight band (340 bp) is a Pfn1 allele containing the loxP sequence. The presence of Tie2-Cre was assessed using a single set of primers along with a set of PCR positive control primers. The activity of Cre was assessed using a PCR conducted with Primer 1 and Primer 3 where a 700 bp band is present when the first exon has been deleted.

Table 2. *Genotype Frequency for the Creation of* $Pfn1^{EC,+,-}$. A summary of the genotypes of the pups generated under the breeding scheme to create heterozygous mice comparing actual frequency to theoretical frequency. $Pfn1^{EC,+/+}$ (* any mouse that is Tie2-$Cre^{-/-}$ is considered $Pfn1^{EC,+/+}$) and $Pfn1^{EC,+/-}$ were generated as expected.

Breeding Scheme: $Pfn1^{fl/fl}$ X $Pfn1^{+/+}$/Tie2-$Cre^{+/-}$

Litter No.	Pups	$Pfn1^{EC,+/+}$ *	$Pfn1^{EC,+/-}$	$Pfn1^{EC,-/-}$
1	4	1	3	0
2	7	3	4	0
3	10	6	4	0
Total	21	10	11	0
%		48%	52%	0%
Theoretical%		50%	50%	0%

Table 3. *Genotype Frequency for Creation of* $Pfn1^{EC,-/-}$. A summary of the genotypes of the pups generated under the breeding scheme to create knockout mice comparing actual frequency to theoretical frequency. $Pfn1^{EC,+/+}$ (* any mouse that is Tie2-$Cre^{-/-}$ is considered $Pfn1^{EC,+/+}$) and $Pfn1^{EC,+/-}$ were generated as expected while no $Pfn1^{EC,-/-}$ were born. (** $p<0.005$)

Breeding Scheme: $Pfn1^{fl/fl}$ X $Pfn1^{fl/+}$/Tie2-$Cre^{+/-}$

Litter No.	Pups	$Pfn1^{EC,+/+}$ *	$Pfn1^{EC,+/-}$	$Pfn1^{EC,-/-}$
1	7	5	2	0
2	1	1	0	0
3	7	7	0	0
4	4	0	4	0
5	4	3	1	0
Total	23	16	7	0**
%		70%	30%	0%
Theoretical%		50%	25%	25%

3.2.5 Heterozygous Knockout of Profilin-1 in Endothelial Cells Delays Sprouting Angiogenesis in Matrigel

Although $Pfn1^{EC,-/-}$ mice could not be generated, the aortas from $Pfn1^{EC,+/-}$ and their $Pfn1^{EC,+/+}$ littermates were isolated and prepared as previously described to begin to address the specific importance of Pfn1 in endothelial cells undergoing sprouting angiogenesis. Aortic rings were embedded in growth factor-reduced matrigel and incubated with medium containing 2.5% FBS and 30 ng-mL^{-1} VEGF-A for 96 hours. The sprouts were counted using phase contrast microscopy at the time points indicated. Representative images of the 72 hour time point of sprouts from aortic rings of $Pfn1^{EC,+/-}$ and $Pfn1^{EC,+/+}$ mice are shown in Figure 6A. Compared to collagen, sprouts formed in matrigel are generally shorter and more cord-like. Similarly, the sprouts are more unstable and began to dissipate between 96 and 120 hours; however, no difference in rate of decay was observed between sprouts originating from $Pfn1^{EC,+/-}$ and $Pfn1^{EC,+/+}$ aortic rings. $Pfn1^{EC,+/-}$ aortic rings exhibited a delay in sprouting as there was a significant decrease in the number of sprouts at 72 hours, but at 96 hours, the time of maximum sprouting, there was no statistical difference (Figure 6B). Aortic rings from these mice were also embedded in collagen using the same setup. Representative images of the resulting sprouting are shown in Figure 6C. Unlike matrigel, embedding in collagen did not yield a significant difference at any time point with the results at the final stage shown in Figure 6D. It is possible that there is a substrate-dependent effect or endothelial cell-specific heterozygous knockout of Pfn1 is simply not sufficient to produce a deficiency in sprouting.

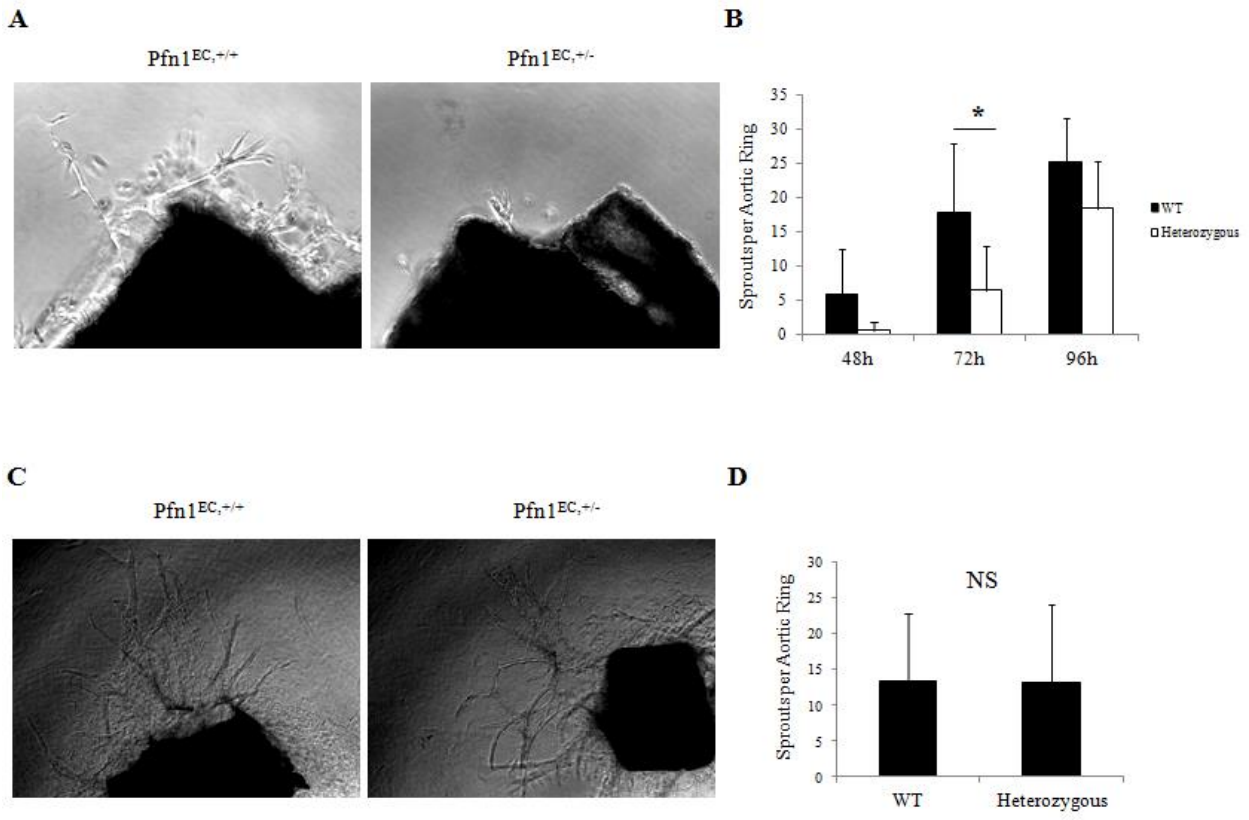

Figure 6. *Effect of Pfn1$^{EC,+/-}$ Genotype on Aortic Ring Sprouting Angiogenesis.* (A) Representative images of Pfn1$^{EC,+/-}$ and Pfn1$^{EC,+/+}$ aortic rings embedded in matrigel and incubated for 72 hours. (B) Quantification of the number of sprouts using phase contrast microscopy after 48, 72, and 96 hours. (C) Representative images of Pfn1$^{EC,+/-}$ and Pfn1$^{EC,+/+}$ aortic rings embedded in collagen and incubated for 96 hours. (D) Quantification of the number of sprouts using phase contrast microscopy after 96 hours. (* $p<0.05$; NS Not Significant)

3.2.6 Attenuation of Profilin-1 is Detrimental to Endothelial Cell Spheroid Sprouting

Endothelial cell-specific Pfn1 knockout mice could not be generated nor was endothelial cell-specific heterozygous knockout of Pfn1 sufficient for reproducing the suppression of sprouting angiogenesis observed for the initial siRNA-mediated knockdown model. While it is certainly possible Pfn1 attenuation had a more significant impact on other cell types resulting in the lower

sprout count, the vital role Pfn1 plays in general endothelial cell movement begs for further analysis. Therefore, to gain an understanding of the importance of Pfn1 in endothelial cells undergoing sprouting angiogenesis, the *in vitro* spheroid sprouting angiogenesis assay was adopted. In this assay, a sphere of 750-1000 tightly-packed endothelial cells are embedded in collagen and allowed to sprout. Although other cell types are absent, spheroids can produce sprouts of sufficient length for meaningful quantification, though they do not approach the size of sprouts generated from aortic rings. Spheroids were embedded in collagen 72 hours after either Control or Pfn1 siRNA treatment and incubated for 48 hours. The extent of knockdown both 72 hours and 120 hours after siRNA treatment is depicted in Figure 7A and representative images of spheroids are shown in Figure 7B. Knockdown of Pfn1 resulted in a significant decrease in the number of sprouts compared to control (Figure 7C). Together, these findings show that Pfn1 is required for endothelial cells to undergo efficient sprouting angiogenesis.

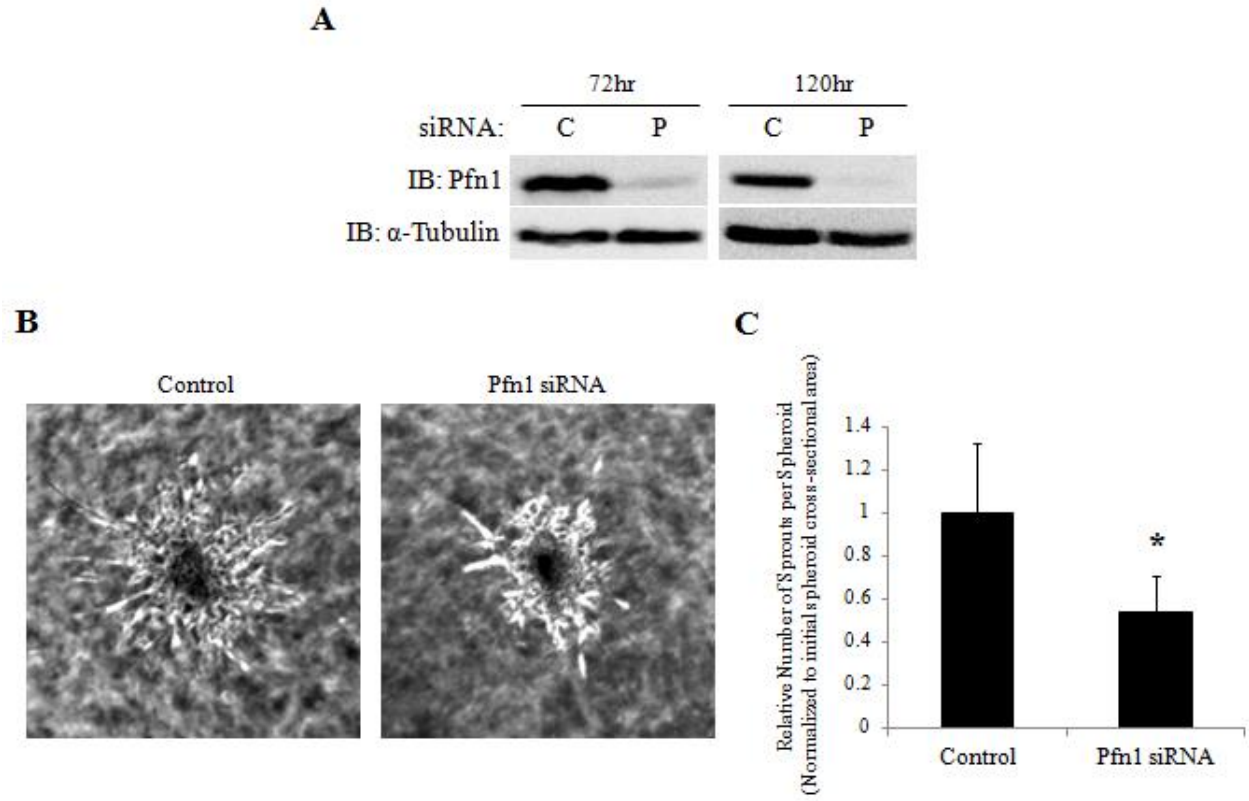

Figure 7. *Importance of Profilin-1 in Sprouting Endothelial Cells.* (A) Western blot showing suppression of Pfn1 expression in HMEC-1 treated with either Control or Pfn1 siRNA after 72 and 120 hours. (B) Representative images of spheroid sprouting following 48 hours incubation. (C) Quantification of the number of sprouts per spheroid normalized to the cross-sectional area of the sprout just after embedding. (* $p<0.0001$)

3.3 DISCUSSION

Depletion studies have indicated that Pfn1 is required for cell migration in a number of physiological and pathological contexts [175-180]. As it pertains to endothelial cells, this and other studies have demonstrated Pfn1 generally promotes cell motility in both HMEC-1 and Human Vein Umbilical Endothelial Cells (HUVEC) [187, 188, 232]. Conversely, attenuation of

Pfn1 in mammary epithelial cells and the metastatic breast cancer cell line MDA-MB-231 enhanced single-cell motility [139]. While nuclear displacement, a typical measure of cell movement also used in this study, was enhanced, closer examination of these cells revealed that loss of Pfn1 actually slowed the rate of membrane protrusion. This phenomenon was similarly observed in endothelial cells where loss of Pfn1 resulted in dramatically lower membrane protrusion velocities [188, 263]. Cell motility is a function of a number of processes and determining Pfn1's specific role in any one of those cannot be achieved solely from displacement analysis; however, membrane protrusion is largely based on F-actin dynamics and is directly proportional to the rates of F-actin polymerization and turnover. Therefore, there is strong evidence for Pfn1 as a promoter of F-actin polymerization in cells, in agreement with prior studies utilizing *in vitro* assay. Given this though, the impact of Pfn1 on cell migration and physiological processes that depend on cell movement likely cannot be generalized and each cell or system of interest needs to be individually considered.

Sprouting angiogenesis requires the coordinated actions of multiple cells to promote neo-vessel formation. This process involves invasion and dynamic morphological modification, both highly dependent on rapid actin polymerization and turnover. Accordingly, Pfn1 becomes an interesting factor for investigation. Because of the apparent context-specific role of Pfn1 in cell migration, we first determined that suppression of Pfn1 expression resulted in reduced endothelial cell single-cell speeds on both plastic, the previously studied substrate, and collagen, a more relevant substrate. Though the control speeds differed somewhat, Pfn1 knockdown slowed the cells to roughly the same extent. This implicates Pfn1 as a general promoter of endothelial cell motility and warrants the study of its role in the angiogenic cascade. Previous studies examining Pfn1 in the context of angiogenesis have relied on morphogenesis assays

[220]. In general, attenuation of Pfn1 expression resulted in decreased 2D and 3D cord formation; however, the relevance of these assays toward sprouting angiogenesis is not clear. Morphogenesis assays involve endothelial cells at sub-confluent levels that are randomly seeded and allowed to assemble into cord- or tube-like structures [264]. This process is therefore qualitatively more comparable to the model of vasculogenesis. Sprouting angiogenesis, in comparison, is the development of an outward growing vessel or cord originating from an approximately confluent layer of cells lining a pre-existing blood vessel [265]. In this regard, we demonstrated that Pfn1 is a factor that generally promotes angiogenic sprouting using the *ex vivo* mouse aortic ring assay in conjunction with siRNA-mediated suppression of Pfn1 expression. Fewer sprouts were observed for the aortic rings treated with Pfn1 siRNA but fluorescent staining revealed the presence of sprouts consisting exclusively of cells with low levels of Pfn1 expression. As a result, we quantitatively segregated sprouts as having either low or normal levels of Pfn1 to analyze differences in characteristic qualities. Interestingly, when comparing these groups there was neither a difference in length nor a difference in propensity to bifurcate. Essentially, without knowledge of the differential Pfn1 expression levels, the two groups of sprouts were qualitatively indistinguishable. In conjunction with the fact that fewer sprouts were observed for Pfn1 siRNA-treated aortic rings, it appears the main role of Pfn1 may be as a promoter of sprout initiation while having a less impactful role once sprouting has begun.

While meaningful in its own right, the previous experiment does not clarify the specific importance of Pfn1 in endothelial cells undergoing sprouting as the use of RNA interference to down-regulate Pfn1 exhibits no cell type specificity. To resolve this, we attempted to generate endothelial cell-specific Pfn1 knockout transgenic mice. Heterozygous mice were born at the expected frequency and did not exhibit any obvious deficiencies compared to their wild-type

littermates. Use of the aortas from these mice in the aortic ring assay only mildly impacted sprouting as a delay was observed only for those rings embedded in matrigel compared to wild-type. It is possible that single-allele knockout is not sufficient to produce a phenotype. Unfortunately, the effort to generate knockout mice was not successful as this genotype appears to be embryonic lethal. While detrimental to the current study, this leads to a possible role for Pfn1 in developmental angiogenesis or vasculogenesis. To continue our pursuit of the importance of Pfn1 in sprouting angiogenesis, we adopted the *in vitro* spheroid sprouting assay. Using this system, we showed that Pfn1-deficienct spheroids exhibited far fewer sprouts. This 3D system has several advantages over the previously utilized morphology assays, not the least of which is the formation of sprouts from an existing structure.

In conclusion, we have identified Pfn1 as a critical factor in endothelial cells undergoing sprouting angiogenesis. As a result, Pfn1 becomes an interesting therapeutic target. Pfn1 activity has direct consequences on the actin cytoskeleton, a key structural element vital to the angiogenic cascade. As such, all pro-angiogenic pathways must promote dynamic change of these structures to promote cellular invasion and morphologic change. Because Pfn1 acts directly on these processes, it becomes a necessary central factor for a number of angiogenic stimulants. Therefore, inhibition of Pfn1 may be one means by which angiogenesis can be generally shutdown. This has important implications in cancer therapeutics, among others, where most anti-angiogenic therapies fail because they target single stimulants and compensatory factors survive. Whether such a therapeutic agent can be realistically created remains to be seen and much more testing will be needed, but it is an interesting starting point. The specific means by which Pfn1 promotes angiogenic sprouting remains unknown. Both G-actin and polyproline binding were required for Pfn1 to promote lamellipodial protrusion and single-cell random

motility in endothelial cells [188]. Similarly, these interactions were imperative for cord morphogenesis. Therefore, it stands to reason that Pfn1 acts through G-actin and polyproline interaction to promote F-actin polymerization permitting endothelial cells to more readily invade and adapt. This hypothesis will be examined in Specific Aim 3.

4.0 PROFILIN-1 CAN BE POST-TRANSLATIONALLY MODIFIED BY PROTEIN KINASE A

4.1 INTRODUCTION

Numerous studies have identified Pfn1 as a vital cog in the machinery that regulates actin polymerization. Though its specific role has evolved over time, the general consensus is that Pfn1 promotes barbed end elongation and actin turnover by coordinately decreasing A_C and A_{CB}. As such, this role requires G-actin interaction. As of yet, there is no model of a G-actin-independent means by which Pfn1 can promote actin polymerization; however, cells do not readily maintain a large pool of Pfn1-G-actin complex [73]. Interestingly, microinjection of actin nuclei and G-actin into quiescent epithelial cells resulted in filaments composed exclusively of exogenous actin that polymerized far slower than endogenous filaments [74, 75]. This shows unregulated actin polymerization is probably not a realistic pathway by which filaments are generated *in vivo*. There are likely further regulatory steps that have yet to be described behind which a pool of polymerization-incompetent G-actin is kept until properly released. Significant effort has been put forth in defining how actin-binding proteins are regulated such that actin polymerization occurs in a predictable manner, but Pfn1 is often overlooked and simply thought to seamlessly facilitate the function of a variety of nucleation and elongation factors.

With advances in mass spectrometry and more sensitive tools for the purification of modified proteins, a number of recent proteomics studies have identified Pfn1 as a target for post-translational modification (See Table 1). While these exploratory studies have augmented our understanding of the proteome, a myriad of cell types and conditions were used to collect these data, so individual modifications cannot be assumed to be ubiquitous. Similarly, the upstream regulation and downstream impact of the identified Pfn1 post-translational modifications have largely not been investigated. To date, the only modification fully characterized in a cellular context is phosphorylation of Y128, an event found to occur downstream VEGF-A stimulation in a VEGFR2- and Src-mediated fashion [232]. This modification increased Pfn1 association with G-actin and generally promoted endothelial migration. That Pfn1 interaction with G-actin can be regulated has important implications in the effort to fully understand the dynamics of the actin cytoskeleton. While the fraction of Pfn1 found associated with G-actin is low in unstimulated cells, this shows Pfn1 is itself regulated to uptake G-actin upon cell activation.

Beyond this, only phosphorylation of S137 has been examined. Both PKCζ and ROCK1 treatment led to S137 phosphorylation *in vitro*, but study of its impact on Pfn1-ligand interaction was inconsistent [86, 250, 251]. No other post-translational modifications of Pfn1 have been investigated. It therefore becomes imperative to address the modification states of Pfn1 in cells and assess their causal upstream pathways and downstream effects to more completely elucidate the regulation of Pfn1.

4.2 RESULTS

4.2.1 Profilin-1 is Post-Translationally Modified in Unstimulated Cells

To investigate the modification status of Pfn1 we utilized 2D electrophoresis. To begin our analysis, we wanted to determine whether or not the endogenous Pfn1 of HMEC-1 was subjected to modification under typical culture conditions (Figure 8A). The theoretical isoelectric point of endogenous, unmodified Pfn1 is ~8.3, therefore we used pH 6-10 IPG strips to maximize resolution. With this, we observed populations of Pfn1 at several isoelectric points in HMEC-1 maintained in growth medium suggesting Pfn1 is indeed post-translationally modified.

The isoelectric point of Pfn1 is basic and isoelectric focusing becomes more difficult because DTT, the reducing agent, becomes negatively charged and migrates away from basic proteins [266]. To combat this, we expressed an acidic, myc-tagged Pfn1 (myc-Pfn1; isoelectric point ~6.1) to improve resolution and more clearly observe the populations of Pfn1 charge states. Both expression in HMEC-1 and HEK-293 showed a similar pattern where the most basic spot represented a very small fraction of the total myc-Pfn1 population (Figure 8B-C). The patterns of the exogenous myc-Pfn1 and endogenous Pfn1 were comparable where it is possible that the streaking observed in the endogenous Pfn1 truly represents multiple populations that were not sufficiently resolved. Therefore there are at least 2, and more likely 3, charge states of Pfn1 and myc-Pfn1 in HMEC-1 and HEK-293 being maintained in appropriate growth medium. Because of the similarity among groups, subsequent 2D electrophoresis experiments will assess the state of exogenously-expressed myc-Pfn1 in HEK-293.

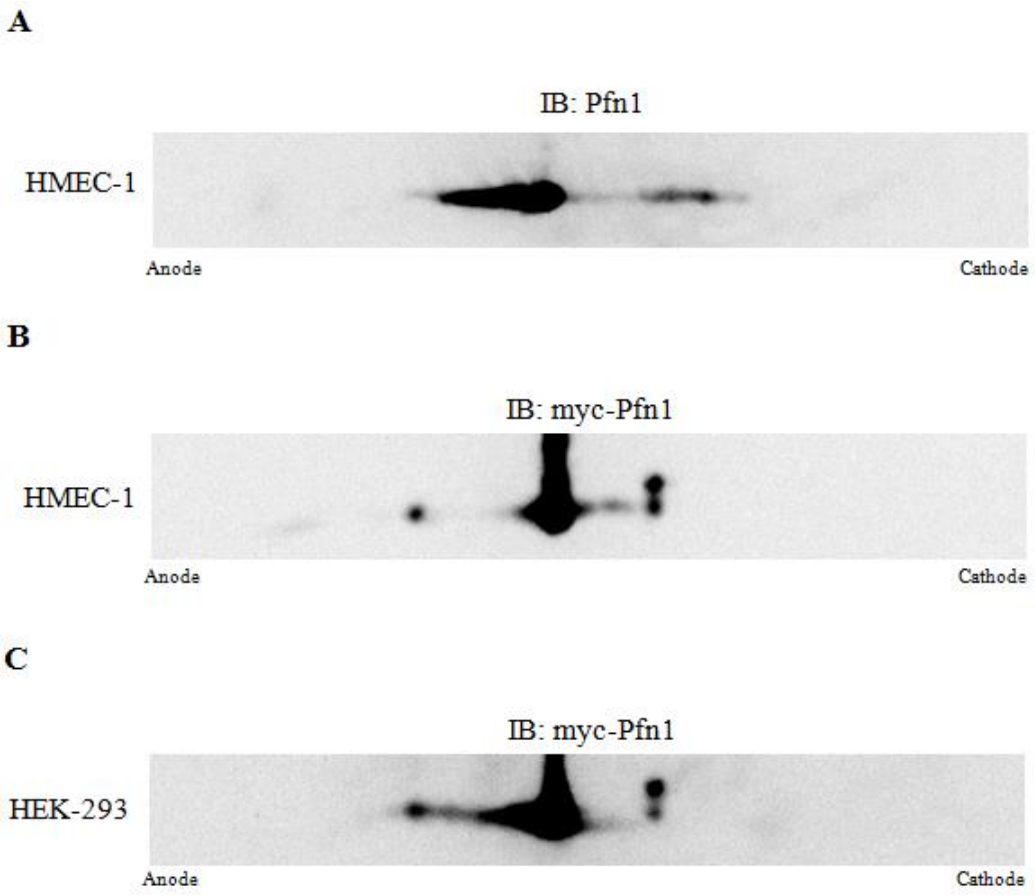

Figure 8. *2D Electrophoresis of Profilin-1 and myc-Pfn1 Expressed in Unstimulated Cells*. (A) 2D electrophoresis of endogenous Pfn1 from HMEC-1 maintained in growth medium. Isoelectric focusing was conducted using a pH 6-10 IPG strip. In all cases, the relative locations of the anode and cathode are labeled. (B) 2D electrophoresis of exogenously-expressed myc-Pfn1 from HMEC-1 maintained in growth medium. Isoelectric focusing was conducted using a pH 4-7 IPG strip. (C) 2D electrophoresis of exogenously-expressed myc-Pfn1 from HEK-293 maintained in growth medium. Isoelectric focusing was conducted using a pH 4-7 IPG strip.

4.2.2 Profilin-1 is Phosphorylated on a Non-Tyrosine Residue in Unstimulated Cells

Table 1 provides a list of known Pfn1 post-translational modifications. There are many varieties of post-translational modification, most of which have not been investigated using proteomic

techniques, so this list is presumably not exhaustive. Phosphorylation is the most widely studied and best-characterized post-translational modification that has implications in every cellular process. It has been suggested that 30% of all proteins in eukaryotic cells are phosphorylated on at least one residue [267]. To assess whether the charge states of myc-Pfn1 resulted from a phosphorylation modification, cell lysate was treated with λ-Protein Phosphatase, a promiscuous phosphatase with low specificity (Figure 9A). A single phosphorylation will alter the net surface charge of a protein by -1, so the basic shift of a significant population of myc-Pfn1 indicates that it is phosphorylated in cells maintained in growth medium. Further investigation using a phosphotyrosine-specific antibody revealed no appreciable level of phosporylated tyrosine. Myc-Pfn1 is therefore phosphorylated on either serine or threonine residues (Figure 9B). In addition to phosphorylation, Pfn1 can also be acetylated on several lysine residues. Like phosphorylation, acetylation modification of a lysine residue will change the net surface charge of a protein by -1. However, none of the spots recognized by an acetylated-lysine-specific antibody aligned with myc-Pfn1, suggesting this is not a major modification under these conditions (Figure 9C).

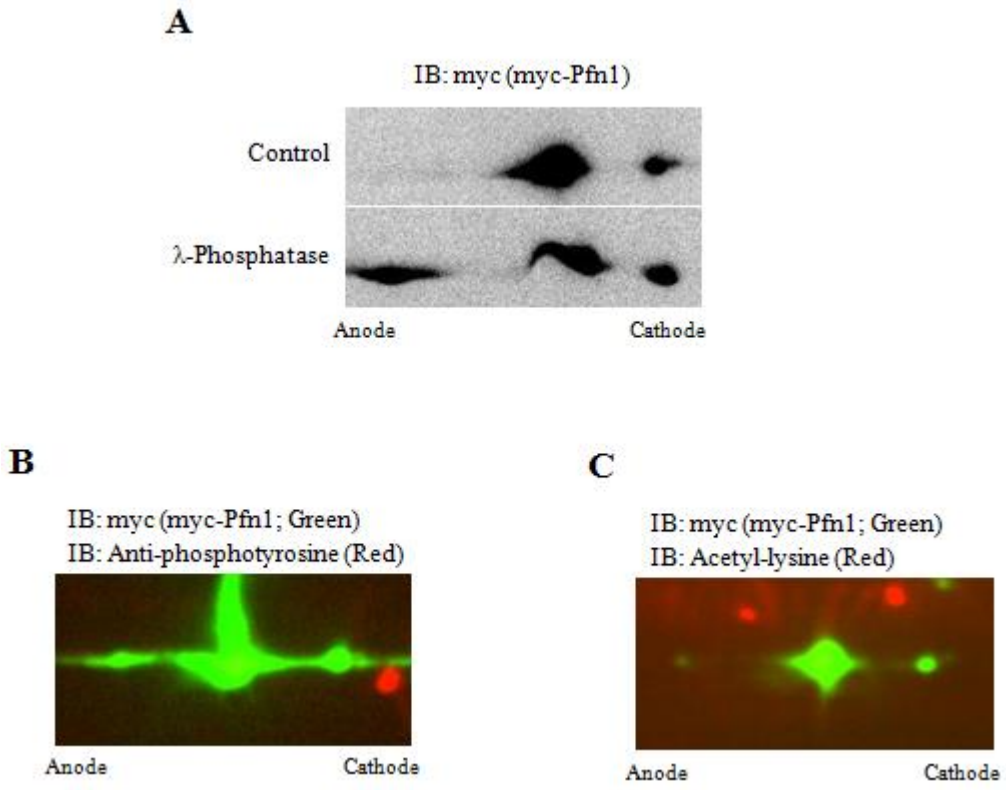

Figure 9. *Assessing the Identity of the Post-Translational Modifications of Profilin-1.* (A) 2D electrophoresis comparing samples either treated with λ-Protein Phosphatase (λ-Phosphatase) or not (Control). Isoelectric focusing was conducted using a pH 4-7 IPG strip. In all cases, the relative locations of the anode and cathode are labeled. (B) 2D electrophoresis of HEK-293 proteins immunoblotted for anti-phosphotyrosine (red) and subsequently immunoblotted for myc-Pfn1 (green) on the same membrane and aligned. Isoelectric focusing was conducted using a pH 4-7 IPG strip. (C) 2D electrophoresis of HEK-293 proteins immunoblotted for anti-acetylated-lysine (red) and subsequently immunoblotted for myc-Pfn1 (green) on the same membrane and aligned. Isoelectric focusing was conducted using a pH 4-7 IPG strip.

4.2.3 Protein Kinase A Phosphorylates Profilin-1 on Threonine 89 *in vitro*

There are several serine and threonine residues previously reported to be phosphorylated on Pfn1, but the upstream regulation has not been characterized. To begin to understand what pathways

could regulate Pfn1, we employed a series of computational prediction algorithms to filter potential targets [268-271]. Although these programs attempt to characterize a variety of kinases, they only represent a small fraction of those that are expressed in a cell, indicating a clear bias in this strategy. Nonetheless, the AGC (Protein Kinase A, G, and C) family kinases consistently scored well with high stringency searches. Of particular interest was Protein Kinase A (PKA) as it was a predicted kinase for several residues, some of which overlapped with previously discovered phosphorylation sites. To test this hypothesis, we treated His-tagged Pfn1 (His-Pfn1) with PKA *in vitro*. This treatment resulted in the acidic shift of a significant population of His-Pfn1 (unmodified isoeletric point pH ~6.5) presenting several new charge states and suggesting phosphorylation on several sites (Figure 10A). To determine the specific residues that were modified, these samples were trypsin-digested and subjected to High Performance Liquid Chromatography (HPCL)-tandem mass spectrometric (MS/MS) analysis. 53% coverage was achieved and three phospho-peptides were identified: DRS**pS**^{57}FYVNGLTLGGQK, **pT**^{89}KSTGGAPTFNVTVTK, and S**pT**^{92}GGAPTFNVTVTK (Figure 10B). His-Pfn1 treated without PKA yielded no phospho-peptides.

His-Pfn1 is a C-terminally-tagged fusion protein and it has been established that tagging Pfn1 on its C-terminus completely abrogates polyproline interaction [272]. This suggests some conformational change in Pfn1. Both the N- and C- terminal helices are in close proximity and participate in polyproline interaction and N-terminal tags do not impact Pfn1 as severely. Although PKA lacks a polyproline stetch, the site of Pfn1-PKA interaction is not known, so we wanted to verify PKA-mediated phosphorylation was not a function of tagging. To accomplish this, we repeated the *in vitro* kinase assay with N-terminally-tagged Glutathione-S-Transferase (GST)-Pfn1. In this case, 81% coverage was achieved and one phospho-peptide was identified:

DRS**pS**[57]FFVNGLTLGGQK. As with His-Pfn1, GST-Pfn1 treated without PKA did not yield any phospho-peptides. It should be noted that Threonine 89 (T89) was not covered in this analysis so its status is unknown. Additionally, the Pfn1 in GST-Pfn1 was *Mus musculus* Pfn1 while that of His-Pfn1 was human Pfn1.

Multiple sequence alignment of Pfn1 in vertebrates revealed a high degree of conservation of T89 and its surrounding residues, suggesting this region may be important in the protein structure or some regulatory pathway (Figure 10C). To investigate if the identified phosphorylation sites could explain any of the acidic Pfn1 populations, phospho-dead S57 (S57A), T89 (T89V), and T92 (T92V) were expressed in cells maintained in unstimulated conditions and extracted for 2D analysis (Figure 10D). Only T89V resulted in the consistent and significant basic shift of a population of myc-Pfn1. Though somewhat modest in terms of absolute amounts of Pfn1, T89V resulted in nearly a 3.5-fold increase in the intensity of the most basic spot relative to that of wild-type. (Figure 10E). While this does not prove phosphorylation, it implicates T89 as an important residue for investigation. Together, these findings suggest a possible role for PKA and T89 phosphorylation in the regulation of Pfn1.

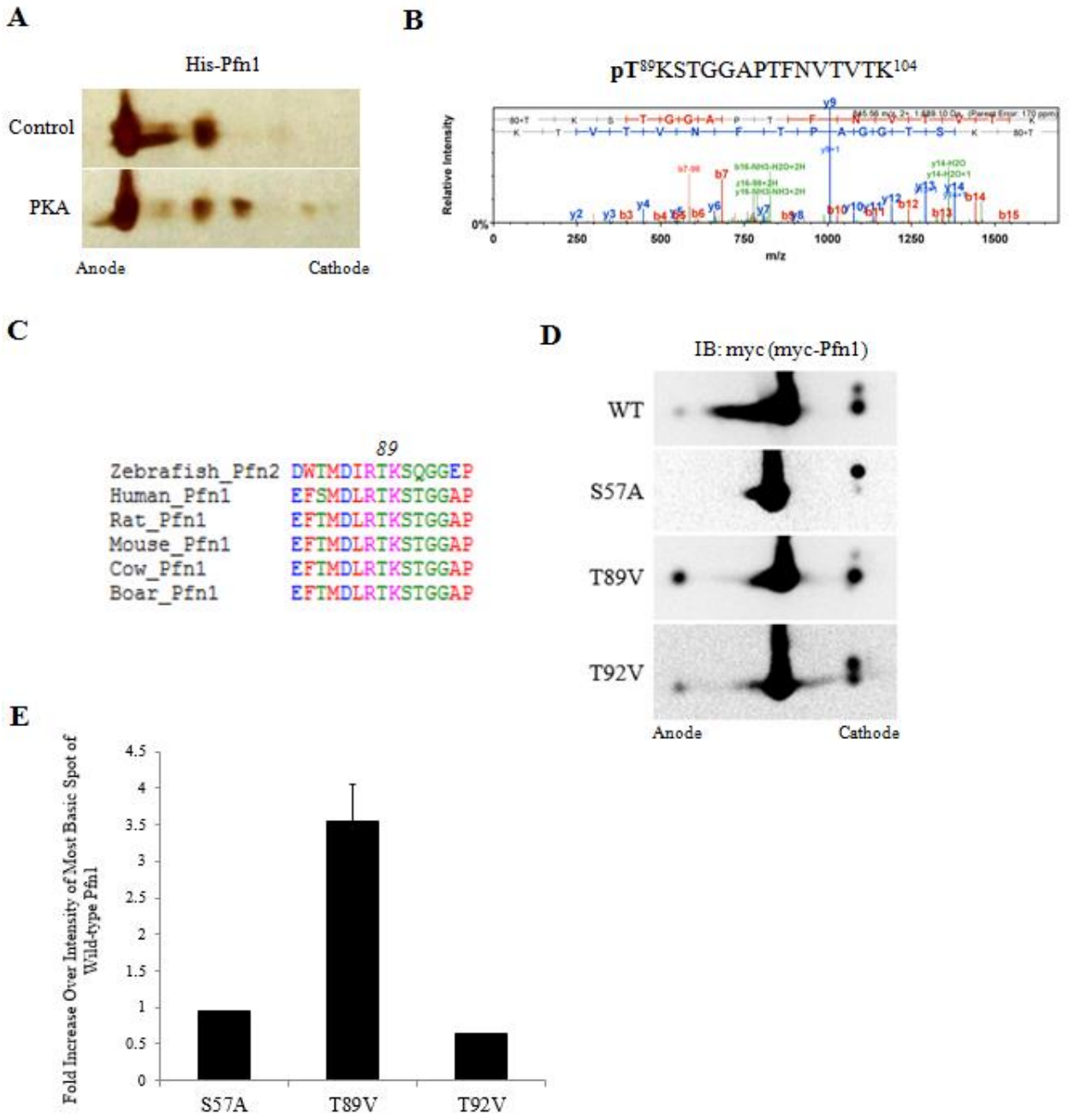

Figure 10. *PKA-Mediated Phosphorylation of Profilin-1 on Threonine 89.* (A) His-Pfn1 was treated with buffer containing ATP with or without PKA followed by 2D electrophoresis and visualized by silver staining. Isoelectric focusing was conducted using a pH 4-7 IPG strip. In all cases, the relative locations of the anode and cathode are labeled. (B) Mass spectrometry reveled PKA-treated His-Pfn1 was phosphorylated on T89. (C) Multiple sequence alignment of Pfn1 focused on T89. (D) 2D electrophoresis of wild-type and phospho-dead S57A, T89V, and T92V

mutant myc-Pfn1 expressed in HEK-293 maintained in growth medium. Isoelectric focusing was conducted using a pH 4-7 IPG strip. (E) The fold increase in the intensity of the most basic spot relative to that of the appropriate control. The error bar for T89V represents the variance of the data over three experiments.

4.2.4 Phospho-mimetic Mutation of Profilin-1 at Threonine 89 Results in Insolubility

Although we do not definitively know whether Pfn1 is phosphorylated at T89 in cells, it is of interest to consider the consequences of such a modification. To this end, both phospho-mimetic (T89D) and phospho-dead (T89V) mutants of myc-Pfn1 were generated to assess their impact on Pfn1-ligand interaction. Interestingly, neither the T89V mutant nor the T89D mutant was completely soluble in NP-40 buffer where T89D was nearly completely insoluble (Figure 11A). In addition, T89D mutation consistently exhibited lower expression when extracted using Laemmli sample buffer. These facts make investigation of T89D mutation on ligand-binding using extra-cellular assay difficult.

4.2.5 In Silico Simulation of Threonine 89 Phosphorylation Confers Backbone Availability for G-Actin Interaction

Therefore, to explore the impact of T89 phosphorylation on actin binding, we utilized computer simulation. We investigated the effect of the T89 mutations by running molecular dynamics simulations on monomeric homology models of Pfn1. The dynamics of the backbone carboxylic acid functional group of T89 were assayed. The double-bonded backbone oxygen of the carboxylic acid functional group of T89 makes a hydrogen bond with Y166 of actin in the bound state (distance $\leq$ 3.0 Å) and does not make an intramolecular hydrogen bond with the nitrogen of the backbone amino functional group of Phenylalanine 98 (F98) (Figure 11B). The distances are

such that T89 cannot interact with both residues simultaneously. Simulation was performed without the influence of actin. The distance between the double-bonded oxygen and the nitrogen of the backbone amino functional group of F98 on Pfn1 over the course of the simulation is shown in Figure 11C-E. In the wild-type simulation, T89 not only samples a conformation where this internal backbone hydrogen bond is made, but also the bond appears to be stable once formed. The T89V mutant also samples this conformation, but it does not appear to be as stable. In contrast, the T89D mutant never samples this conformation. Since the internal hydrogen bond is not being made, the backbone oxygen is free to bond elsewhere, such as to Y166 of actin. Therefore, based on these simulations, it appears that T89D-mutated Pfn1 presents a more 'actin-friendly' interface. [Portions reproduced with the permission of Dr. David Koes, University of Pittsburgh (Collaborator)]

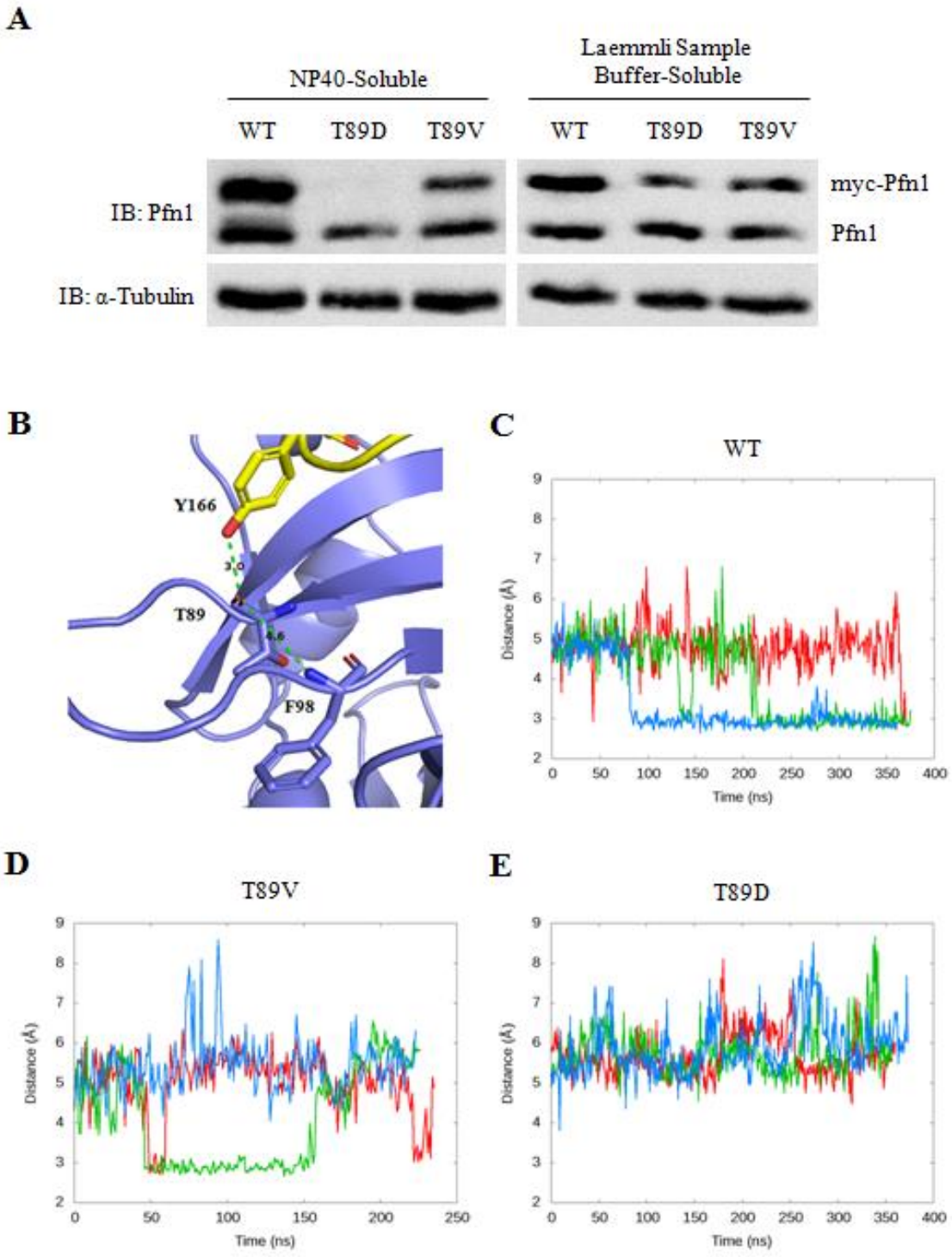

Figure 11. *Phospho-mimetic Mutation of Threonine 89 Confers an Actin-Friendly Interface*. (A) myc-Pfn1 or the T89D and T89V mutants were expressed in HEK-293 and extracted using the indicated buffers and solubility

assessed using Western blot. (B) Molecular model of the Pfn1 (blue)-G-actin (yellow) complex (PDB 2BTF). The enhanced view shows the Pfn1 T89-Actin Y166 hydrogen bond as well as Pfn1 T89-Pfn1 F98 proximity. Dashed green lines represent the two potential hydrogen bonds. (C-E) The distance between the double-bonded oxygen of the carboxylic acid functional group of T89 and the nitrogen of the backbone amino functional group of F98 on Pfn1 over the course of the simulations. A value $\leq$ 3.0 Å means a hydrogen bond is being made. The three colors represent three unique simulations. Every simulation was run for 144 hours, resulting in approximately 360ns of simulation per run (an I/O error terminated the T89V simulation early). [Simulation results and molecular model reproduced with the permission of Dr. David Koes, University of Pittsburgh (Collaborator)]

4.3 DISCUSSION

The advent of advanced mass spectrometry techniques and tools for concentrating proteins with modification has led to the discovery of a number of Pfn1 post-translational modifications. Pfn1 exerts its influence on the actin cytoskeleton through its interaction with G-actin, polyprolines, and phosphoionsitides [258]. Correspondingly, many of the identified modifications of Pfn1 are either adjacent to or within the regions responsible for interaction. Previous study with regard to Pfn1 post-translational modification is limited, but both investigated sites, namely Y128 and S137, had strong impacts on regulating Pfn1-ligand binding [86, 232, 257]. With these exceptions, no other modifications have been characterized.

To begin to investigate Pfn1 post-translational modification and its downstream implications, we wanted to determine if it was basally modified. By utilizing 2D electrophoresis, we showed endogenous Pfn1 and exogenous myc-Pfn1 exhibit a comparable pattern and exist at three distinct isoelectric points. By combining modification-specific antibodies and phosphatase treatment, we determined at least some population of Pfn1 was phosphorylated on either a serine

or threonine residue under these unstimulated culture conditions. Both serine and threonine phosphorylation of Pfn1 is not without precedent as several such sites have been discovered, but their upstream regulation is completely unknown. Following several bioinformatics searches, we found PKA could phosphorylate Pfn1 *in vitro* on at least three residues: S57, T89, and T92. Two of these modifications, T89 and T92, are novel and have yet to be seen *in vivo*. In testing if phosphorylation at any of these sites was at least partially responsible for the acidic shifts previously observed using 2D analysis we found that phospho-dead mutation of T89 resulted in the basic shift of a small, but repeatable population of Pfn1. Though this does not prove that T89 is phosphorylated *in vivo*, the 3D molecular model of Pfn1 indicated the backbone of T89 forms a hydrogen bond with Y166 of actin, implicating it as a residue of interest.

To better understand T89 modification on Pfn1 function, we wanted to assess its impact on Pfn1-G-actin binding. Interestingly, neither the phospho-dead T89V nor the phospho-mimetic T89D was completely soluble in non-denaturing NP-40 buffer, where T89D was completely insoluble. Previous studies have mutated residues near and adjacent to T89, including R88 and K90, with no impact on solubility [15, 273]. However, several residues of Pfn1 found to be mutated in familial Amyotrophic Lateral Sclerosis (ALS) resulted in protein insolubility, so such behavior is not completely unfounded [274]. These facts further implicate T89 as a residue that is important for Pfn1 function and possibly stability, although the solubility issue presents a complication in exploring its impact on Pfn1-ligand interaction using conventional means. As a result, we relied on computer simulation to determine if T89 phosphorylation had any structural importance and what effect it might have on the backbone hydrogen bond with Y166 of actin. The simulations were run starting from the G-actin-bound conformation of Pfn1 and without the influence of actin. Wild-type Pfn1 repeatedly stabilized to a conformation where the backbone of

T89 interacted intramolecularly with F98. We observed that when this interaction is made, the backbone of T89 is unavailable for interaction with Y166 of actin. Similarly, T89V also reached this state, but with less consistency and less stability. T89D, however, never sampled this conformation at any time point over the course of any of the simulations. Accordingly, the backbone of T89D was maintained at a distance that would permit hydrogen bonding with Y166 of actin. We therefore hypothesize that T89 phosphorylation would result in an 'actin-friendly' conformation because an extra hydrogen bond could be made, increasing the strength of interaction. The physiological implications of such regulation of Pfn1 by PKA are not yet known but phosphorylation at T89 might push equilibrium toward an increase in levels of Pfn1-G-actin complex, at least locally. PKA activity has been linked with Rho GTPase activation [275]. In this way PKA might promote cytoskeletal reorganization by increasing Pfn1-G-actin while concomitantly promoting the activity of actin elongation and nucleation factors. PKA, however, can also be detrimental to protrusion [276]. Therefore, the meaning behind this regulatory event requires further study.

In conclusion, Pfn1 can be phosphorylated at T89 by PKA *in vitro*, and this modification would result in both insolubility and an 'actin-friendly' conformation. We theorize that this would lead to a general increase in G-actin binding, though whether this would have a positive or negative impact on Pfn1 function must be investigated. While increasing the pool of Pfn1-G-actin should theoretically promote F-actin polymerization, Pfn1 must be able to release its G-actin. If, for instance, the increase in complex stability is too great, Pfn1 may simply sequester the G-actin, making it unavailable for polymerization. It also remains to be seen whether PKA can regulate Pfn1 *in vivo*. This and the impact of PKA on sprouting angiogenesis will be addressed in Specific Aim 3.

5.0 PROTEIN KINASE A-MEDIATED POST-TRANSLATIONAL MODIFICATION OF PROFILIN-1 CORRELATES WITH IMPAIRED SPROUTING ANGIOGENESIS

5.1 INTRODUCTION

We demonstrated that Pfn1 is required for proper sprouting angiogenesis and is subject to PKA-mediated phosphorylation *in vitro*. These modifications, along with those investigated in previous studies, suggest a role for the post-translational modification of Pfn1 in regulating its ligand interaction. Both Pfn1-G-actin and Pfn1-polyproline interactions were critical in endothelial cell migration and invasion [188]; however, the role of these interactions in sprouting angiogenesis and whether they can be regulated downstream PKA has not been addressed.

5.2 RESULTS

5.2.1 Forskolin Treatment Causes a Protein Kinase A-Dependent Post-Translational Modification of Profilin-1

The physiological regulation of Pfn1-ligand interaction is largely not understood. Because PKA can phosphorylate Pfn1 *in vitro*, we wanted to investigate whether this phenomenon was relevant in cells. Treating HEK-293 with Forskolin, a potent activator of PKA, resulted in the acidic shift

of a small, but repeatable population of myc-Pfn1 (Figure 12A). Unexpectedly, the acidic shift observed was more than 1 pH unit, a dramatic change not typically observed; however, there is evidence that Pfn2a, having the same isoelectric point as the myc-Pfn1 construct, undergoes post-translational modification downstream ROCK2 resulting in a similar shift [277]. Although observed shift can be a function of a number of parameters including unmodified isoelectric point and size, many outliers exist and each protein must be considered individually [278]. Blocking PKA activity with the PKA-specific inhibitor H89 prevented the observed acidic shift indicating that Forskolin treatment acts through PKA to induce Pfn1 post-translational modification (Figure 12B). Together, this suggests a role for PKA in the regulation of Pfn1 in cells.

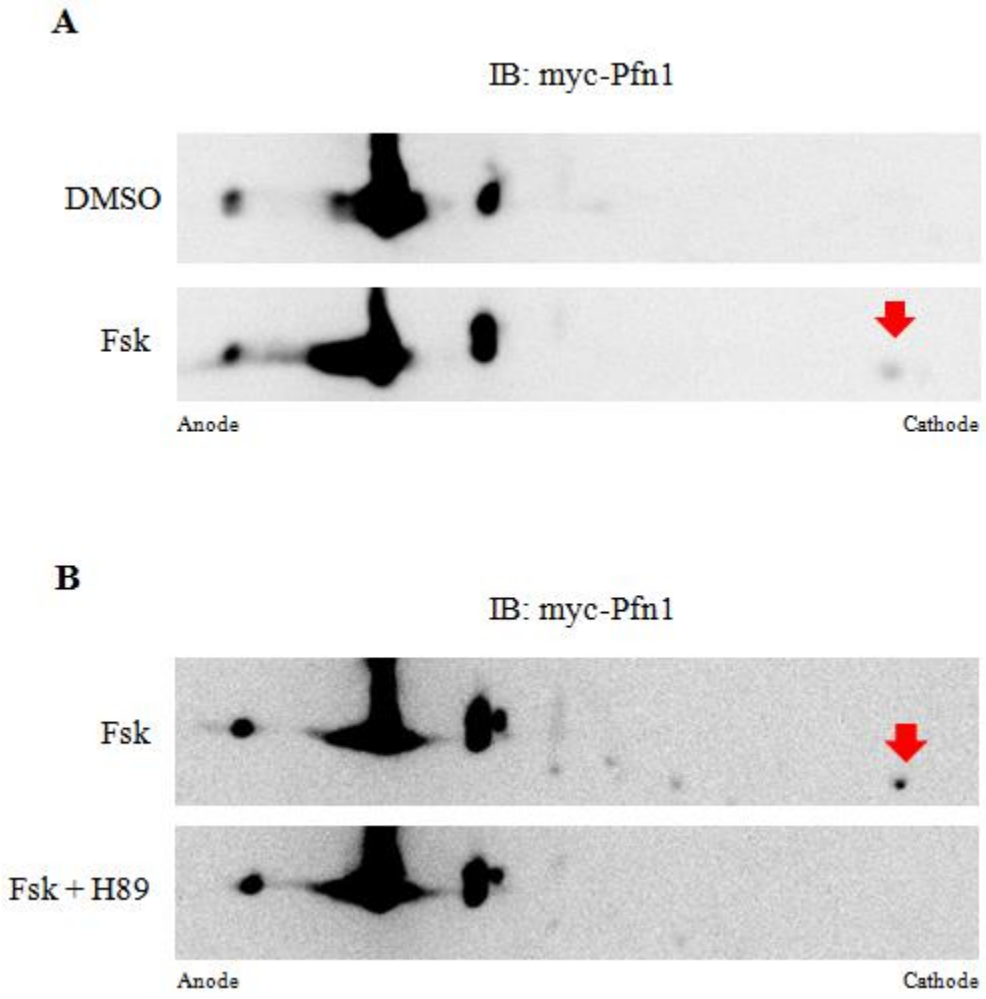

Figure 12. *Forskolin Mediates Profilin-1 Post-Translational Modification through PKA.* (A) 2D electrophoresis of myc-Pfn1 from HEK-293 treated with 50 µM Forskolin (Fsk) or DMSO for 30 minutes. Isoelectric focusing was conducted using a pH 4-7 IPG strip. In all cases, the relative locations of the anode and cathode are labeled. Spot representing acidic shift denoted with arrow (B) 2D electrophoresis of myc-Pfn1 from HEK-293 treated with 10 µM H89 or DMSO in the presence of 50 µM Forskolin (Fsk) for 30 minutes. Cells were pre-treated with 10 µM H89 or DMSO for 10 minutes before changing to Forskolin-containing medium. Isoelectric focusing was conducted using a pH 4-7 IPG strip. Spot representing acidic shift denoted with arrow.

5.2.2 Forskolin Treatment Reduces Profilin-1-Polyproline Interaction Downstream Protein Kinase A

Because Forskolin induces a PKA-dependent post-translational modification in Pfn1, we next wanted to determine whether this correlated with any interaction changes. Forskolin induced a time-dependent decrease in Pfn1-VASP interaction (Figure 13A). Incidentally, VASP is phosphorylated by PKA at Serine 157 (S157), a residue adjacent to its polyproline region. This event, however, does not affect Pfn1 interaction, so binding changes could be due to modification of Pfn1 [279]. Verification of PKA activity is seen by the apparent mass shift of VASP during electrophoresis, as phosphorylation at S157 results in a 2-3 kDa shift (Figure 13B). Inhibiting the activity of PKA rescued the Forskolin-induced decrease in Pfn1-VASP binding, suggesting the regulation of this interaction works downstream PKA (Figure 13C). Forskolin, therefore, inhibits Pfn1-VASP binding in a PKA-mediated manner.

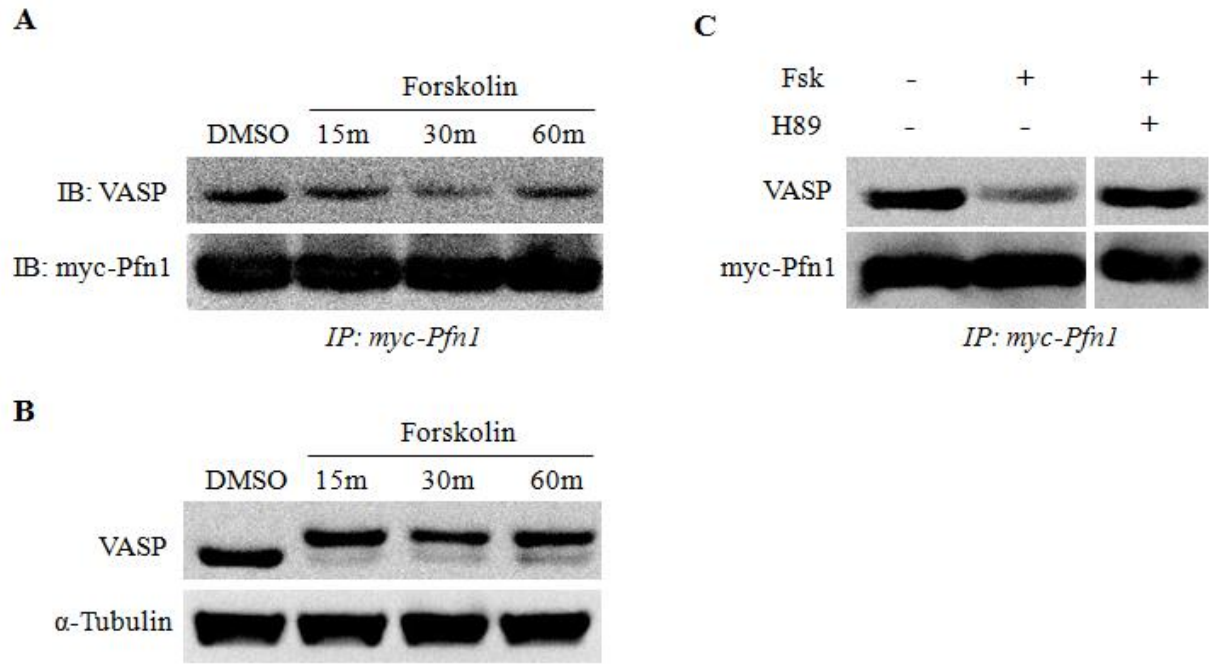

Figure 13. *Forskolin Mediates Profilin-1-Polyproline Interaction through PKA.* (A) Co-immunoprecipitation of VASP with myc-Pfn1 from HEK-293 treated with 50 µM Forskolin or DMSO for the indicated times. (B) Relative protein levels of VASP and myc-Pfn1 that were subjected to co-immunoprecipitation. The apparent mass shift of VASP is a function of phosphorylated S157, indicating PKA is strongly activated by Forksolin. (C) Co-immunoprecipitation of VASP with myc-Pfn1 from HEK-293 treated with 10 µM H89 or DMSO in the presence of 50 µM Forskolin (Fsk) for 30 minutes. Cells were pre-treated with 10 µM H89 or DMSO for 10 minutes before changing to Forskolin-containing medium.

5.2.3 Profilin-1-Polyproline Interaction is Required for Endothelial Cell Spheroid Sprouting

While we established that Pfn1 is required to promote proper sprouting angiogenesis, we wanted to determine if Pfn1-polyproline interactions were playing a role. To investigate this, we used green fluorescent protein (GFP)-tagged Pfn1 that was modified with two silent point mutations

that do not affect protein translation or peptide sequence, but negatively impact the recognition of our Pfn1 siRNA [188]. With this system, we can introduce mutant Pfn1 in an endogenous Pfn1-null background and explore its specific effect on various cellular processes. Here, we have expressed either wild-type GFP-Pfn1 or GFP-Pfn1-H133S, a mutation that strongly abrogates polyproline interaction [14]. The efficiency of our system in introducing specific Pfn1 constructs to HMEC-1 is seen in Figure 14A. GFP-Pfn1 is expressed at a slightly higher level compared to endogenous Pfn1, but is completely immune to Pfn1 siRNA treatment. Additionally, greater than 95% knockdown of endogenous Pfn1 is maintained for 48 hours. Use of these cells in the spheroid sprouting assay showed a significant reduction in sprouting in the H133S group (Figure 14B-C). These data suggest Pfn1 requires polyproline interaction to promote sprouting angiogenesis.

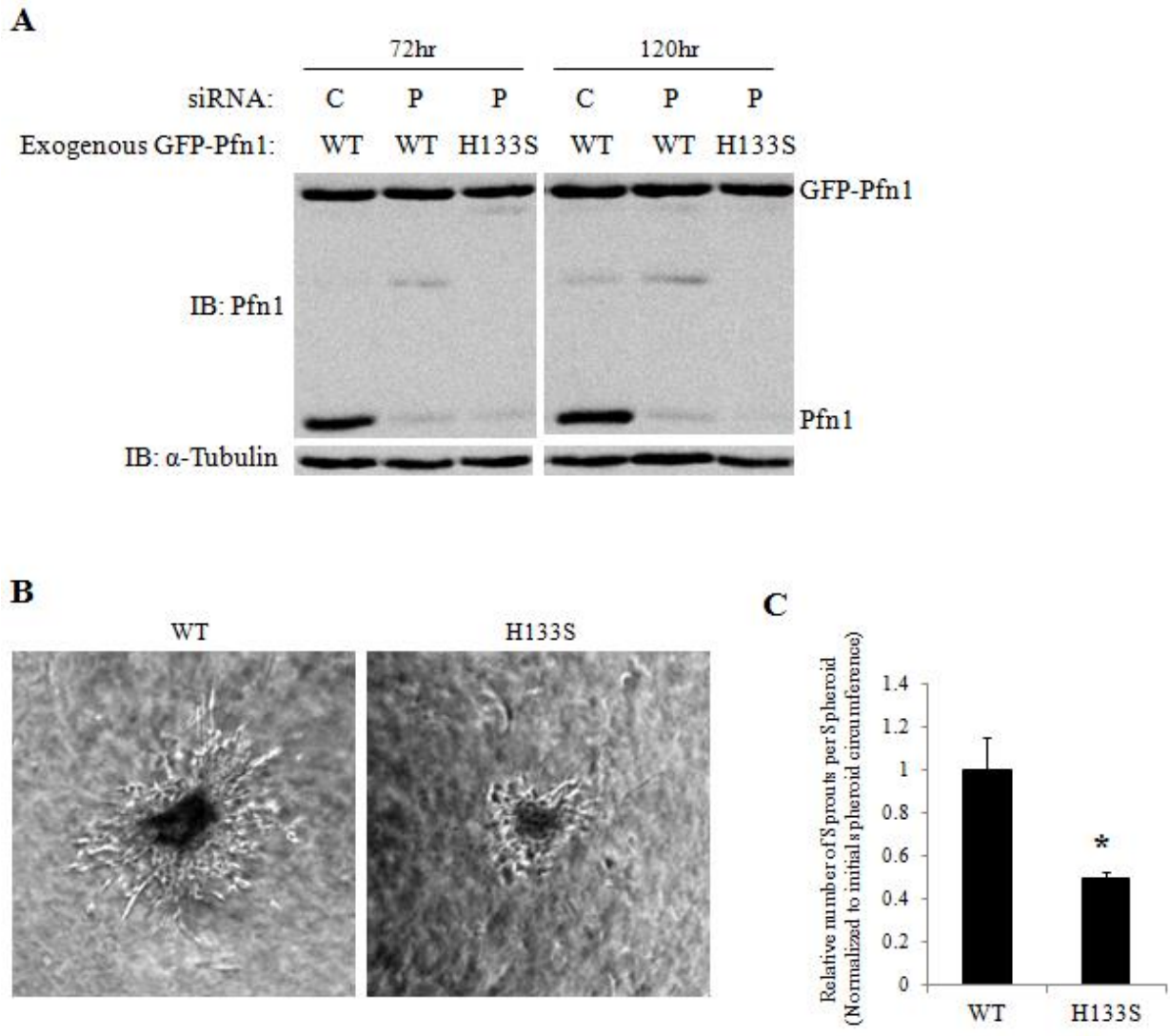

Figure 14. *Impact of Profilin-1-Polyproline Interaction on Endothelial Cell Spheroid Sprouting.* (A) Western blot of HMEC-1 cells expressing siRNA-resistant GFP-Pfn1 or H133S mutant with Control (C) or Pfn1 siRNA (P). (B) Representative images of spheroid sprouting following 48 hours incubation. (C) Quantification of the number of sprouts per spheroid normalized to the cross-sectional area of the sprout just after embedding. (* $p<0.001$)

5.2.4 Forskolin Treatment Inhibits Endothelial Cell Motility Partially through Protein Kinase A Activity

Pfn1-polyproline interaction is required for endothelial cell motility and can be negatively regulated by Forskolin in a PKA-mediated manner; therefore we next determined the effect of PKA on endothelial cell migration. In general, Forskolin treatment significantly reduced single-cell random motility of HMEC-1 while H89 alone had no impact (Figure 15A). The Forskolin-induced drop in motility could be partially, but significantly, rescued by H89 indicating that Forskolin inhibits endothelial cell migration, at least partially, through PKA.

5.2.5 Forskolin Inhibits Endothelial Cell Spheroid Sprouting

Similarly, Pfn1-polyproline interaction was shown to be imperative for proper spheroid sprouting. In this regard, HMEC-1 spheroids incubated in the presence of Forskolin exhibited a significant reduction in the number of sprouts (Figure 15B-C). Together, these data show Forskolin treatment results in a similar phenotype to polyproline binding-deficient Pfn1, although no direct relationship is established.

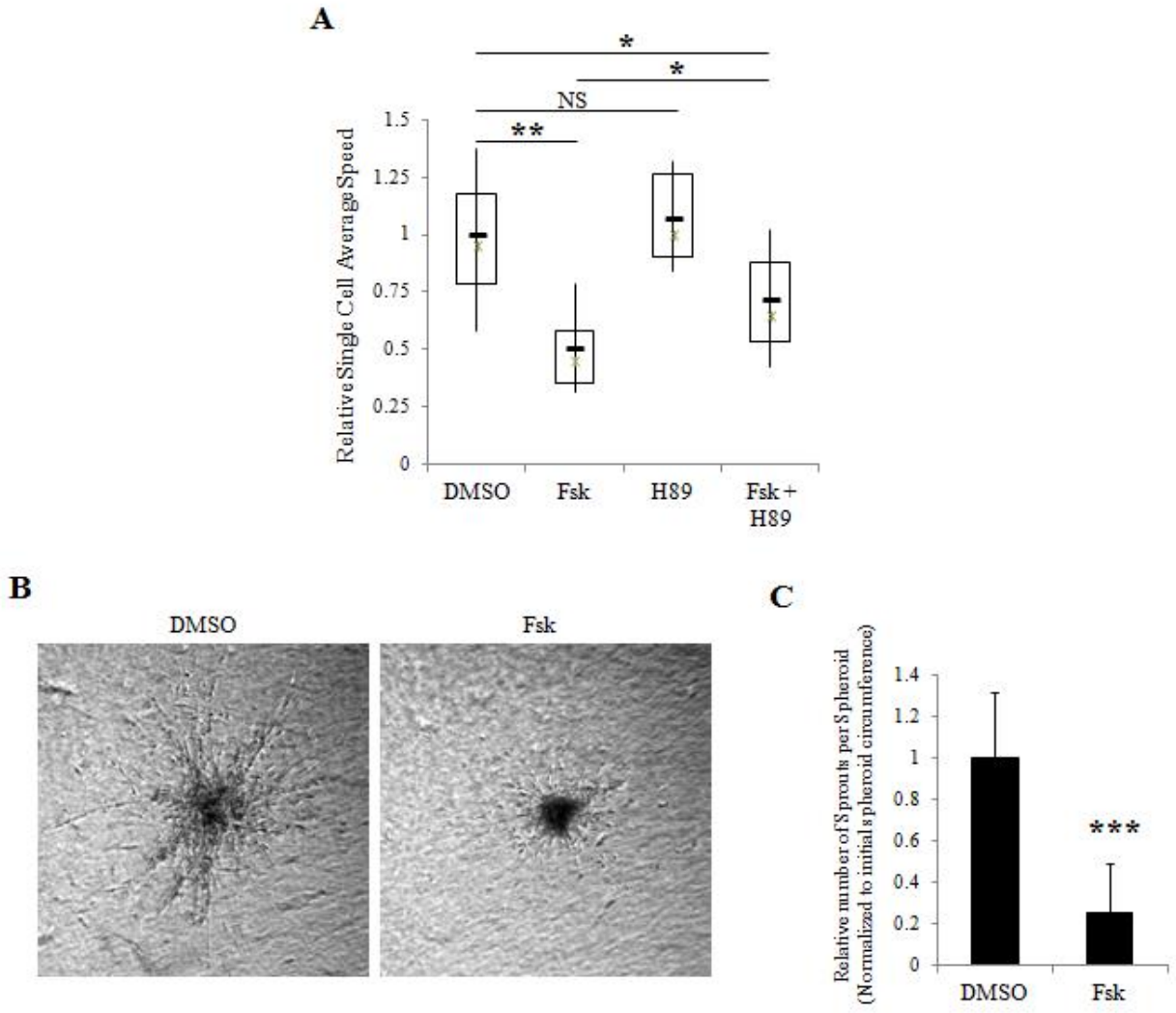

Figure 15. *Forskolin Inhibits Endothelial Cell Motility and Spheroid Sprouting.* (A) Box-and-whisker plots of the average cell speed of Forskolin- (Fsk), H89-, Forskolin/H89-, and DMSO-treated HMEC-1 seeded on a collagen-coated dish normalized to the DMSO group. The average speed of the DMSO cells was 0.81 μm-min^{-1}. (B) Representative images of spheroid sprouting following 48 hours incubation. (C) Quantification of the number of sprouts per spheroid normalized to the cross-sectional area of the sprout just after embedding. (* $p<0.05$; ** $p<0.005$; *** $p<0.0001$; NS Not Significant)

5.2.6 Phospho-mimetic Mutation of Profilin-1 on Protein Kinase A Targets Does Not Affect Profilin-1-Ligand Interaction

Together, the prior data suggest PKA plays a role in regulating Pfn1-polyproline interaction and forskolin mediates a phenotype in endothelial cells similar to that of polyproline binding-deficient Pfn1. To attempt to link these two correlative observations through Pfn1, it is necessary to determine what specific residue PKA is modifying. Therefore, we next examined whether the previously determined targets of *in vitro* PKA phosphorylation, namely Serine 57 (S57), T89, and Threonine 92 (T92), could impact Pfn1-ligand interaction using a pulldown assay. In addition to these three sites, Serine 91 (S91) was also included in the analysis because it is the only residue in Pfn1 with a consensus sequence for PKA phosphorylation (Arginine-X-X-Serine, where X can be any amino acid). Phospho-mimetic mutation of these residues had no effect on Pfn1-VASP or Pfn1-G-actin binding (Figure 16A). Interestingly, much like eukaryotic cells, Pfn1-T89D could not be extracted from bacteria.

5.2.7 Protein Kinase A May Phosphorylate Profilin-1 on Serine 137 *in vitro*

It is possible that other sites were phosphorylated by PKA but mass spectrometric analysis missed them because of low levels or poor coverage. One such site is Serine 137 (S137). Using tryptic digestion, S137 will reside on a peptide comprised of four amino acids, too small for mass spectrometric analysis, and will therefore always be missed. Using a PKA phosphorylated substrate antibody raised against phosphorylated Arginine-Arginine-X-Serine/Threonine (pRRXS/T), where X can be any amino acid, we see both PKA-treated GST-Pfn1 and His-Pfn1 are recognized (Figure 16B-C); however, Pfn1 contains no such sequence. In fact, the only

consecutive Arginine residues reside on the N-terminal side of S137 (RRS). How stringent this antibody is with regard to the presence of the amino acid separating the RR and S is not clear, but this suggests Pfn1 may be phosphorylated at S137 by PKA *in vitro*.

5.2.8 Phospho-mimetic Mutation of Profilin-1 at Serine 137 Inhibits Profilin-1-Polyproline Interaction

Although several studies have assessed the impact of S137 phosphorylation on polyproline interaction, the results were not consistent. This could possibly be due to confounding factors or some sort of context-specificity. Therefore, we wanted to determine the significance of S137 phosphorylation on interaction changes in endothelial cells. Phospho-mimetic S137 (S137E) mutation resulted in nearly complete ablation of Pfn1-VASP interaction while phospho-dead S137 (S137A) had a more mild effect (Figure 16D). Therefore, it is likely that S137 phosphorylation negatively impacts Pfn1-polyproline interaction in endothelial cells.

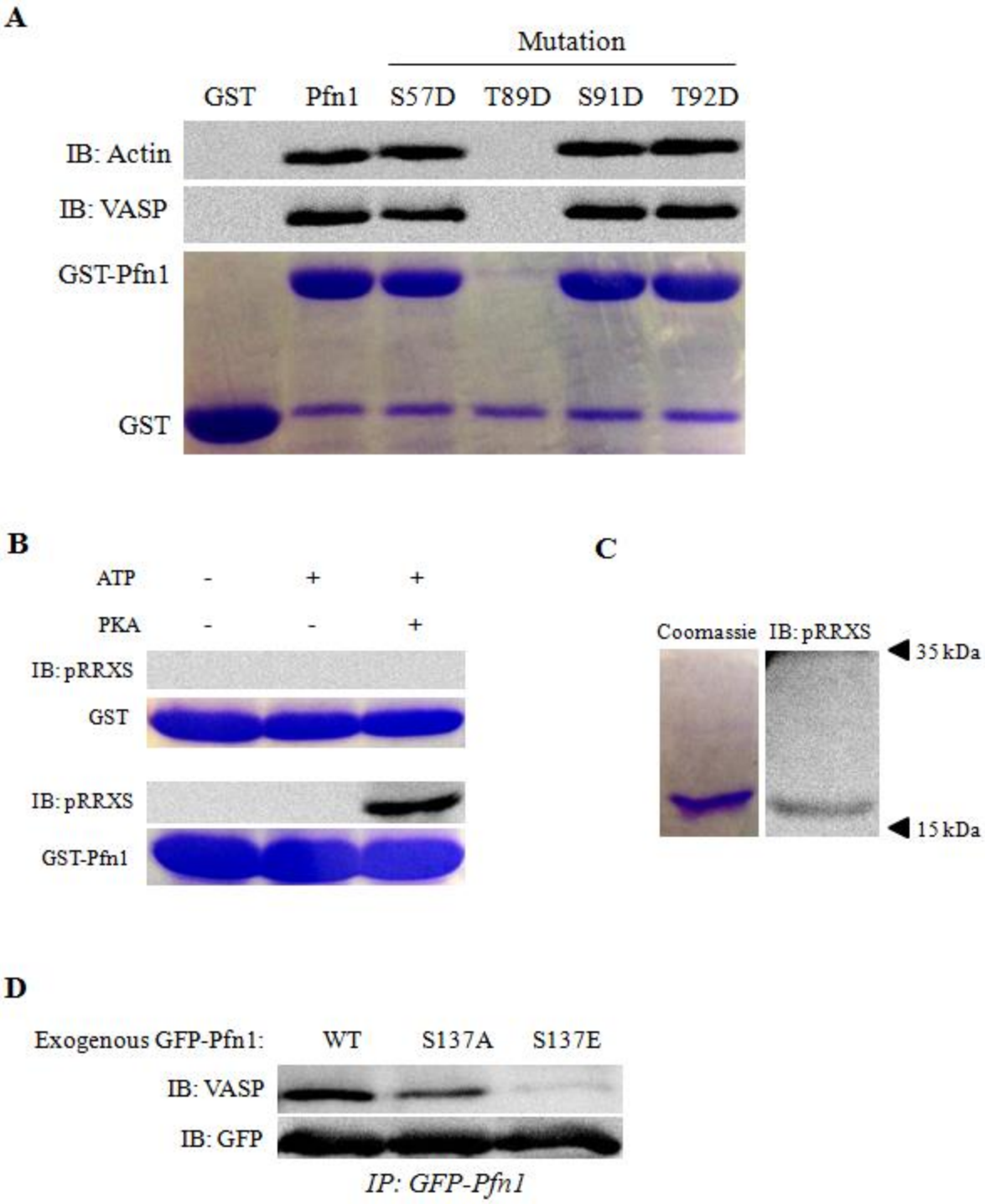

Figure 16. *PKA May Negatively Regulate Profilin-1-Polyproline Interaction through Serine 137 Phosphorylation.* (A) Parallel Western blot and coomassie stain following GST pulldown using the indicated Pfn1 mutant constructs. Proteins were eluted from beads and supernatant equally split for analysis. The presence of GST in all groups is a

result of residual GST-conjugated beads following pre-clear of the whole-cell lysate, but GST group alone confirms it had no impact on pulldown. (B) Parallel Western blot and coomassie stain of GST-Pfn1 following *in vitro* PKA kinase assay. Proteins were similarly eluted from beads and split equally. Treatments are indicated. (C) Parallel Western blot and coomassie stain of His-Pfn1 following *in vitro* PKA kinase assay. Protein was split equally. (D) Co-immunoprecipitation of VASP with GFP-Pfn1 or S137 mutants from HMEC-1.

5.2.9 Phospho-mimetic Mutation of Profilin-1 at Serine 137 Reduces Endothelial Cell Motility

The importance of Pfn1-ligand interaction on endothelial cell migration has been previously discussed [188]. It was determined that Pfn1 must maintain both polyproline and actin interaction to promote single-cell random motility. Because phospho-mimetic mutation of Pfn1 at S137 reduced Pfn1-VASP interaction in endothelial cells, we wanted to determine if it had a similar impact on cell migration. To accomplish this, we employed the same Pfn1 siRNA-resistant GFP-Pfn1 construct and expressed both the S137A and S137E mutations. The success of this system in this regard can be seen in Figure 17A. S137E mutation significantly reduced endothelial cell motility while, as previously seen while assessing polyproline interaction, S137A had a mild and insignificant effect (Figure 17B). Phospho-mimetic mutation of S137, therefore, produces the same phenotype as other polyproline binding-deficient Pfn1 mutations.

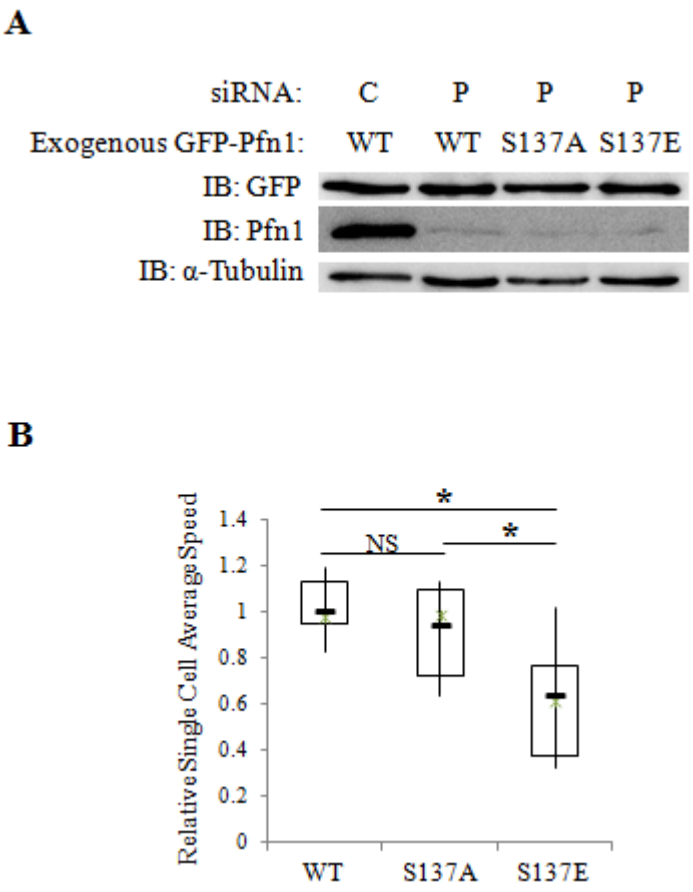

Figure 17. *Phospho-mimetic Mutation of Profilin-1 at Serine 137 Reduces Endothelial Cell Motility.* (A) Western blot of HMEC-1 cells expressing siRNA-resistant GFP-Pfn1 or S137A or S137E mutants with Control (C) or Pfn1 siRNA (P). (B) Box-and-whisker plots of the average cell speed of Pfn1 siRNA-treated HMEC-1 expressing respective constructs seeded on a collagen-coated dish normalized to the GFP-Pfn1 group. The average speed of the GFP-Pfn1 cells was 0.31 μm-min^{-1}. Time-lapse imaging was carried out 96 hours post-transfection after cells were incubated 24 hours. (* $p<0.01$; NS Not Significant)

5.3 DISCUSSION

This study previously demonstrated the importance of Pfn1 in sprouting angiogenesis and the capacity for it to be phosphorylated by PKA *in vitro*. To combine these observations, we asked what impact PKA might have on Pfn1 function *in vivo* and endothelial sprouting. We first determined that Pfn1 was post-translationally modified *in vivo* downstream PKA. Additionally, Pfn1-polyproline interaction, as assessed by Pfn1-VASP interaction, was disrupted downstream PKA. Although VASP is strongly phosphorylated by PKA, this modification has no impact on Pfn1-VASP interaction, so binding changes could be due to modification of Pfn1 [279]. These data suggest a role for PKA in the regulation of Pfn1 function.

Similar to polyproline binding-deficient Pfn1, Forskolin treatment inhibited single-cell random migration downstream PKA. Accordingly, Forskolin treatment also inhibited endothelial cell spheroid sprouting. Because it had yet to be investigated, we next determined that Pfn1 must maintain polyproline interaction to promote sprouting. This result is not surprising as polyproline binding-deficient Pfn1 inhibited both endothelial cell migration and morphogenesis [188]. Therefore, we have correlative observations that (1) Pfn1-polyproline interaction is inhibited downstream PKA; (2) Pfn1 must maintain polyproline binding-capacity to promote sprouting angiogenesis; and (3) PKA negatively regulates endothelial cell migration and spheroid sprouting similar to polyproline binding-deficient Pfn1. It follows that we must determine which residues on Pfn1 are specifically regulated downstream PKA to establish a complete relationship; however, none of the residues previously identified to be phosphorylated by PKA *in vitro* affected Pfn1-ligand interation. The only exception was T89 because, just like with eukaryotic cells, it could not be extracted from bacteria using non-denaturing buffer. In general, T89 cannot be commented on, but its position relative to the polyproline binding site may indicate that it

would not be involved. A phosphorylated substrate-specific antibody (pRRXS/T) recognized both GST-Pfn1 and His-Pfn1 following PKA treatment *in vitro*. S137 was the most likely target of this antibody as it is the only residue in Pfn1 adjacent to two consecutive arginines (RRS). Interestingly, phospho-mimetic mutation of S137 both decreased endothelial cell migration and inhibited Pfn1-polyproline interaction, making it an interesting target for future study.

In conclusion, we have established a possible role for Pfn1 in PKA-mediated inhibition of sprouting angiogenesis. To determine whether PKA inhibits endothelial cell function through its action on Pfn1, the specific post-translational modification to which Pfn1 is subjected must be identified. We presented evidence that S137 could be one such residue, but proof of its phosphorylation in cells is lacking. Mass spectrometry could be used if Pfn1 is digested using a different enzyme. In addition, a phospho-dead S137 could be treated with PKA to determine if the utilized antibody was truly recognizing S137 phosphorylation. Other previously identified serine and threonine phosphorylation sites could also be considered in a similar manner. Ultimately, the capacity to rescue the PKA-mediated decrease in endothelial sprouting by introducing a phospho-dead mutation will need to be examined to establish a causal relationship. This will lead to knowledge that PKA can negatively impact endothelial cell function and sprouting angiogenesis by directly affecting the regulation of the actin cytoskeleton in a novel manner.

6.0 CONCLUSIONS

We determined that Pfn1 is required for endothelial sprouting using both *in vitro* and *ex vivo* angiogenesis assays. Further characterization revealed that in order to promote such behavior, Pfn1 must maintain its polyproline binding-capacity. This interaction, however, was disrupted by Forskolin downstream PKA. Similarly, Pfn1 was post-translationally modified downstream PKA *in vivo*. Although this does not prove PKA directly phosphorylates Pfn1 in cells, use of an *in vitro* kinase assay suggested this event is possible. Mass spectrometry identified Pfn1 was phosphorylated on S57, T89, and T92. Further characterization using a post-translational modification-specific antibody – anti-pRRXS – suggested S137 may also be modified by PKA. Using computer-aided simulation, we determined T89 phosphorylation might confer Pfn1 into a conformation that permits increased G-actin binding, but proof of this in cells was made difficult due to its insolubility. Phospho-mimetic mutation of the other sites determined by mass spectrometry did not affect Pfn1-polyproline interaction, but S137 mutation caused dramatically reduced binding. Accordingly, S137 mutation also impaired endothelial cell motility much like PKA activation. These data support a role for Pfn1 in PKA-mediated inhibition of endothelial cell motility and sprouting angiogenesis.

7.0 FUTURE DIRECTIONS

7.1 EXPLORING THE IMPORTANCE OF PROFILIN-1 IN SPROUTING ANGIOGENESIS IN VIVO

The present study establishes endothelial cell-specific knockout of Pfn1 as an embryonic lethal genotype, preventing study of its impact in an animal setting. To attempt to remedy this, an inducible mouse model can be generated by mating our $Pfn1^{fl/fl}$ mice with a commercially available Cdh5-Cre-ERT2 mouse (Cancer Research Technology). This transgenic mouse strain expresses Cre-ERT2 (under the Cdh5 or VE-Cadherin promoter, specific to endothelial cells), a fusion protein that consists of Cre fused to a mutant form of human estrogen receptor (ER) which only binds to a synthetic ER ligand such as 4-hydroxytamoxifen (OHT). The same mating scheme can be used to create $Pfn1^{fl/fl}$/ Cdh5-Cre-$ERT2^{+/-}$ mice. To study angiogenesis using the reteinal angiogenesis assay, post-natal knockout can be achieved by injecting pups with OHT in their stomach daily for 3 days from post-natal day 1 (P1) to P3.

Additionally, these mice can be used to study angiogenesis in the context of other physiological and pathological processes by inducing knockout at a later stage of life. Both would healing and cancer are highly dependent on angiogenesis. Mice generated using the schematic above should be theoretically viable and grow to adulthood. Injection of OHT into the local bloodstream should sufficiently knockout Pfn1 in the adjacent endothelial cells in the area

of interest. These mice can then be subjected to typical wound healing or tumor development and dissemination assays. Depending on the process that is being studied, either wound closure or tumor growth can be observed. Especially in the case of tumor development, these experiments could begin to elucidate the specific importance of vessels that arise from the native vasculature, as this has become a point of interest in some recent studies.

7.2 USE OF THE ENDOTHELIAL CELL-SPECIFIC PROFILIN-1 KNOCKOUT MICE

Pfn1 was also implicated as an important factor in endothelial cell-mediated activities during embryogenesis. Prior investigation into the role of the actin cytoskeleton during development showed knockout of all three mammalian Ena/VASP proteins – VASP, Mena, and EVL – exhibited deficiencies in vascular morphology as well as severe hemorrhaging due to reduced barrier function [280]. This mouse model was not endothelial cell-specific, so other deformities were observed, but this, along with other studies establishes a role for the actin cytoskeleton in the development of the vasculature [217]. It is not known to what stage of development $Pfn1^{EC,-/-}$ mice reach, but Tie2 is expressed as early as the first endothelial cells arise in the late primitive streak [281]. Therefore, investigation into the role of Pfn1 in endothelial development will begin during the gastrulation phase. Indeed, Pfn1 depletion impaired cell movement during gastrulation for several organisms, so it is possible Pfn1 is required for endothelial cell function as early as they are first differentiated [177, 179]. It would be interesting to determine how Pfn1 regulates endothelial cell function and fate in these early embryonic mice.

7.3 CHARACTERIZATION OF PROFILIN-1 POST-TRANSLATIONAL MODIFICATIONS

Finally, although this study attempted to characterize some known post-translational modifications of Pfn1, there are a number of others that have yet to be investigated. Not only determining how they are specifically regulated, but how they change Pfn1 intracellular function or localization. Phosphorylation of Pfn1 as a regulator of interaction has some precedence, but no study has considered lysine-acetylation and its role. In addition, it will be interesting to see how Pfn1 might be differentially regulated in other cell types, like cancer. Pfn1 associates with a number of proteins involved in many aspects of cellular homeostasis and signaling through its polyproline interaction, so knowledge of this will enhance our understanding of many aspects of cellular function.

BIBLIOGRAPHY

1. Metzler, W.J., et al., *Refined solution structure of human profilin I.* Protein Sci, 1995. **4**(3): p. 450-9.

2. Carlsson, L., et al., *Actin polymerizability is influenced by profilin, a low molecular weight protein in non-muscle cells.* J Mol Biol, 1977. **115**(3): p. 465-83.

3. Honore, B., et al., *Cloning and expression of a novel human profilin variant, profilin II.* FEBS Lett, 1993. **330**(2): p. 151-5.

4. Braun, A., et al., *Genomic organization of profilin-III and evidence for a transcript expressed exclusively in testis.* Gene, 2002. **283**(1-2): p. 219-25.

5. Obermann, H., et al., *Novel testis-expressed profilin IV associated with acrosome biogenesis and spermatid elongation.* Mol Hum Reprod, 2005. **11**(1): p. 53-64.

6. Karakesisoglou, I., et al., *Plant profilins rescue the aberrant phenotype of profilin-deficient Dictyostelium cells.* Cell Motil Cytoskeleton, 1996. **34**(1): p. 36-47.

7. Witke, W., et al., *Profilin I is essential for cell survival and cell division in early mouse development.* Proc Natl Acad Sci U S A, 2001. **98**(7): p. 3832-6.

8. Witke, W., et al., *In mouse brain profilin I and profilin II associate with regulators of the endocytic pathway and actin assembly.* EMBO J, 1998. **17**(4): p. 967-76.

9. Di Nardo, A., et al., *Alternative splicing of the mouse profilin II gene generates functionally different profilin isoforms.* J Cell Sci, 2000. **113 Pt 21**: p. 3795-803.

10. Lambrechts, A., et al., *Profilin II is alternatively spliced, resulting in profilin isoforms that are differentially expressed and have distinct biochemical properties.* Mol Cell Biol, 2000. **20**(21): p. 8209-19.

11. Tilney, L.G., *The polymerization of actin. II. How nonfilamentous actin becomes nonrandomly distributed in sperm: evidence for the association of this actin with membranes.* J Cell Biol, 1976. **69**(1): p. 51-72.

12. Tanaka, M. and H. Shibata, *Poly(L-proline)-binding proteins from chick embryos are a profilin and a profilactin.* Eur J Biochem, 1985. **151**(2): p. 291-7.

13. Lassing, I. and U. Lindberg, *Specific interaction between phosphatidylinositol 4,5-bisphosphate and profilactin.* Nature, 1985. **314**(6010): p. 472-4.

14. Bjorkegren, C., et al., *Mutagenesis of human profilin locates its poly(L-proline)-binding site to a hydrophobic patch of aromatic amino acids.* FEBS Lett, 1993. **333**(1-2): p. 123-6.

15. Sohn, R.H., et al., *Localization of a binding site for phosphatidylinositol 4,5-bisphosphate on human profilin.* J Biol Chem, 1995. **270**(36): p. 21114-20.

16. Lambrechts, A., et al., *Mutational analysis of human profilin I reveals a second PI(4,5)-P2 binding site neighbouring the poly(L-proline) binding site.* BMC Biochem, 2002. **3**: p. 12.

17. Metzler, W.J., et al., *Characterization of the three-dimensional solution structure of human profilin: 1H, 13C, and 15N NMR assignments and global folding pattern.* Biochemistry, 1993. **32**(50): p. 13818-29.

18. Ferron, F., et al., *Structural basis for the recruitment of profilin-actin complexes during filament elongation by Ena/VASP.* EMBO J, 2007. **26**(21): p. 4597-606.

19. Baek, K., et al., *Modulation of actin structure and function by phosphorylation of Tyr-53 and profilin binding.* Proc Natl Acad Sci U S A, 2008. **105**(33): p. 11748-53.

20. Tilney, L.G., *The role of actin in nonmuscle cell motility.* Soc Gen Physiol Ser, 1975. **30**: p. 339-88.

21. Tobacman, L.S. and E.D. Korn, *The kinetics of actin nucleation and polymerization.* J Biol Chem, 1983. **258**(5): p. 3207-14.

22. Pollard, T.D., *Polymerization of ADP-actin.* J Cell Biol, 1984. **99**(3): p. 769-77.

23. Cooper, J.A., et al., *Kinetic evidence for a monomer activation step in actin polymerization.* Biochemistry, 1983. **22**(9): p. 2193-202.

24. Lal, A.A., E.D. Korn, and S.L. Brenner, *Rate constants for actin polymerization in ATP determined using cross-linked actin trimers as nuclei.* J Biol Chem, 1984. **259**(14): p. 8794-800.

25. Woodrum, D.T., S.A. Rich, and T.D. Pollard, *Evidence for biased bidirectional polymerization of actin filaments using heavy meromyosin prepared by an improved method.* J Cell Biol, 1975. **67**(1): p. 231-7.

26. Wegner, A., *Head to tail polymerization of actin.* J Mol Biol, 1976. **108**(1): p. 139-50.

27. Brenner, S.L. and E.D. Korn, *On the mechanism of actin monomer-polymer subunit exchange at steady state.* J Biol Chem, 1983. **258**(8): p. 5013-20.

28. Carlier, M.F. and D. Pantaloni, *Direct evidence for ADP-Pi-F-actin as the major intermediate in ATP-actin polymerization. Rate of dissociation of Pi from actin filaments.* Biochemistry, 1986. **25**(24): p. 7789-92.

29. Carlier, M.F., *Actin polymerization and ATP hydrolysis.* Adv Biophys, 1990. **26**: p. 51-73.

30. Neidl, C. and J. Engel, *Exchange of ADP, ATP and 1: N6-ethenoadenosine 5'-triphosphate at G-actin. Equilibrium and kinetics.* Eur J Biochem, 1979. **101**(1): p. 163-9.

31. Hegyi, G., L. Szilagyi, and J. Belagyi, *Influence of the bound nucleotide on the molecular dynamics of actin.* Eur J Biochem, 1988. **175**(2): p. 271-4.

32. Carlier, M.F., D. Pantaloni, and E.D. Korn, *The mechanisms of ATP hydrolysis accompanying the polymerization of Mg-actin and Ca-actin.* J Biol Chem, 1987. **262**(7): p. 3052-9.

33. Pollard, T.D., *Rate constants for the reactions of ATP- and ADP-actin with the ends of actin filaments.* J Cell Biol, 1986. **103**(6 Pt 2): p. 2747-54.

34. Pollard, T.D. and J.A. Cooper, *Actin and actin-binding proteins. A critical evaluation of mechanisms and functions.* Annu Rev Biochem, 1986. **55**: p. 987-1035.

35. Wegner, A. and G. Isenberg, *12-fold difference between the critical monomer concentrations of the two ends of actin filaments in physiological salt conditions.* Proc Natl Acad Sci U S A, 1983. **80**(16): p. 4922-5.

36. Wang, Y.L., *Exchange of actin subunits at the leading edge of living fibroblasts: possible role of treadmilling.* J Cell Biol, 1985. **101**(2): p. 597-602.

37. Le Clainche, C. and M.F. Carlier, *Regulation of actin assembly associated with protrusion and adhesion in cell migration.* Physiol Rev, 2008. **88**(2): p. 489-513.

38. dos Remedios, C.G., et al., *Actin binding proteins: regulation of cytoskeletal microfilaments.* Physiol Rev, 2003. **83**(2): p. 433-73.

39. Tobacman, L.S. and E.D. Korn, *The regulation of actin polymerization and the inhibition of monomeric actin ATPase activity by Acanthamoeba profilin.* J Biol Chem, 1982. **257**(8): p. 4166-70.

40. Tobacman, L.S., S.L. Brenner, and E.D. Korn, *Effect of Acanthamoeba profilin on the pre-steady state kinetics of actin polymerization and on the concentration of F-actin at steady state.* J Biol Chem, 1983. **258**(14): p. 8806-12.

41. Tseng, P.C. and T.D. Pollard, *Mechanism of action of Acanthamoeba profilin: demonstration of actin species specificity and regulation by micromolar concentrations of MgCl2.* J Cell Biol, 1982. **94**(1): p. 213-8.

42. Goldschmidt-Clermont, P.J., et al., *The control of actin nucleotide exchange by thymosin beta 4 and profilin. A potential regulatory mechanism for actin polymerization in cells.* Mol Biol Cell, 1992. **3**(9): p. 1015-24.

43. Perelroizen, I., et al., *Role of nucleotide exchange and hydrolysis in the function of profilin in action assembly.* J Biol Chem, 1996. **271**(21): p. 12302-9.

44. Yarmola, E.G., D.A. Dranishnikov, and M.R. Bubb, *Effect of profilin on actin critical concentration: a theoretical analysis.* Biophys J, 2008. **95**(12): p. 5544-73.

45. Tilney, L.G., et al., *Actin from Thyone sperm assembles on only one end of an actin filament: a behavior regulated by profilin.* J Cell Biol, 1983. **97**(1): p. 112-24.

46. Pollard, T.D. and J.A. Cooper, *Quantitative analysis of the effect of Acanthamoeba profilin on actin filament nucleation and elongation.* Biochemistry, 1984. **23**(26): p. 6631-41.

47. Pring, M., A. Weber, and M.R. Bubb, *Profilin-actin complexes directly elongate actin filaments at the barbed end.* Biochemistry, 1992. **31**(6): p. 1827-36.

48. Nyman, T., et al., *A cross-linked profilin-actin heterodimer interferes with elongation at the fast-growing end of F-actin.* J Biol Chem, 2002. **277**(18): p. 15828-33.

49. DiNubile, M.J. and S. Huang, *Capping of the barbed ends of actin filaments by a high-affinity profilin-actin complex.* Cell Motil Cytoskeleton, 1997. **37**(3): p. 211-25.

50. Pantaloni, D. and M.F. Carlier, *How profilin promotes actin filament assembly in the presence of thymosin beta 4.* Cell, 1993. **75**(5): p. 1007-14.

51. Romero, S., et al., *How ATP hydrolysis controls filament assembly from profilin-actin: implication for formin processivity.* J Biol Chem, 2007. **282**(11): p. 8435-45.

52. Kinosian, H.J., et al., *Actin filament barbed end elongation with nonmuscle MgATP-actin and MgADP-actin in the presence of profilin.* Biochemistry, 2002. **41**(21): p. 6734-43.

53. Yarmola, E.G. and M.R. Bubb, *Profilin: emerging concepts and lingering misconceptions.* Trends Biochem Sci, 2006. **31**(4): p. 197-205.

54. Gutsche-Perelroizen, I., et al., *Filament assembly from profilin-actin.* J Biol Chem, 1999. **274**(10): p. 6234-43.

55. Nishida, E., S. Maekawa, and H. Sakai, *Cofilin, a protein in porcine brain that binds to actin filaments and inhibits their interactions with myosin and tropomyosin.* Biochemistry, 1984. **23**(22): p. 5307-13.

56. Yeoh, S., et al., *Determining the differences in actin binding by human ADF and cofilin.* J Mol Biol, 2002. **315**(4): p. 911-25.

57. Andrianantoandro, E. and T.D. Pollard, *Mechanism of actin filament turnover by severing and nucleation at different concentrations of ADF/cofilin.* Mol Cell, 2006. **24**(1): p. 13-23.

58. Didry, D., M.F. Carlier, and D. Pantaloni, *Synergy between actin depolymerizing factor/cofilin and profilin in increasing actin filament turnover.* J Biol Chem, 1998. **273**(40): p. 25602-11.

59. Stossel, T.P., *On the crawling of animal cells.* Science, 1993. **260**(5111): p. 1086-94.

60. Southwick, F.S. and D.L. Purich, *Dynamic remodeling of the actin cytoskeleton: lessons learned from Listeria locomotion.* Bioessays, 1994. **16**(12): p. 885-91.

61. Malm, B., L.E. Nystrom, and U. Lindberg, *The effect of proteolysis on the stability of the profilactin complex.* FEBS Lett, 1980. **113**(2): p. 241-4.

62. Markey, F., T. Persson, and U. Lindberg, *Characterization of platelet extracts before and after stimulation with respect to the possible role of profilactin as microfilament precursor.* Cell, 1981. **23**(1): p. 145-53.

63. Southwick, F.S. and C.L. Young, *The actin released from profilin--actin complexes is insufficient to account for the increase in F-actin in chemoattractant-stimulated polymorphonuclear leukocytes.* J Cell Biol, 1990. **110**(6): p. 1965-73.

64. Cassimeris, L., et al., *Thymosin beta 4 sequesters the majority of G-actin in resting human polymorphonuclear leukocytes.* J Cell Biol, 1992. **119**(5): p. 1261-70.

65. Nachmias, V.T., et al., *Thymosin beta 4 (T beta 4) in activated platelets.* Eur J Cell Biol, 1993. **61**(2): p. 314-20.

66. Safer, D. and V.T. Nachmias, *Beta thymosins as actin binding peptides.* Bioessays, 1994. **16**(8): p. 590.

67. Yarmola, E.G. and M.R. Bubb, *Effects of profilin and thymosin beta4 on the critical concentration of actin demonstrated in vitro and in cell extracts with a novel direct assay.* J Biol Chem, 2004. **279**(32): p. 33519-27.

68. Theriot, J.A., et al., *Involvement of profilin in the actin-based motility of L. monocytogenes in cells and in cell-free extracts.* Cell, 1994. **76**(3): p. 505-17.

69. Schafer, D.A. and J.A. Cooper, *Control of actin assembly at filament ends.* Annu Rev Cell Dev Biol, 1995. **11**: p. 497-518.

70. Schafer, D.A., P.B. Jennings, and J.A. Cooper, *Dynamics of capping protein and actin assembly in vitro: uncapping barbed ends by polyphosphoinositides.* J Cell Biol, 1996. **135**(1): p. 169-79.

71. Carlier, M.F. and D. Pantaloni, *Control of actin dynamics in cell motility.* J Mol Biol, 1997. **269**(4): p. 459-67.

72. Dufort, P.A. and C.J. Lumsden, *How profilin/barbed-end synergy controls actin polymerization: a kinetic model of the ATP hydrolysis circuit.* Cell Motil Cytoskeleton, 1996. **35**(4): p. 309-30.

73. Babcock, G. and P.A. Rubenstein, *Control of profilin and actin expression in muscle and nonmuscle cells.* Cell Motil Cytoskeleton, 1993. **24**(3): p. 179-88.

74. Sanders, M.C. and Y.L. Wang, *Exogenous nucleation sites fail to induce detectable polymerization of actin in living cells.* J Cell Biol, 1990. **110**(2): p. 359-65.

75. Handel, S.E., K.A. Hendry, and P. Sheterline, *Microinjection of covalently cross-linked actin oligomers causes disruption of existing actin filament architecture in PtK2 cells.* J Cell Sci, 1990. **97 (Pt 2)**: p. 325-33.

76. Lindberg, U., et al., *The use of poly(L-proline)-Sepharose in the isolation of profilin and profilactin complexes.* Biochim Biophys Acta, 1988. **967**(3): p. 391-400.

77. Reinhard, M., et al., *The proline-rich focal adhesion and microfilament protein VASP is a ligand for profilins.* EMBO J, 1995. **14**(8): p. 1583-9.

78. Gertler, F.B., et al., *Mena, a relative of VASP and Drosophila Enabled, is implicated in the control of microfilament dynamics.* Cell, 1996. **87**(2): p. 227-39.

79. Watanabe, N., et al., *p140mDia, a mammalian homolog of Drosophila diaphanous, is a target protein for Rho small GTPase and is a ligand for profilin.* EMBO J, 1997. **16**(11): p. 3044-56.

80. Miki, H., S. Suetsugu, and T. Takenawa, *WAVE, a novel WASP-family protein involved in actin reorganization induced by Rac.* EMBO J, 1998. **17**(23): p. 6932-41.

81. Lafuente, E.M., et al., *RIAM, an Ena/VASP and Profilin ligand, interacts with Rap1-GTP and mediates Rap1-induced adhesion.* Dev Cell, 2004. **7**(4): p. 585-95.

82. Boukhelifa, M., et al., *The proline-rich protein palladin is a binding partner for profilin.* FEBS J, 2006. **273**(1): p. 26-33.

83. Ramesh, N., et al., *WIP, a protein associated with wiskott-aldrich syndrome protein, induces actin polymerization and redistribution in lymphoid cells.* Proc Natl Acad Sci U S A, 1997. **94**(26): p. 14671-6.

84. Yayoshi-Yamamoto, S., I. Taniuchi, and T. Watanabe, *FRL, a novel formin-related protein, binds to Rac and regulates cell motility and survival of macrophages.* Mol Cell Biol, 2000. **20**(18): p. 6872-81.

85. Alvarez-Martinez, M.T., et al., *Characterization of the interaction between annexin I and profilin.* Eur J Biochem, 1996. **238**(3): p. 777-84.

86. Shao, J., et al., *Phosphorylation of profilin by ROCK1 regulates polyglutamine aggregation.* Mol Cell Biol, 2008. **28**(17): p. 5196-208.

87. Mammoto, A., et al., *Interactions of drebrin and gephyrin with profilin.* Biochem Biophys Res Commun, 1998. **243**(1): p. 86-9.

88. Wang, X., et al., *Aczonin, a 550-kD putative scaffolding protein of presynaptic active zones, shares homology regions with Rim and Bassoon and binds profilin.* J Cell Biol, 1999. **147**(1): p. 151-62.

89. Miyagi, Y., et al., *Delphilin: a novel PDZ and formin homology domain-containing protein that synaptically colocalizes and interacts with glutamate receptor delta 2 subunit.* J Neurosci, 2002. **22**(3): p. 803-14.

90. Giesemann, T., et al., *A role for polyproline motifs in the spinal muscular atrophy protein SMN. Profilins bind to and colocalize with smn in nuclear gems.* J Biol Chem, 1999. **274**(53): p. 37908-14.

91. Stuven, T., E. Hartmann, and D. Gorlich, *Exportin 6: a novel nuclear export receptor that is specific for profilin.actin complexes.* EMBO J, 2003. **22**(21): p. 5928-40.

92. Lederer, M., B.M. Jockusch, and M. Rothkegel, *Profilin regulates the activity of p42POP, a novel Myb-related transcription factor.* J Cell Sci, 2005. **118**(Pt 2): p. 331-41.

93. Machesky, L.M. and T.D. Poland, *Profilin as a potential mediator of membrane-cytoskeleton communication.* Trends Cell Biol, 1993. **3**(11): p. 381-5.

94. Metzler, W.J., et al., *Identification of the poly-L-proline-binding site on human profilin.* J Biol Chem, 1994. **269**(6): p. 4620-5.

95. Mahoney, N.M., P.A. Janmey, and S.C. Almo, *Structure of the profilin-poly-L-proline complex involved in morphogenesis and cytoskeletal regulation.* Nat Struct Biol, 1997. **4**(11): p. 953-60.

96. Mullins, R.D., J.A. Heuser, and T.D. Pollard, *The interaction of Arp2/3 complex with actin: nucleation, high affinity pointed end capping, and formation of branching networks of filaments.* Proc Natl Acad Sci U S A, 1998. **95**(11): p. 6181-6.

97. Millard, T.H., S.J. Sharp, and L.M. Machesky, *Signalling to actin assembly via the WASP (Wiskott-Aldrich syndrome protein)-family proteins and the Arp2/3 complex.* Biochem J, 2004. **380**(Pt 1): p. 1-17.

98. Rodal, A.A., et al., *Conformational changes in the Arp2/3 complex leading to actin nucleation.* Nat Struct Mol Biol, 2005. **12**(1): p. 26-31.

99. Pruyne, D., et al., *Role of formins in actin assembly: nucleation and barbed-end association.* Science, 2002. **297**(5581): p. 612-5.

100. Pring, M., et al., *Mechanism of formin-induced nucleation of actin filaments.* Biochemistry, 2003. **42**(2): p. 486-96.

101. Zigmond, S.H., et al., *Formin leaky cap allows elongation in the presence of tight capping proteins.* Curr Biol, 2003. **13**(20): p. 1820-3.

102. Ramalingam, N., et al., *Phospholipids regulate localization and activity of mDia1 formin.* Eur J Cell Biol, 2010. **89**(10): p. 723-32.

103. Kurokawa, K. and M. Matsuda, *Localized RhoA activation as a requirement for the induction of membrane ruffling.* Mol Biol Cell, 2005. **16**(9): p. 4294-303.

104. Nicholson-Dykstra, S., H.N. Higgs, and E.S. Harris, *Actin dynamics: growth from dendritic branches.* Curr Biol, 2005. **15**(9): p. R346-57.

105. Urban, E., et al., *Electron tomography reveals unbranched networks of actin filaments in lamellipodia.* Nat Cell Biol, 2010. **12**(5): p. 429-35.

106. Yang, C., et al., *Novel roles of formin mDia2 in lamellipodia and filopodia formation in motile cells.* PLoS Biol, 2007. **5**(11): p. e317.

107. Yang, C. and T. Svitkina, *Filopodia initiation: focus on the Arp2/3 complex and formins.* Cell Adh Migr, 2011. **5**(5): p. 402-8.

108. Quinlan, M.E., et al., *Drosophila Spire is an actin nucleation factor.* Nature, 2005. **433**(7024): p. 382-8.

109. Baum, B. and P. Kunda, *Actin nucleation: spire - actin nucleator in a class of its own.* Curr Biol, 2005. **15**(8): p. R305-8.

110. Montaville, P., et al., *Spire and Formin 2 synergize and antagonize in regulating actin assembly in meiosis by a ping-pong mechanism.* PLoS Biol, 2014. **12**(2): p. e1001795.

111. Ahuja, R., et al., *Cordon-bleu is an actin nucleation factor and controls neuronal morphology.* Cell, 2007. **131**(2): p. 337-50.

112. Chereau, D., et al., *Leiomodin is an actin filament nucleator in muscle cells.* Science, 2008. **320**(5873): p. 239-43.

113. Hug, C., et al., *Capping protein levels influence actin assembly and cell motility in dictyostelium.* Cell, 1995. **81**(4): p. 591-600.

114. Kovar, D.R., et al., *Control of the assembly of ATP- and ADP-actin by formins and profilin.* Cell, 2006. **124**(2): p. 423-35.

115. Kovar, D.R. and T.D. Pollard, *Progressing actin: Formin as a processive elongation machine.* Nat Cell Biol, 2004. **6**(12): p. 1158-9.

116. Applewhite, D.A., et al., *Ena/VASP proteins have an anti-capping independent function in filopodia formation.* Mol Biol Cell, 2007. **18**(7): p. 2579-91.

117. Krause, M., et al., *Ena/VASP proteins: regulators of the actin cytoskeleton and cell migration.* Annu Rev Cell Dev Biol, 2003. **19**: p. 541-64.

118. Breitsprecher, D., et al., *Molecular mechanism of Ena/VASP-mediated actin-filament elongation.* EMBO J, 2011. **30**(3): p. 456-67.

119. Breitsprecher, D., et al., *Clustering of VASP actively drives processive, WH2 domain-mediated actin filament elongation.* EMBO J, 2008. **27**(22): p. 2943-54.

120. Hansen, S.D. and R.D. Mullins, *VASP is a processive actin polymerase that requires monomeric actin for barbed end association.* J Cell Biol, 2010. **191**(3): p. 571-84.

121. Krause, M., et al., *Lamellipodin, an Ena/VASP ligand, is implicated in the regulation of lamellipodial dynamics.* Dev Cell, 2004. **7**(4): p. 571-83.

122. Loisel, T.P., et al., *Reconstitution of actin-based motility of Listeria and Shigella using pure proteins.* Nature, 1999. **401**(6753): p. 613-6.

123. Boujemaa-Paterski, R., et al., *Listeria protein ActA mimics WASp family proteins: it activates filament barbed end branching by Arp2/3 complex.* Biochemistry, 2001. **40**(38): p. 11390-404.

124. Wiesner, S., et al., *A biomimetic motility assay provides insight into the mechanism of actin-based motility.* J Cell Biol, 2003. **160**(3): p. 387-98.

125. Romero, S., et al., *Formin is a processive motor that requires profilin to accelerate actin assembly and associated ATP hydrolysis.* Cell, 2004. **119**(3): p. 419-29.

126. Smith, G.A., J.A. Theriot, and D.A. Portnoy, *The tandem repeat domain in the Listeria monocytogenes ActA protein controls the rate of actin-based motility, the percentage of moving bacteria, and the localization of vasodilator-stimulated phosphoprotein and profilin.* J Cell Biol, 1996. **135**(3): p. 647-60.

127. Niebuhr, K., et al., *A novel proline-rich motif present in ActA of Listeria monocytogenes and cytoskeletal proteins is the ligand for the EVH1 domain, a protein module present in the Ena/VASP family.* EMBO J, 1997. **16**(17): p. 5433-44.

128. Grenklo, S., et al., *A crucial role for profilin-actin in the intracellular motility of Listeria monocytogenes.* EMBO Rep, 2003. **4**(5): p. 523-9.

129. Yarar, D., et al., *Motility determinants in WASP family proteins.* Mol Biol Cell, 2002. **13**(11): p. 4045-59.

130. Ezezika, O.C., et al., *Incompatibility with formin Cdc12p prevents human profilin from substituting for fission yeast profilin: insights from crystal structures of fission yeast profilin.* J Biol Chem, 2009. **284**(4): p. 2088-97.

131. Laurent, V., et al., *Role of proteins of the Ena/VASP family in actin-based motility of Listeria monocytogenes.* J Cell Biol, 1999. **144**(6): p. 1245-58.

132. Auerbuch, V., et al., *Ena/VASP proteins contribute to Listeria monocytogenes pathogenesis by controlling temporal and spatial persistence of bacterial actin-based motility.* Mol Microbiol, 2003. **49**(5): p. 1361-75.

133. Geese, M., et al., *Contribution of Ena/VASP proteins to intracellular motility of listeria requires phosphorylation and proline-rich core but not F-actin binding or multimerization.* Mol Biol Cell, 2002. **13**(7): p. 2383-96.

134. Gau, D., et al., *Fluorescence Resonance Energy Transfer (FRET)-based Detection of Profilin-VASP Interaction.* Cell Mol Bioeng, 2011. **4**(1): p. 1-8.

135. Hartwig, J.H., et al., *Association of profilin with filament-free regions of human leukocyte and platelet membranes and reversible membrane binding during platelet activation.* J Cell Biol, 1989. **109**(4 Pt 1): p. 1571-9.

136. Lu, P.J., et al., *Lipid products of phosphoinositide 3-kinase bind human profilin with high affinity.* Biochemistry, 1996. **35**(44): p. 14027-34.

137. Moens, P.D. and L.A. Bagatolli, *Profilin binding to sub-micellar concentrations of phosphatidylinositol (4,5) bisphosphate and phosphatidylinositol (3,4,5) trisphosphate.* Biochim Biophys Acta, 2007. **1768**(3): p. 439-49.

138. Krishnan, K., et al., *Profilin interaction with phosphatidylinositol (4,5)-bisphosphate destabilizes the membrane of giant unilamellar vesicles.* Biophys J, 2009. **96**(12): p. 5112-21.

139. Bae, Y.H., et al., *Loss of profilin-1 expression enhances breast cancer cell motility by Ena/VASP proteins.* J Cell Physiol, 2009. **219**(2): p. 354-64.

140. Das, T., et al., *Profilin-1 overexpression upregulates PTEN and suppresses AKT activation in breast cancer cells.* J Cell Physiol, 2009. **218**(2): p. 436-43.

141. Bae, Y.H., et al., *Profilin1 regulates PI(3,4)P2 and lamellipodin accumulation at the leading edge thus influencing motility of MDA-MB-231 cells.* Proc Natl Acad Sci U S A, 2010. **107**(50): p. 21547-52.

142. Zhao, H., M. Hakala, and P. Lappalainen, *ADF/cofilin binds phosphoinositides in a multivalent manner to act as a PIP(2)-density sensor.* Biophys J, 2010. **98**(10): p. 2327-36.

143. Rohatgi, R., H.Y. Ho, and M.W. Kirschner, *Mechanism of N-WASP activation by CDC42 and phosphatidylinositol 4, 5-bisphosphate.* J Cell Biol, 2000. **150**(6): p. 1299-310.

144. Krahn, M.P. and A. Wodarz, *Phosphoinositide lipids and cell polarity: linking the plasma membrane to the cytocortex.* Essays Biochem, 2012. **53**: p. 15-27.

145. Small, J.V., et al., *The lamellipodium: where motility begins.* Trends Cell Biol, 2002. **12**(3): p. 112-20.

146. Svitkina, T.M., et al., *Mechanism of filopodia initiation by reorganization of a dendritic network.* J Cell Biol, 2003. **160**(3): p. 409-21.

147. Nobes, C.D. and A. Hall, *Rho GTPases control polarity, protrusion, and adhesion during cell movement.* J Cell Biol, 1999. **144**(6): p. 1235-44.

148. Das, B., et al., *Control of intramolecular interactions between the pleckstrin homology and Dbl homology domains of Vav and Sos1 regulates Rac binding.* J Biol Chem, 2000. **275**(20): p. 15074-81.

149. Yoshida, S., S. Bartolini, and D. Pellman, *Mechanisms for concentrating Rho1 during cytokinesis.* Genes Dev, 2009. **23**(7): p. 810-23.

150. Sit, S.T. and E. Manser, *Rho GTPases and their role in organizing the actin cytoskeleton.* J Cell Sci, 2011. **124**(Pt 5): p. 679-83.

151. Pertz, O., et al., *Spatiotemporal dynamics of RhoA activity in migrating cells.* Nature, 2006. **440**(7087): p. 1069-72.

152. Machacek, M., et al., *Coordination of Rho GTPase activities during cell protrusion.* Nature, 2009. **461**(7260): p. 99-103.

153. Zigmond, S.H., *Formin-induced nucleation of actin filaments.* Curr Opin Cell Biol, 2004. **16**(1): p. 99-105.

154. Lammers, M., et al., *Specificity of interactions between mDia isoforms and Rho proteins.* J Biol Chem, 2008. **283**(50): p. 35236-46.

155. Nishita, M., et al., *Spatial and temporal regulation of cofilin activity by LIM kinase and Slingshot is critical for directional cell migration.* J Cell Biol, 2005. **171**(2): p. 349-59.

156. Worthylake, R.A. and K. Burridge, *RhoA and ROCK promote migration by limiting membrane protrusions.* J Biol Chem, 2003. **278**(15): p. 13578-84.

157. Kunisaki, Y., et al., *DOCK2 is a Rac activator that regulates motility and polarity during neutrophil chemotaxis.* J Cell Biol, 2006. **174**(5): p. 647-52.

158. Nishikimi, A., et al., *Sequential regulation of DOCK2 dynamics by two phospholipids during neutrophil chemotaxis.* Science, 2009. **324**(5925): p. 384-7.

159. McCarty, O.J., et al., *Rac1 is essential for platelet lamellipodia formation and aggregate stability under flow.* J Biol Chem, 2005. **280**(47): p. 39474-84.

160. Tomasevic, N., et al., *Differential regulation of WASP and N-WASP by Cdc42, Rac1, Nck, and PI(4,5)P2.* Biochemistry, 2007. **46**(11): p. 3494-502.

161. Lorenz, M., et al., *Imaging sites of N-wasp activity in lamellipodia and invadopodia of carcinoma cells.* Curr Biol, 2004. **14**(8): p. 697-703.

162. Stradal, T.E. and G. Scita, *Protein complexes regulating Arp2/3-mediated actin assembly.* Curr Opin Cell Biol, 2006. **18**(1): p. 4-10.

163. Rottner, K., A. Hall, and J.V. Small, *Interplay between Rac and Rho in the control of substrate contact dynamics.* Curr Biol, 1999. **9**(12): p. 640-8.

164. Arthur, W.T. and K. Burridge, *RhoA inactivation by p190RhoGAP regulates cell spreading and migration by promoting membrane protrusion and polarity.* Mol Biol Cell, 2001. **12**(9): p. 2711-20.

165. Gupton, S.L. and F.B. Gertler, *Filopodia: the fingers that do the walking.* Sci STKE, 2007. **2007**(400): p. re5.

166. Snapper, S.B., et al., *N-WASP deficiency reveals distinct pathways for cell surface projections and microbial actin-based motility.* Nat Cell Biol, 2001. **3**(10): p. 897-904.

167. Peng, J., et al., *Disruption of the Diaphanous-related formin Drf1 gene encoding mDia1 reveals a role for Drf3 as an effector for Cdc42.* Curr Biol, 2003. **13**(7): p. 534-45.

168. Nobes, C.D. and A. Hall, *Rho, rac and cdc42 GTPases: regulators of actin structures, cell adhesion and motility.* Biochem Soc Trans, 1995. **23**(3): p. 456-9.

169. Wu, X., et al., *Cdc42 is crucial for the establishment of epithelial polarity during early mammalian development.* Dev Dyn, 2007. **236**(10): p. 2767-78.

170. Weber, K.S., et al., *Chemokine-induced monocyte transmigration requires cdc42-mediated cytoskeletal changes.* Eur J Immunol, 1998. **28**(7): p. 2245-51.

171. Miano, J.M., X. Long, and K. Fujiwara, *Serum response factor: master regulator of the actin cytoskeleton and contractile apparatus.* Am J Physiol Cell Physiol, 2007. **292**(1): p. C70-81.

172. Sun, Q., et al., *Defining the mammalian CArGome.* Genome Res, 2006. **16**(2): p. 197-207.

173. Arsenian, S., et al., *Serum response factor is essential for mesoderm formation during mouse embryogenesis.* EMBO J, 1998. **17**(21): p. 6289-99.

174. Alberti, S., et al., *Neuronal migration in the murine rostral migratory stream requires serum response factor.* Proc Natl Acad Sci U S A, 2005. **102**(17): p. 6148-53.

175. Haugwitz, M., et al., *Dictyostelium amoebae that lack G-actin-sequestering profilins show defects in F-actin content, cytokinesis, and development.* Cell, 1994. **79**(2): p. 303-14.

176. Verheyen, E.M. and L. Cooley, *Profilin mutations disrupt multiple actin-dependent processes during Drosophila development.* Development, 1994. **120**(4): p. 717-28.

177. Smith, L.C., et al., *The sea urchin profilin gene is specifically expressed in mesenchyme cells during gastrulation.* Dev Biol, 1994. **164**(2): p. 463-74.

178. Sato, A., et al., *Profilin is an effector for Daam1 in non-canonical Wnt signaling and is required for vertebrate gastrulation.* Development, 2006. **133**(21): p. 4219-31.

179. Lai, S.L., et al., *Diaphanous-related formin 2 and profilin I are required for gastrulation cell movements.* PLoS One, 2008. **3**(10): p. e3439.

180. Kullmann, J.A., et al., *Profilin1 is required for glial cell adhesion and radial migration of cerebellar granule neurons.* EMBO Rep, 2012. **13**(1): p. 75-82.

181. Janke, J., et al., *Suppression of tumorigenicity in breast cancer cells by the microfilament protein profilin 1.* J Exp Med, 2000. **191**(10): p. 1675-86.

182. Wang, W., et al., *Identification and testing of a gene expression signature of invasive carcinoma cells within primary mammary tumors.* Cancer Res, 2004. **64**(23): p. 8585-94.

183. Gronborg, M., et al., *Biomarker discovery from pancreatic cancer secretome using a differential proteomic approach.* Mol Cell Proteomics, 2006. **5**(1): p. 157-71.

184. Zoidakis, J., et al., *Profilin 1 is a potential biomarker for bladder cancer aggressiveness.* Mol Cell Proteomics, 2012. **11**(4): p. M111 009449.

185. Roy, P. and K. Jacobson, *Overexpression of profilin reduces the migration of invasive breast cancer cells.* Cell Motil Cytoskeleton, 2004. **57**(2): p. 84-95.

186. Zou, L., et al., *Profilin-1 is a negative regulator of mammary carcinoma aggressiveness.* Br J Cancer, 2007. **97**(10): p. 1361-71.

187. Ding, Z., et al., *Silencing profilin-1 inhibits endothelial cell proliferation, migration and cord morphogenesis.* J Cell Sci, 2006. **119**(Pt 19): p. 4127-37.

188. Ding, Z., et al., *Both actin and polyproline interactions of profilin-1 are required for migration, invasion and capillary morphogenesis of vascular endothelial cells.* Exp Cell Res, 2009. **315**(17): p. 2963-73.

189. Carmeliet, P., *Mechanisms of angiogenesis and arteriogenesis.* Nat Med, 2000. **6**(4): p. 389-95.

190. Risau, W. and I. Flamme, *Vasculogenesis.* Annu Rev Cell Dev Biol, 1995. **11**: p. 73-91.

191. Lee, S., et al., *Autocrine VEGF signaling is required for vascular homeostasis.* Cell, 2007. **130**(4): p. 691-703.

192. Hellstrom, M., et al., *Dll4 signalling through Notch1 regulates formation of tip cells during angiogenesis.* Nature, 2007. **445**(7129): p. 776-80.

193. Bentley, K., H. Gerhardt, and P.A. Bates, *Agent-based simulation of notch-mediated tip cell selection in angiogenic sprout initialisation.* J Theor Biol, 2008. **250**(1): p. 25-36.

194. Carmeliet, P., *Angiogenesis in health and disease.* Nat Med, 2003. **9**(6): p. 653-60.

195. Ferrara, N., H.P. Gerber, and J. LeCouter, *The biology of VEGF and its receptors.* Nat Med, 2003. **9**(6): p. 669-76.

196. Bauer, S.M., R.J. Bauer, and O.C. Velazquez, *Angiogenesis, vasculogenesis, and induction of healing in chronic wounds.* Vasc Endovascular Surg, 2005. **39**(4): p. 293-306.

197. Jakobsson, L., et al., *Endothelial cells dynamically compete for the tip cell position during angiogenic sprouting.* Nat Cell Biol, 2010. **12**(10): p. 943-53.

198. Dorrell, M.I., E. Aguilar, and M. Friedlander, *Retinal vascular development is mediated by endothelial filopodia, a preexisting astrocytic template and specific R-cadherin adhesion.* Invest Ophthalmol Vis Sci, 2002. **43**(11): p. 3500-10.

199. Gerhardt, H., et al., *VEGF guides angiogenic sprouting utilizing endothelial tip cell filopodia.* J Cell Biol, 2003. **161**(6): p. 1163-77.

200. Adams, R.H. and A. Eichmann, *Axon guidance molecules in vascular patterning.* Cold Spring Harb Perspect Biol, 2010. **2**(5): p. a001875.

201. Adams, R.H. and K. Alitalo, *Molecular regulation of angiogenesis and lymphangiogenesis.* Nat Rev Mol Cell Biol, 2007. **8**(6): p. 464-78.

202. Herbert, S.P. and D.Y. Stainier, *Molecular control of endothelial cell behaviour during blood vessel morphogenesis.* Nat Rev Mol Cell Biol, 2011. **12**(9): p. 551-64.

203. Chrzanowska-Wodnicka, M., et al., *Defective angiogenesis, endothelial migration, proliferation, and MAPK signaling in Rap1b-deficient mice.* Blood, 2008. **111**(5): p. 2647-56.

204. Brouty-Boye, D. and B.R. Zetter, *Inhibition of cell motility by interferon.* Science, 1980. **208**(4443): p. 516-8.

205. Starzec, A., et al., *Antiangiogenic and antitumor activities of peptide inhibiting the vascular endothelial growth factor binding to neuropilin-1.* Life Sci, 2006. **79**(25): p. 2370-81.

206. Xu, Y., et al., *A novel antiangiogenic peptide derived from hepatocyte growth factor inhibits neovascularization in vitro and in vivo.* Mol Vis, 2010. **16**: p. 1982-95.

207. Li, S., N.F. Huang, and S. Hsu, *Mechanotransduction in endothelial cell migration.* J Cell Biochem, 2005. **96**(6): p. 1110-26.

208. Lamalice, L., F. Le Boeuf, and J. Huot, *Endothelial cell migration during angiogenesis.* Circ Res, 2007. **100**(6): p. 782-94.

209. Connolly, J.O., et al., *Rac regulates endothelial morphogenesis and capillary assembly.* Mol Biol Cell, 2002. **13**(7): p. 2474-85.

210. Park, H.J., et al., *3-hydroxy-3-methylglutaryl coenzyme A reductase inhibitors interfere with angiogenesis by inhibiting the geranylgeranylation of RhoA.* Circ Res, 2002. **91**(2): p. 143-50.

211. Hoang, M.V., M.C. Whelan, and D.R. Senger, *Rho activity critically and selectively regulates endothelial cell organization during angiogenesis.* Proc Natl Acad Sci U S A, 2004. **101**(7): p. 1874-9.

212. Fryer, B.H. and J. Field, *Rho, Rac, Pak and angiogenesis: old roles and newly identified responsibilities in endothelial cells.* Cancer Lett, 2005. **229**(1): p. 13-23.

213. Budd, S., et al., *Reduction in endothelial tip cell filopodia corresponds to reduced intravitreous but not intraretinal vascularization in a model of ROP.* Exp Eye Res, 2009. **89**(5): p. 718-27.

214. Yamazaki, D., et al., *WAVE2 is required for directed cell migration and cardiovascular development.* Nature, 2003. **424**(6947): p. 452-6.

215. van Nieuw Amerongen, G.P., et al., *Involvement of RhoA/Rho kinase signaling in VEGF-induced endothelial cell migration and angiogenesis in vitro.* Arterioscler Thromb Vasc Biol, 2003. **23**(2): p. 211-7.

216. Chai, J., M.K. Jones, and A.S. Tarnawski, *Serum response factor is a critical requirement for VEGF signaling in endothelial cells and VEGF-induced angiogenesis.* FASEB J, 2004. **18**(11): p. 1264-6.

217. Franco, C.A., et al., *Serum response factor is required for sprouting angiogenesis and vascular integrity.* Dev Cell, 2008. **15**(3): p. 448-61.

218. Franco, C.A., et al., *SRF selectively controls tip cell invasive behavior in angiogenesis.* Development, 2013. **140**(11): p. 2321-33.

219. Smith, J.T., J.T. Elkin, and W.M. Reichert, *Directed cell migration on fibronectin gradients: effect of gradient slope.* Exp Cell Res, 2006. **312**(13): p. 2424-32.

220. Salazar, R., S.E. Bell, and G.E. Davis, *Coordinate induction of the actin cytoskeletal regulatory proteins gelsolin, vasodilator-stimulated phosphoprotein, and profilin during capillary morphogenesis in vitro.* Exp Cell Res, 1999. **249**(1): p. 22-32.

221. Sui, S., et al., *Phosphoproteome analysis of the human Chang liver cells using SCX and a complementary mass spectrometric strategy.* Proteomics, 2008. **8**(10): p. 2024-34.

222. Kim, W., et al., *Systematic and quantitative assessment of the ubiquitin-modified proteome.* Mol Cell, 2011. **44**(2): p. 325-40.

223. Meierhofer, D., et al., *Quantitative analysis of global ubiquitination in HeLa cells by mass spectrometry.* J Proteome Res, 2008. **7**(10): p. 4566-76.

224. Xu, G., J.S. Paige, and S.R. Jaffrey, *Global analysis of lysine ubiquitination by ubiquitin remnant immunoaffinity profiling.* Nat Biotechnol, 2010. **28**(8): p. 868-73.

225. Danielsen, J.M., et al., *Mass spectrometric analysis of lysine ubiquitylation reveals promiscuity at site level.* Mol Cell Proteomics, 2011. **10**(3): p. M110 003590.

226. Shi, Y., et al., *A data set of human endogenous protein ubiquitination sites.* Mol Cell Proteomics, 2011. **10**(5): p. M110 002089.

227. Wagner, S.A., et al., *A proteome-wide, quantitative survey of in vivo ubiquitylation sites reveals widespread regulatory roles.* Mol Cell Proteomics, 2011. **10**(10): p. M111 013284.

228. Wagner, S.A., et al., *Proteomic analyses reveal divergent ubiquitylation site patterns in murine tissues.* Mol Cell Proteomics, 2012. **11**(12): p. 1578-85.

229. Pan, C., et al., *Global effects of kinase inhibitors on signaling networks revealed by quantitative phosphoproteomics.* Mol Cell Proteomics, 2009. **8**(12): p. 2796-808.

230. Olsen, J.V., et al., *Quantitative phosphoproteomics reveals widespread full phosphorylation site occupancy during mitosis.* Sci Signal, 2010. **3**(104): p. ra3.

231. Gu, T.L., et al., *Survey of tyrosine kinase signaling reveals ROS kinase fusions in human cholangiocarcinoma.* PLoS One, 2011. **6**(1): p. e15640.

232. Fan, Y., et al., *Stimulus-dependent phosphorylation of profilin-1 in angiogenesis.* Nat Cell Biol, 2012. **14**(10): p. 1046-56.

233. Mayya, V., et al., *Quantitative phosphoproteomic analysis of T cell receptor signaling reveals system-wide modulation of protein-protein interactions.* Sci Signal, 2009. **2**(84): p. ra46.

234. Kim, S.C., et al., *Substrate and functional diversity of lysine acetylation revealed by a proteomics survey.* Mol Cell, 2006. **23**(4): p. 607-18.

235. Choudhary, C., et al., *Lysine acetylation targets protein complexes and co-regulates major cellular functions.* Science, 2009. **325**(5942): p. 834-40.

236. Rush, J., et al., *Immunoaffinity profiling of tyrosine phosphorylation in cancer cells.* Nat Biotechnol, 2005. **23**(1): p. 94-101.

237. Rikova, K., et al., *Global survey of phosphotyrosine signaling identifies oncogenic kinases in lung cancer.* Cell, 2007. **131**(6): p. 1190-203.

238. Kim, J.E. and F.M. White, *Quantitative analysis of phosphotyrosine signaling networks triggered by CD3 and CD28 costimulation in Jurkat cells.* J Immunol, 2006. **176**(5): p. 2833-43.

239. Wolf-Yadlin, A., et al., *Effects of HER2 overexpression on cell signaling networks governing proliferation and migration.* Mol Syst Biol, 2006. **2**: p. 54.

240. Guo, A., et al., *Signaling networks assembled by oncogenic EGFR and c-Met.* Proc Natl Acad Sci U S A, 2008. **105**(2): p. 692-7.

241. Luo, W., et al., *Global impact of oncogenic Src on a phosphotyrosine proteome.* J Proteome Res, 2008. **7**(8): p. 3447-60.

242. Heibeck, T.H., et al., *An extensive survey of tyrosine phosphorylation revealing new sites in human mammary epithelial cells.* J Proteome Res, 2009. **8**(8): p. 3852-61.

243. Jorgensen, C., et al., *Cell-specific information processing in segregating populations of Eph receptor ephrin-expressing cells.* Science, 2009. **326**(5959): p. 1502-9.

244. Moritz, A., et al., *Akt-RSK-S6 kinase signaling networks activated by oncogenic receptor tyrosine kinases.* Sci Signal, 2010. **3**(136): p. ra64.

245. Gu, T.L., et al., *Identification of activated Tnk1 kinase in Hodgkin's lymphoma.* Leukemia, 2010. **24**(4): p. 861-5.

246. Pighi, C., et al., *Phospho-proteomic analysis of mantle cell lymphoma cells suggests a pro-survival role of B-cell receptor signaling.* Cell Oncol (Dordr), 2011. **34**(2): p. 141-53.

247. Artemenko, K.A., et al., *Optimization of immunoaffinity enrichment and detection: toward a comprehensive characterization of the phosphotyrosine proteome of K562 cells by liquid chromatography-mass spectrometry.* Analyst, 2011. **136**(9): p. 1971-8.

248. Bergstrom Lind, S., et al., *Toward a comprehensive characterization of the phosphotyrosine proteome.* Cell Signal, 2011. **23**(8): p. 1387-95.

249. Bai, Y., et al., *Phosphoproteomics identifies driver tyrosine kinases in sarcoma cell lines and tumors.* Cancer Res, 2012. **72**(10): p. 2501-11.

250. Hansson, A., et al., *Protein kinase C-dependent phosphorylation of profilin is specifically stimulated by phosphatidylinositol bisphosphate (PIP2).* Biochem Biophys Res Commun, 1988. **150**(2): p. 526-31.

251. Singh, S.S., et al., *Phosphoinositide-dependent in vitro phosphorylation of profilin by protein kinase C. Phospholipid specificity and localization of the phosphorylation site.* Recept Signal Transduct, 1996. **6**(2): p. 77-86.

252. Vemuri, B. and S.S. Singh, *Protein kinase C isozyme-specific phosphorylation of profilin.* Cell Signal, 2001. **13**(6): p. 433-9.

253. Kasina, S., et al., *Nitration of profilin effects its interaction with poly (L-proline) and actin.* J Biochem, 2005. **138**(6): p. 687-95.

254. Kasina, S., et al., *Phorbol ester mediated activation of inducible nitric oxide synthase results in platelet profilin nitration.* Nitric Oxide, 2006. **14**(1): p. 65-71.

255. Goldschmidt-Clermont, P.J., et al., *Mechanism of the interaction of human platelet profilin with actin.* J Cell Biol, 1991. **113**(5): p. 1081-9.

256. Vinson, V.K., et al., *Three-dimensional solution structure of Acanthamoeba profilin-I.* J Cell Biol, 1993. **122**(6): p. 1277-83.

257. Sathish, K., et al., *Phosphorylation of profilin regulates its interaction with actin and poly (L-proline).* Cell Signal, 2004. **16**(5): p. 589-96.

258. Ding, Z., Y.H. Bae, and P. Roy, *Molecular insights on context-specific role of profilin-1 in cell migration.* Cell Adh Migr, 2012. **6**(5): p. 442-9.

259. Baker, M., et al., *Use of the mouse aortic ring assay to study angiogenesis.* Nat Protoc, 2012. **7**(1): p. 89-104.

260. Korff, T. and H.G. Augustin, *Integration of endothelial cells in multicellular spheroids prevents apoptosis and induces differentiation.* J Cell Biol, 1998. **143**(5): p. 1341-52.

261. Korff, T. and H.G. Augustin, *Tensional forces in fibrillar extracellular matrices control directional capillary sprouting.* J Cell Sci, 1999. **112 (Pt 19)**: p. 3249-58.

262. Masson, V.V., et al., *Mouse Aortic Ring Assay: A New Approach of the Molecular Genetics of Angiogenesis.* Biol Proced Online, 2002. **4**: p. 24-31.

263. Fan, Y., et al., *Spatial coordination of actin polymerization and ILK-Akt2 activity during endothelial cell migration.* Dev Cell, 2009. **16**(5): p. 661-74.

264. Goodwin, A.M., *In vitro assays of angiogenesis for assessment of angiogenic and anti-angiogenic agents.* Microvasc Res, 2007. **74**(2-3): p. 172-83.

265. Ribatti, D. and E. Crivellato, *"Sprouting angiogenesis", a reappraisal.* Dev Biol, 2012. **372**(2): p. 157-65.

266. Hoving, S., et al., *Preparative two-dimensional gel electrophoresis at alkaline pH using narrow range immobilized pH gradients.* Proteomics, 2002. **2**(2): p. 127-34.

267. Ubersax, J.A. and J.E. Ferrell, Jr., *Mechanisms of specificity in protein phosphorylation.* Nat Rev Mol Cell Biol, 2007. **8**(7): p. 530-41.

268. Xue, Y., et al., *GPS 2.1: enhanced prediction of kinase-specific phosphorylation sites with an algorithm of motif length selection.* Protein Eng Des Sel, 2011. **24**(3): p. 255-60.

269. Blom, N., et al., *Prediction of post-translational glycosylation and phosphorylation of proteins from the amino acid sequence.* Proteomics, 2004. **4**(6): p. 1633-49.

270. Wong, Y.H., et al., *KinasePhos 2.0: a web server for identifying protein kinase-specific phosphorylation sites based on sequences and coupling patterns.* Nucleic Acids Res, 2007. **35**(Web Server issue): p. W588-94.

271. Neuberger, G., G. Schneider, and F. Eisenhaber, *pkaPS: prediction of protein kinase A phosphorylation sites with the simplified kinase-substrate binding model.* Biol Direct, 2007. **2**: p. 1.

272. Wittenmayer, N., et al., *Functional characterization of green fluorescent protein-profilin fusion proteins.* Eur J Biochem, 2000. **267**(16): p. 5247-56.

273. Skare, P. and R. Karlsson, *Evidence for two interaction regions for phosphatidylinositol(4,5)-bisphosphate on mammalian profilin I.* FEBS Lett, 2002. **522**(1-3): p. 119-24.

274. Wu, C.H., et al., *Mutations in the profilin 1 gene cause familial amyotrophic lateral sclerosis.* Nature, 2012. **488**(7412): p. 499-503.

275. Leve, F., W. de Souza, and J.A. Morgado-Diaz, *A cross-link between protein kinase A and Rho-family GTPases signaling mediates cell-cell adhesion and actin cytoskeleton organization in epithelial cancer cells.* J Pharmacol Exp Ther, 2008. **327**(3): p. 777-88.

276. Newell-Litwa, K.A. and A.R. Horwitz, *Cell migration: PKA and RhoA set the pace.* Curr Biol, 2011. **21**(15): p. R596-8.

277. Nolle, A., et al., *The spinal muscular atrophy disease protein SMN is linked to the Rho-kinase pathway via profilin.* Hum Mol Genet, 2011. **20**(24): p. 4865-78.

278. Zhu, K., et al., *Protein pI shifts due to posttranslational modifications in the separation and characterization of proteins.* Anal Chem, 2005. **77**(9): p. 2745-55.

279. Harbeck, B., et al., *Phosphorylation of the vasodilator-stimulated phosphoprotein regulates its interaction with actin.* J Biol Chem, 2000. **275**(40): p. 30817-25.

280. Furman, C., et al., *Ena/VASP is required for endothelial barrier function in vivo.* J Cell Biol, 2007. **179**(4): p. 761-75.

281. Schlaeger, T.M., et al., *Uniform vascular-endothelial-cell-specific gene expression in both embryonic and adult transgenic mice.* Proc Natl Acad Sci U S A, 1997. **94**(7): p. 3058-63.